Climate Impacts to Restoration Practices – Project Report

September 18, 2020

PREPARED FOR

Sadie Drescher
Director, Restoration Programs
Chesapeake Bay Trust
108 Severn Avenue,
Annapolis, MD 21403
(410) 974-2941 x105
sdrescher@cbtrust.org

PREPARED BY

Jonathan Butcher
Tetra Tech
One Park Drive, Suite 200
PO Box 14409
Research Triangle Park, NC 27709
(919) 485-8278
jon.butcher@tetratech.com

Contributing authors
Scott Job, Nancy Roth, Bryan Groza, Brian Pickard, and Peter Kwon

CBT Request #16928, D**eliverable** # 1**1**

100-IWM-T39881

TETRA TECH

This page left intentionally blank

CONTENTS

EXECUTIVE SUMMARY **1**

1.0 INTRODUCTION **5**

2.0 METHODS **7**

2.1 Statistical Theory 8

2.1.1 IDF Updates 8

2.1.2 Peaks over Threshold Analysis for Sub-yearly Events 11

2.2 Runoff and BMP Simulation with SWMM 14

2.2.1 Bioretention 16

2.2.2 Extended Wet Detention Basin 16

2.2.3 BMP Sizing with Maryland Environmental Site Design 17

3.0 DATA **19**

3.1 NOAA IDF Curve Stations in Maryland 19

3.2 Climate Model Selection 21

4.0 RESULTS – EXTREME PRECIPITATION **37**

5.0 RESULTS – EVENT RUNOFF AND BMP SIMULATIONS **41**

5.1 Runoff 41

5.2 Bioretention BMP 42

5.3 Extended Wet Detention BMP 47

6.0 IMPLICATIONS FOR DESIGN **51**

6.1 Channel Stability 51

6.2 Roadway Flooding Risk 58

6.3 Urban BMP Performance 67

6.3.1 BMP Systems: Environmental Site Design 68

6.3.2 Design of Individual Practices 72

7.0 DISCUSSION **75**

7.1 Potential Use of Continuous Simulation 75

7.2 Adaptation of BMPs in a Changing Climate 76

7.3 Stream Restoration Design Considerations 78

8.0 REFERENCES **81**

APPENDIX A. PYTHON CODE **89**

A-1. IDF Updates 89

A-2. Peaks-over-Threshold Analysis 108
A-3. SWMM Simulations 120

TABLES

Table 2-1. Curve Numbers for Environmental Site Design Simulations (MDE, 2009) 18
Table 3-1. Key to NOAA Atlas 14 Sites 20
Table 3-2. Key to CMIP5 GCM Scenarios in the LOCA Downscaled Climate Data Archive 23
Table 3-3. Bounding Scenarios for Analysis of Changes in Precipitation Volume, ca. 2056 24
Table 3-4. Bounding Scenarios for Analysis of Changes in Precipitation Volume, ca. 2085 27
Table 3-5. Bounding Scenarios for Analysis of the 90th Percentile 24-hour Precipitation Event, ca. 2056 30
Table 3-6. Bounding Scenarios for Analysis of the 90th Percentile 24-hour Precipitation Event, ca. 2085 33
Table 5-1. Summary of Response of Bioretention to 90th-percentile Event 43
Table 5-2. Summary of Responses of Bioretention to Future 1-year through 100-year Events 44
Table 5-3. Summary of Response of Extended Wet Detention to 90th-percentile Event 47
Table 5-4. Summary of Responses of Extended Wet Detention to Future 1-year through 100-year Events 48
Table 6-1. Probability of Channel Instability for Runoff from 1 Acre with $S/\sqrt{d_{50}}$ = 1.75, with and without Bioretention BMPs 55
Table 6-2. Probability of Channel Instability for Runoff from 1 Acre Parcel with Alternative $S/\sqrt{d_{50}}$ at 80% Imperviousness 55
Table 6-3. Probability of Channel Instability for Runoff from 25-Acre Parcel based on 1-yr 24-hr Event with Alternative Values of $S/\sqrt{d_{50}}$ 58
Table 6-4. HY-8 Results, Local Road Culvert 63
Table 6-5. HY-8 Results, Minor Arterial Culvert 64
Table 6-6. Polynomial Coefficients for Relationship of Headwater Elevation and Outlet Velocity to Flow 66
Table 6-7. Curve Numbers for Environmental Site Design Simulations 69
Table 6-8. Treatment Volume (Q_E, inches) for Historic and Predicted Future Climate for Hydrologic Group D Soils, Developed Land at 80% Imperviousness 70
Table 6-9. Relationship of Excess Stormwater Volume to Q_E Calculated using Environmental Site Design Procedure from 2009 Design Manual (MDE, 2009) – Hydrologic Soil Group A 70
Table 6-10. Relationship of Excess Stormwater Volume to Q_E Calculated using Environmental Site Design Procedure from 2009 Design Manual (MDE, 2009) – Hydrologic Soil Group B 71
Table 6-11. Relationship of Excess Stormwater Volume to Q_E Calculated using Environmental Site Design Procedure from 2009 Design Manual (MDE, 2009) – Hydrologic Soil Group C 71
Table 6-12. Relationship of Excess Stormwater Volume to Q_E Calculated using Environmental Site Design Procedure from 2009 Design Manual (MDE, 2009) – Hydrologic Soil Group D 72

FIGURES

Figure 2-1. Threshold Value Detected by the Python Algorithm for Site 18-7140 14
Figure 2-2. Future 90th-percentile Rainfall Event Predictions for Different GCMs at Site 18-7140 14
Figure 2-3. Schematic of IDF Analysis Tool 15
Figure 2-4. Curve Number Prediction of Runoff as a Function of Precipitation for Hydrologic Group D Soils, Developed Land at 80% Imperviousness 18
Figure 3-1. NOAA Atlas 14 Sites in Maryland and the District of Columbia 19
Figure 3-2. Example Biplot of Forecast Changes in Average Annual Precipitation and Air Temperature for Durham North Carolina for 2050 - 2080 vs. 1950 – 2005 21
Figure 4-1. Projected 25-year IDF Curves for Baltimore WSO Airport ca. 2055 38
Figure 4-2. Projected 25-year IDF Curves for Baltimore WSO Airport ca. 2085 39
Figure 4-3. Projected Results for 90th Percentile 24-hour Precipitation Event, Aberdeen-Phillips Field 40
Figure 5-1. Historic and Future Peak Flow Averages by Recurrence 42
Figure 5-2. Bioretention Simulation Results for Peak Outflow as a Function of Total Storm Depth 45
Figure 5-3. Bioretention Simulation Results for Overflow Volume as a Function of Total Storm Depth 46
Figure 5-4. Extended Wet Detention Basin Simulation Results for Peak Outflow as a Function of Total Storm Depth 49
Figure 5-5. Extended Wet Detention Simulation Results for Overflow Volume as a Function of Total Storm Depth 50
Figure 6-1. Stability Transition Frontier for Sand Bed Stream with 1-acre Drainage 53
Figure 6-2. Average Mobility Index for 25% (left) and 80% (right) Impervious Cover 1-acre Parcel, $S/\sqrt{d_{50}}$ = 1.75 $m^{-0.5}$ 54
Figure 6-3. Predicted Probability of Channel Instability at 25% Imperviousness for Runoff from a 1 Acre Site with $S/\sqrt{d_{50}}$ = 1.75 using the Logistic Regression of Bledsoe and Watson (2001) 54
Figure 6-4. Histogram of Individual Station/GCM/Imperviousness for Probability of Channel Instability with $S/\sqrt{d_{50}}$ = 1.75, 1 Acre Drainage, and no BMP 56
Figure 6-5. Inverse Cumulative Distribution Function (Percentage Greater than Specified Level) of Individual Station/GCM/Imperviousness for Probability of Channel Instability with $S/\sqrt{d_{50}}$ = 1.75, 1 Acre Drainage, and no BMP 56
Figure 6-6. Average Mobility Index for 25% (left) and 80% (right) Impervious Cover, 25-acre Parcel, $S/\sqrt{d_{50}}$ = 0.35 $m^{-0.5}$ 57
Figure 6-7. Average Mobility Index for 80% Impervious Cover, 25-acre Parcel, $S/\sqrt{d_{50}}$ = 0.35 $m^{-0.5}$ (left) and $S/\sqrt{d_{50}}$ = 1.0 $m^{-0.5}$ (right) 57
Figure 6-8. Minor Arterial Road Culvert, HY-8 Specifications 60
Figure 6-9. Local Road Culvert HY-8 Specifications 61
Figure 6-10. Relationship between Peak Flow from 1-acre (80% Impervious) and 24-hour Precipitation Depth 62
Figure 6-11. Relationship of Headwater Elevation and Outlet Velocity to Flow for Local Road (Left) and Minor Arterial (Right) Culvert Designs 65
Figure 6-12. Predicted Frequency of Road Overtopping under Future Climate, Local Road Culvert 66
Figure 6-13. Predicted Frequency of Road Overtopping under Future Climate, Minor Arterial Culvert 67
Figure 6-14. Curve Number Prediction of Runoff as a Function of Precipitation for Hydrologic Group D Soils, Developed Land at 80% Imperviousness 69

(This page left intentionally blank.)

EXECUTIVE SUMMARY

Intense precipitation events are increasing in the mid-Atlantic region and climate models suggest this trend may continue. We derive projections of future extreme precipitation and runoff events throughout Maryland. These suggest that infrastructure sized to handle historic weather may be inadequate in future and that urban stream channels may become less stable; however, pollutant removal functions of stormwater best management practices appear less likely to be adversely affected.

Warmer air can hold more precipitable water and associated potential energy. A warming climate can thus increase the risk of extreme rainfall events. Recent observations document an increased frequency of extreme rainfall events throughout the eastern United States and in the Chesapeake Bay watershed. Climate models generally predict that these trends will continue. However, there is also considerable uncertainty about the practical implications of these predicted trends for designers and planners. First it is not precipitation itself, but the runoff generated by precipitation that is of most concern to the performance of stormwater infrastructure and the protection of stream channel integrity. Further, while a general trend of increases in extreme precipitation events is well supported by broad spatial averages over the ensemble of multiple climate model runs, predicted results at specific locations and in individual climate models can be quite different from one another.

In many U.S. jurisdictions, including Maryland, designs for stormwater infrastructure rely on estimates of the recurrence interval or frequency (F) of a storm of a given intensity (I) and duration (D) – the so-called IDF curve. For example, regulations might require that a minor road culvert be designed to pass the flow resulting from the precipitation associated with the 24-hour storm event that would reoccur, on average, once every 25 years. The National Oceanic and Atmospheric Administration (NOAA) has published IDF curves for weather stations throughout most of the U.S. For Maryland, these IDF curves are developed by a statistical extreme value fit to series of annual maximum daily precipitation recorded through December 2000.

Use of the NOAA IDF curves implicitly assumes that weather observed through 2000 is applicable to current and future conditions. The evidence already suggests that changes in the IDF relationships have occurred since 2000, while climate models predict continuing changes.

How can we account for such changes, especially regarding future conditions that may be encountered during the design life of a project? Global climate models have limited skill at predicting extreme precipitation events. For one, many of the most intensive rainfall events are associated with convective storms that occur at spatial scales that are smaller than the grid size of global climate models and with tropical storm events that are inherently difficult to predict. One potential solution is to use a regional weather model to predict more local responses when used with the global climate model providing boundary conditions. This is an informative exercise, but different regional models also differ, further increasing the multiplicity and potentially the range of results. More importantly, regional models are computationally expensive to run. The Coupled Model Intercomparison Project of the World Climate Research Programme in its most recently completed 5th round of experiments (CMIP5) includes output from over 32 different global climate models, each of which was run for at least two greenhouse gas forcing scenarios and it is not readily feasible to run all these permutations through a regional model – especially as the results of the new CMIP6 updated runs are now becoming available.

For this project we take a different, more computationally efficient approach to evaluating IDF curves consistent with CMIP5 global climate results. Essentially, we ask the question “What would the NOAA

IDF curves look like if they had been calculated from annual maximum precipitation series that had been modified to reflect changes in climate conditions indicated by the global climate models?" To do this we first make use of readily available climate prediction series that have already been downscaled to a smaller spatial scale and a daily time step. This is done using a "constructed analogs" approach, in which a library of historical observation series is used to scale from a monthly to a daily time step, ensuring a reasonable representation of the temporal structure of local rainfall, coupled with a spatial bias correction step based on comparison to historic observations that reduces the spatial size of the output grid to 1/16 degree (approximately 6.9 x 5.4 km at the latitude of Baltimore).

Our approach does not assume that the downscaled global climate models are able to provide accurate estimates of future extreme rainfall events. Rather, we assume that, for a given global climate model, the relative change between historic and future conditions for events of a given recurrence can be used to assess the likely change in the annual maxima series used to develop NOAA's IDF curves. We then re-fit the extreme value distribution to the revised maxima series to generate a climate modified IDF curve. This method is computationally efficient and allows us to generate potential future IDF relationships using multiple climate models at all 74 Maryland stations for which NOAA has published IDF curves.

Design of "green" management practices for water quality treatment is often based on retaining the runoff from the 90th or 95th percentile (i.e., sub-yearly) 24-hour precipitation event. The IDF analysis based on annual maxima series is not applicable to sub-yearly events. However, a similar updating procedure was constructed on a peaks-over-threshold analysis. A database containing estimates of future IDF curves and 90th percentile events was constructed for all 74 Maryland stations analyzed by NOAA. For each station this includes estimates of conditions centered at 2055 and 2085 from four different climate models, selected to represent a drier case (10th percentile of all models in total rainfall volume), a wetter case (90th percentile), and two cases near the median for a low and a high greenhouse gas emissions scenario.

Results of the IDF analysis suggest a widespread risk under future conditions of increased intensity of extreme precipitation events of a given duration and recurrence. However, this increase is not consistent among GCM scenarios downscaled by LOCA, with some models predicting drier conditions with a lesser frequency of extreme rainfall events. Consistent changes were not predicted in the magnitude of the 90th percentile event. This is in line with studies that suggest total annual precipitation volume will most likely increase under future climate, but that much of this increase will be associated with more extreme, low-recurrence events. The 90th percentile results thus appear to be "good news" as they suggest that many water quality best management practices (BMPs) that are optimized to capture and treat pollutants associated with sub-yearly recurrence events are likely to continue to provide expected services under future climate.

Once estimates of the precipitation distributions are obtained it is necessary to calculate runoff. This was done by routing the precipitation through EPA's Storm Water Management Model (SWMM) using a generic unit-area representation of an urban landscape with varying levels of impervious. SWMM was also used to represent performance of bioretention cells and extended wet detention pond BMPs, representative of green and gray approaches to stormwater management.

As with precipitation, there is a wide range of predictions from different climate models and different stations for extreme runoff. However, by the end of the century, peak runoff rates are predicted to increase, on average, about 13 – 14 percent, with slightly higher increases for longer recurrence intervals and lower impervious percentages.

Both bioretention and extended wet detention BMPs tended, on average, to produce less outflow and lower peak flows in response to the 90th percentile event under future climate. However, for large, longer recurrence events future predictions include increased peak flows and a larger volume of flow that overflowed or bypassed the BMP.

We undertook three additional analyses to evaluate practical consequence of these predicted changes in precipitation and runoff:

- **Channel Stability and Stream Restoration Design:** Stream restoration design seeks to create stable, resilient channels. Stability is highly site-specific and, in addition to runoff, depends on channel substrate, slope, and existing morphology. However, analysis of stability indices for channel-forming flows suggest that changes in IDF relationships will increase the risk that some streams will shift from stable to unstable conditions.
- **Roadway Flooding Risk and Culvert Design:** Undersized culverts are a common cause of hazardous road overtopping during high flow events. Maryland specifies design standards for culverts based on road class and service life. For example, a culvert on a local road must be designed to safely pass the peak runoff from a 10-year 24-hour storm and has a minimum service life goal of 50 years. Model simulations suggest that a culvert designed for the current 10-year storm may have, on average, a risk of overtopping of about 15% by 2055 and a risk of 37% by 2085. This may indicate a need to revise design standards to address nearer-term conditions and the possible need for a larger culvert at the end of the 50-year service life.
- **BMP Performance Efficiency:** The Maryland Department of the Environment has adopted an Environmental Site Design approach for new development under which the combination of BMPs on a site needs to control runoff in response to the 1-year 24-hour storm so that it is no greater than the runoff that would be expected for the same site with a cover of undeveloped woods in good condition. We examined how these design criteria might fare under future climate and found that only a small increase in risk is anticipated on average, largely because the projected changes in the 1-year event are small.

Adaptation to a changing climate is challenging because models, while numerous, are uncertain, there is no single best predictor of the future, and the course of climate response will depend on human political and economic decisions. Exercises like this report help inform us about the range of risks that may need to be faced but deciding where to balance risk and cost is inherently political. What is clear is that it is preferable to employ solutions that are resilient and adaptable – able to perform well under a variety of future conditions and amenable to be adjusted with low regret costs if the future is not as predicted. In this context, stormwater management using green components such as bioretention that can be expanded or altered as needed are likely preferable to gray infrastructure such as retention basins that, if they turn out to be undersized, are difficult and expensive to replace. Low-regret opportunities that benefit resource management regardless of whether and how climate changes are preferable.

For climate-smart stream restoration design, resilience and adaptability should be explicit objectives. Maintaining floodplain connectivity is one key to building natural resilience and designs should anticipate greater uncertainty in the flow regime, not just increases in large events. The overall goal is to maximize the ability of the stream to adjust gradually to a range of potential, but uncertain, hydrometeorological changes over the design life of the project.

(This page left intentionally blank.)

1.0 INTRODUCTION

Engineering design for stormwater management is largely based on empirical evidence obtained from past data with the assumption that the frequency of extreme events that is likely to be seen in the future can be inferred from the historical record. This implies that climate is stationary; however, in many regions of the U.S., the intensity and frequency of major precipitation events is projected to increase (Hayhoe et al., 2018). Predicted changes in future climate imply the end of the assumption of stationarity that has provided the foundation of water management for decades, as was announced by Milly et al. (2008). Commenting on the "death of stationarity", Galloway (2011) noted "there is also a great need to provide those in the field the information they require now to plan, design, and operate today's projects."

Kunkel et al. (2013) identified increasing trends in the number of 2-dau precipitation events exceeding a once-in-five-year threshold throughout the eastern half of the U.S. Easterling et al. (2017) in the Fourth National Climate Assessment reported changes in both the number and magnitude of large precipitation events. Hoerling et al. (2016) looked at precipitation above the 95th percentile daily event and found consistent increases in the Northeast but not in the Southeast U.S. (Maryland is on the border between the two regions). Howarth et al. (2019) summarize recent observations for the Northeast U.S. and identified statistically significant increases in the top one percent of daily rainfall events. Expected increases in the frequency of intense rain events in the Chesapeake Bay watershed is supported by the 4th National Climate Assessment (Dupigny-Giroux et al., 2018). Thibeault and Seth (2014) and Lynch et al. (2016) also document recent observed and future projected increases in intense rain events in the area.

Design of urban stormwater BMPs typically begins with consideration of rainfall recurrence intervals, which may be translated into design storm specifications or runoff depth. Practices are designed to achieve a level of service or performance associated with controlling a certain design storm, combination of design storms, and/or runoff depth to reduce flooding, stream erosion, and pollutant loading. In most areas, design standards for BMPs incorporate sizing requirements based on storms of a specified intensity, duration, and frequency (IDF analysis). The performance of stormwater practices is dictated primarily by precipitation IDF, impervious surface area, and soils, along with life cycle maintenance (Berndtsson, 2010; Claytor and Schueler, 1996; Gallo et al., 2012, Hunt et al., 2012, Kadlec and Knight, 1996, Khan et al., 2012; Roseen et al., 2009). If the IDF relationships change, the design standards for both gray and green infrastructure components should change as well to preserve retention capacity and treatment contact times that are essential to treatment efficiency.

IDF curves graphically summarize the relationship between precipitation intensity and the duration of precipitation events for a given frequency or recurrence interval. IDF curves provide important information for engineering design and planning purposes. From one perspective, updating IDF curves for future climate is simple – conditional on reliable estimates of the distribution of future precipitation events. Unfortunately, the skill of GCMs in predicting individual precipitation events is limited, especially convective storm events that provide the most intense storms yet occur at spatial scales smaller than the resolution of GCMs. For light precipitation, GCMs tend to overestimate the frequency but reproduce the observed patterns of intensity relatively well. For heavy precipitation, GCMs roughly reproduce the observed frequency, but underestimate the intensity (Sun et al. 2006; Sillmann et al. 2013; Mehran et al. 2014). Some of the biases inherent in GCMs are resolved by downscaling results to a finer, local scale, often with a bias correction step. However, Maraun et al. (2010) conclude that serious deficiencies

remain in the ability of downscaling methods to generate local precipitation series with the correct temporal variability.

For most of the U.S. (including Maryland), estimates of precipitation frequency at pre-defined recurrence intervals of once per year through once per 1,000 years for specific weather observation stations are provided as IDF curves and tables in the National Oceanic and Atmospheric Administration (NOAA)'s Atlas 14 (e.g., Perica et al., 2013) and companion Precipitation Frequency Data Server (https://hdsc.nws.noaa.gov/hdsc/pfds/). A specific objective of the work described in this report is to provide a method to update Atlas 14 IDF curves to reflect potential future changes in model-predicted local climate. To satisfy this objective it is important to understand the way in which the Atlas 14 estimates were created.

Frequency estimates in Atlas 14 are based on fitting an extreme value distribution (in most cases, a generalized extreme value [GEV] distribution) to the time series of annual maximum precipitation (AMP) amounts at a station for seventeen durations ranging from 15 minutes to 60 days. The AMP series consists of one measurement per year (the largest depth observed for a given duration) and does not account for the possibility of more than one event in a year exceeding a threshold of interest. The true probability of occurrence of events of a given intensity and duration should be derived from the partial duration series, which includes all events of a specified duration and above a pre-defined volume threshold. Frequency estimates for partial duration series were developed by NOAA for Atlas 14 from the series of AMPs using Langbein's conversion formula, which transforms a partial duration series-based average recurrence interval (*ARI*) to an annual exceedance probability (*AEP*):

$$AEP = 1 - \exp\left(-\frac{1}{ARI}\right) \qquad \text{Equation 1}$$

Selected partial duration *ARI*s are first converted to *AEP*s using this formula, and frequency estimates were then calculated for the *AEP* using the GEV fit to annual maxima.

For Atlas 14, NOAA fit the GEV for each station using the method of L-moments (Hosking and Wallis, 1997), incorporating regionalization across approximately the 10 nearest stations for higher order L-moments. NOAA does not release the fitted coefficients of the GEV distribution, although the AMP series are provided via ftp server. Because the NOAA method is ultimately based only on annual maxima (the AMP series), only AMPs are needed for future climate conditions and not the complete time series. The theoretical basis for updating Atlas 14 IDF curves is presented in Section 2.1.

Storms of more frequent occurrence than once per year are also relevant to BMP and restoration design but cannot be reliably analyzed from AMPs alone. Analysis of these more frequent storms requires a somewhat different "peaks over threshold" approach, as is also described in Section 2.10.

The size of precipitation events is generally of less direct concern than the amount of runoff produced by the event, which in addition to precipitation, depends on antecedent moisture conditions, the extent to which the landscape produces direct runoff (which is closely related to the amount of impervious surfaces that are present), and the degree to which management practices retain or infiltrate stormwater. Evaluating runoff requires combining precipitation estimates with a rainfall-runoff model (Section 2.2).

These tools are combined with climate model projections (Section 3.0) to produce precipitation and runoff results under future climate for Atlas 14 stations throughout Maryland (Sections 4.0 and 5.0). The remaining sections investigate how projected changes may affect aspects of stormwater infrastructure design and stream restoration activities

2.0 METHODS

Updating the IDF curves in Atlas 14 or similar statistical estimates of large precipitation events for future climate requires understanding how the extreme value distribution fit to annual maximum precipitation series may change. Over the past two decades – and especially since the 2008 call-to-arms of Milly et al. – numerous researchers have explored methods for predicting future changes in extreme precipitation and IDF relationships. While many different methods have been used, all have in common a recognition that the current generation of GCMs has relatively low skill in predicting extreme precipitation events, especially those associated with convective storms, which occur at scales smaller than GCM grids. In essence, predicting extreme precipitation events is a specific form of the general problem of downscaling from global models that produce monthly-scale climate projections to place-based predictions at daily and sub-daily time scales. Research in this field falls into four general classes (with terminology in part adapted from Arnbjerg-Nielsen et al., 2013):

1. **Conditional Probability (weather generators)**: One response to the deficiencies in GCM simulation of extreme events is to not use the GCM output directly at all, but rather to use information from the GCMs to populate statistical weather generators, which are then used to estimate meteorological time-series at the desired spatial and temporal resolution. Conditional probability methods for precipitation have long been in use for spatial analyses and were adopted for evaluation of climate response by Fowler et al., (2005), Kilsby et al. (2007), Prodanovic and SImonovic (2007), and Onof and Arnbjerg-Nielsen (2009). The method remains popular for areas that lack long term rainfall data (e.g., Shrestha et al., 2017). A fundamental challenge of this approach is determining the short duration statistical moments of the weather generator from GCM output that does not provide the necessary temporal resolution

2. **Empirical Transfer Functions**: Another approach that avoids direct use of GCM precipitation output is to develop a surrogate relationship between extreme precipitation and other GCM outputs that are presumed to be predicted with greater accuracy. For example, Willems and Vrac (2011) developed transfer functions based on atmospheric pressure, while Dahm et al. (2019) developed an approach to project rainfall extremes by scaling the empirical relationship to dewpoint temperature. While promising, this approach appears to require development of transfer function relationships on a site by site basis to obtain robust predictions.

3. **Dynamical Downscaling (Regional Climate Models)**: An alternative approach to improving rainfall projections for future climate is to use GCM output as boundary conditions to drive a smaller-scale regional climate model (RCM), or even smaller scale local area model (LAM) that presumably has better predictive capabilities for local rainfall events. This approach is known as dynamical downscaling. Future precipitation time series are typically obtained directly from the RCM or LAM output. Use of dynamical downscaling for precipitation extreme analysis has soared in popularity with the increasing availability of RCM output produced as part of the CORDEX (Coordinated Regional Climate Downscaling Experiment; http://www.cordex.org/) effort. Examples include Rosenberg et al. (2010), DeGaetano and Castellano (2017), Li et al. (2017), Lettenmaier et al. (2017), Vu et al. (2018), Kristvik et al. (2019), and Cannon and Innocenti (2019). The advantages of this approach depend on the level of accuracy that is achieved by the smaller-scale model. One problem with direct use of RCMs is that they generally still do not explicitly model small-scale cloud processes that cause intense convective storms, for which LAMs with horizontal scales finer than about 3 km may be needed (Arnbjerg-Nielsen et al., 2013).

Validation of these models is required before they can be used as input for local climate change impact studies (Arnbjerg-Nielsen et al., 2013). Further, dynamical downscaling is a time-consuming process, and results at the RCM scale are not available for many GCMs, much less LAM analyses.

4. **Statistical Downscaling**: In recent years, statistical approaches to downscaling have become widely available. Statistical downscaling is based on relationships that interpolate large-scale GCM output to observations of historical weather and climate (Wood et al., 2004; Maurer et al., 2007). Recent advances in statistical downscaling, such as the LOCA (Pierce et al., 2014) and MACA (Abatzoglou and Brown, 2012) archives, use a constructed analogs approach, in which a library of historical observation series is used to scale from monthly to daily time step, ensuring a reasonable representation of the temporal structure of local rainfall. The downscaling process incorporates a bias correction step and ensures that local, daily time series projections exhibit patterns similar to historical observed data. This achieves a spatial resolution of 1/6 degree (approximately 6.9 x 5.4 km at the latitude of Baltimore). The LOCA downscaling approach was developed to address some shortcomings of the older bias-correction constructed analog approaches to avoid damping of local precipitation extremes. Statistically downscaled time series from a GCM could be used to directly estimate IDF relationships or used to describe the relative change in the extreme value distribution underlying the IDF relationship (e.g., Srivastav et al., 2014a), as described below. A potential refinement of the approach is to select the downscaling analogs specifically on the basis of representation of extreme precipitation events (Castellano and DeGaetano, 2017; DeGaetano and Castellano, 2017; So et al., 2017). The refined approach focusing on extreme values appears promising but has not been implemented on a national basis. Any statistical downscaling approach is subject to the caveat of an implicit assumption that it assumes historical spatial relationships between GCM output and local climate will remain unchanged over time (Nover et al., 2016).

Some authors have also suggested that the whole framework of IDF curves, with assumption of constant or stationary parameters (conditional on climate) is misguided and that it is instead preferable to use an extreme value distribution with non-stationary parameters that could be derived either empirically (based on observations) or in reference to climate models. This type of approach is combined with Bayesian conditioning and uncertainty analysis by Cheng and AghaKouchak (2014), and Ragno et al. (2018); see also Huard et al. (2010).

2.1 STATISTICAL THEORY

2.1.1 IDF Updates

Many of the approaches described above for downscaling precipitation extremes are complex and require detailed site-specific analyses. Which approach is theoretically optimal for prediction appears to remain an open question. Our intention here is to use methods that are efficient, use widely available statistically downscaled data, are consistent with Atlas 14 procedures and results that are incorporated into many local regulations and design guides, and are model agnostic. A simple, computationally efficient approach to updating IDF curves was proposed by Srivastav et al. (2014a, 2014b). Their insight was that the essence of the problem was the need to update extreme value distributions for future conditions, and that this could be done through a direct analysis of the distributions. The general concept of the approach of Srivastav et al. (2014a) is described as follows: "…quantile-mapping functions can be directly applied

to establish the statistical relationship between the AMPs of a GCM and sub-daily observed data rather than using complete records. Further, the IDF is a distributional function; therefore, it would be easy to derive the functional relationships between the distributions of the GCM AMPs and sub-daily observed data. One way of deriving such relationship is by using quantile-mapping functions."

Quantile mapping (QM) methods, otherwise known as cumulative distribution function (CDF) matching methods, have long been used as a method to correct for local biases in GCM output. The method first establishes a statistical relationship or transfer function between model outputs and historical observations, then applies the transfer function to future model projections (Panofsky and Brier, 1968) and has been successfully used as a downscaling method in various climate impact studies (e.g., Hayhoe et al., 2004).

Using the notation of Li et al. (2010), for a climate variable *x*, the QM method for finding the bias-adjusted future value of a climate variable can be written as:

$$\hat{x}_{m-p.adjst.} = F_{o-c}^{-1}\left(F_{m-c}(x_{m-p})\right) \quad \text{Equation 2}$$

where *F* is the CDF of either the observations (o) or model (m) for observed current climate (c) or future projected climate (p), and F^{-1} is the inverse of the cumulative distribution function. The bias correction for a future period is thus done by finding the corresponding percentile values for these future projection points in the CDF of the model for current observations, then locating the observed values for the same CDF values of the observations.

A significant weakness of the QM method is that it assumes that the climate CDF does not change much over time, and that, as the mean changes, the variance and skew do not change, which is likely not true (e.g., Milly et al., 2008). To address these issues, Li et al. (2010) proposed the equidistant quantile mapping (EQM) method, which incorporates additional information from the CDF of the model projection. The method assumes that the difference between the model and observed value during the current calibration period also applies to the future period; however, the difference between the shape of the CDFs for the future and historic periods is also taken into account. This is written as:

$$\hat{x}_{m-p.adjst.} = x_{m-p} + F_{o-c}^{-1}\left(F_{m-p}(x_{m-p})\right) - F_{m-c}^{-1}\left(F_{m-p}(x_{m-p})\right) \quad \text{Equation 3}$$

where the form and parameters of the CDF are not yet specified. Srivastav et al. (2014a) argue for using EQM to update IDF curves; however, the specific method of Srivastav et al. (2014b) is not directly applicable to updating Atlas 14 IDF curves in the US for several reasons:

- Bias-corrected statistically downscaled climate model output were not widely available for Canada; therefore, the Srivastav et al. (2014a) method must also incorporate a spatial downscaling step from the coarse scale of GCMs, whereas output that is already spatially downscaled to a fine resolution grid is readily available for the US.
- The method of Srivastav et al. justifies use of EQM, but largely consists of a multi-step QM procedure, without full implementation of the EQM corrections proposed by Li et al. (2010).
- Canada assumes that the AMP series follows a Gumbel, rather than the GEV distribution that is mostly commonly used in the U.S.

To address these issues, we re-derived under contract with USEPA an EQM method that is consistent with U.S. design guidelines and makes use of statistically downscaled climate data readily available from GCM output.

Our approach uses a combination of EQM and QM to update IDF curves for any location conditional on output of GCMs for future climate conditions, implemented in Python code. The EQM approach can be used to update IDF curves for any location conditional on downscaled output of GCMs for future climate conditions. The process begins with GCM output that has already been subject to spatial bias correction and downscaling to a finer spatial scale. The calculation step consists of additional spatial downscaling from the climate output grid to the specific point location of a weather station used by Atlas 14 along with bias correction for the AMP series (as distinct from the general bias correction of the complete precipitation series) using the EQM method for different time durations from sub-hourly to daily.

The historical data for this analysis are the historical AMP series used by Atlas 14 (X_{amp}^{STN}). Model data include the predicted AMP series from 1950 to 2005 as historical period (X_{amp}^{GCM}) and future period (e.g., 2050- 2080, centered at 2065) of interest ($X_{amp}^{GCM_{FUT}}$). A GEV distribution is fit to each of these series, using the L-moments method (Hosking and Wallis, 1997; implemented in Python in *lmoments3* v1.0.4 [Hollebrandse et al., 2015]), consistent with Atlas 14 methods.

To apply the EQM method, quantiles of modeled future AMP series are matched to the distribution for historical AMPs. For a given percentile, it is assumed that the difference between the model and observed value also applies to the future period. There are two EQM factors as in Equation 3. The first is:

$$\boldsymbol{Y_{amp}^{adj1} = F_{o-c}^{-1}\left(F_{m-p}(x_{m-p})\right) = F^{-1}((F(X_{amp}^{GCM_{FUT}}|\theta^{GCM_{FUT}}))|\theta^{STN})}, \quad \text{Equation 4}$$

where the vertical bar "|" indicates conditional dependence, i.e., $F(X_{amp}^{GCM_{FUT}}|\theta^{GCM_{FUT}})$ indicates the cumulative distribution function (GEV for this case) of the future GCM AMP series calculated at the cumulative probability corresponding to $X_{amp}^{GCM_{FUT}}$ using the parameter set $\theta^{GCM_{FUT}}$ calculated for that future series. θ^{STN} represents the GEV parameters from fit to the Atlas 14 AMP series. To account for the difference between the CDFs for the model outputs of future and current periods, a second adjustment factor is calculated:

$$\boldsymbol{Y_{amp}^{adj2} = F_{m-c}^{-1}\left(F_{m-p}(x_{m-p})\right) = F^{-1}((F(X_{amp}^{GCM_{FUT}}|\theta^{GCM_{FUT}}))|\theta^{GCM})} \quad \text{Equation 5}$$

The projected AMP series is then calculated as:

$$\boldsymbol{Y_{amp}^{STN_FUT} = X_{amp}^{GCM_FUT} + Y_{amp}^{adj1} - Y_{amp}^{adj2}} \quad \text{Equation 6}$$

Once this series is calculated, a GEV fit is applied to estimate the full distribution of the future extreme events for the local station. This EQM step is applied to update the 24-hour IDF curves. We include corrections for constrained data (i.e., results for a given duration that are artificially truncated by crossing over the midnight boundary) using the Atlas 14 factors at this step. The CDFs and inverse CDFs of the GEV and other extreme value distributions are provided by the *lmoments3* Python library.

The second step in adjusting the IDF curves is temporal downscaling to convert future daily extremes into sub-daily extremes. The QM method was used for this purpose: First find the corresponding percentile values for these future projection points in the CDF of the model for the historical period, then locate the observed values for the same CDF values of the sub-daily observations. For rainfall duration *i*:

$$\boldsymbol{Y_{amp,i}^{GCM_FUT_sub24} = F^{-1}\left((F(Y_{amp}^{GCM_FUT_24h}|\theta^{STN_24h})|\theta_i^{STN_{sub24}})\right)} \quad \text{Equation 7}$$

As noted in later volumes of Atlas 14 (e.g., Perica et al., 2013), estimates for shorter durations can be noisy due to limited data availability and are improved by smoothing. To account for the short modeling

simulation period, the modeled extreme values with less than 24 hours' duration are thus smoothed by fitting them to a linear regression relative to the daily maximum series before fitting them to the GEV distribution. Atlas 14 uses a regression with an intercept for this purpose:

$$Y_{amp}^{GCM_sub24} = a_1 * Y_{amp}^{GCM_24h} + b_1 \quad \text{Equation 8}$$

$$Y_{amp}^{GCM_FUT_sub24} = a_2 * Y_{amp}^{GCM_FUT_24h} + b_2 \quad \text{Equation 9}$$

We found that for some Maryland stations the recommended smoothing step could produce negative estimates of AMS depths. This was resolved by switching to a zero-intercept regression in which b_1 and b_2 are constrained to be zero.

The adjusted model predictions ($Y_{amp}^{GCM_FUT}$) are then used to fit the GEV distribution with the L-moments method, and the model predicted partial duration series (PDS) series were retrieved from the derived GEV distribution at given annual exceedance probability (*AEP*).

$$Y_{pds}^{GCM_FUT} = F^{-1}((F(Y_{amp}^{GCM_{FUT}}|\theta_Y^{GCM_{FUT}}))|AEP) \quad \text{Equation 10}$$

In cases where there are discrepancies between different sub-daily durations (e.g., the 1-hour estimate is greater than the 2-hour estimate), Atlas 14 suggests maintaining consistency by increasing the estimate for the longer return interval. This proved problematic because the shorter sub-daily durations (often estimated from limited data at a station) are much less stable than the daily estimates (which typically have long runs of data), especially for high recurrence intervals. We revised the approach by enforcing consistency from the more stable daily estimates downwards to the shorter intervals. For example, if the 1-hour estimate was greater than the 2-hour estimate we reduced the 1-hour estimate rather than increasing the 2-hour estimate.

The final future 1 to 24-hour IDF ordinates are estimated by multiplying the Atlas 14 published values by the ratio of fitted GEV PDS results for climate-adjusted future conditions to the fitted GEV PDS results obtained for the Atlas 14 observed data:

$$IDF_{FUT} = IDF_{Atlas} * \frac{Y^{GCM_FUT}}{Y^{STN}} \quad \text{Equation 11}$$

This last step adjusts for the regional representation of higher L moments that is incorporated in the original Atlas 14 calculations but not explicitly documented for individual stations.

2.1.2 Peaks over Threshold Analysis for Sub-yearly Events

The IDF procedures described above are applicable to storm events with a return period of 1 year or greater and is most relevant to flood and channel stability analyses. For water quality, design of individual management practices for water quality treatment is most commonly based on more frequent events, such as the 90th percentile 24-hour rainfall event. The distribution of a sub-yearly event can be analyzed in a manner analogous to the AMP series for IDF. The primary difference is that the distribution of the 90th percentile event can be described by a Peaks-over-Threshold (POT) approach, which characterizes the frequency of events greater than a specified magnitude (Serinaldi and Kilsby, 2014). As the value of the threshold (u) increases, the distribution of the POT (prob $Y = (X\text{-}u)|X > u$) converges to a generalized Pareto distribution (GPD; Pickands, 1975; Balkema and de Haan, 1974):

$$H(y) = 1 - \left(1 + \xi\frac{y}{\tilde{\sigma}}\right)^{-1/\xi} \quad \text{Equation 12}$$

in which $\{y: y > 0 \text{ and } 1 + \xi\frac{y}{\tilde{\sigma}} > 0\}$ and $\tilde{\sigma} = \sigma + \xi(u - \mu)$, μ is the location parameter, $\sigma > 0$ is the scale parameter, and ξ is the shape parameter. An EQM updating procedure for the GPD, analogous to that described above for the GEV distribution using *H(y)* and its inverse, was developed to estimate the distribution of future 90th percentile events and map the changes implied in historic and future GCM runs onto historic data.

Unlike the AMP analysis, the POT analysis requires working with a complete series of daily precipitation depths, along with multiple iterations to determine the appropriate threshold for the analysis of events. Precipitation gauge series typically have missing or accumulated data, which complicate the automation of the analysis. As with the IDF analysis, we address this issue by using PRISM daily gridded precipitation estimates that are fit to observed records but filled to provide complete "observed" time series with bias correction (http://prism.oregonstate.edu).

An important issue for the POT analysis is determining the appropriated threshold for the GPD, which can have a significant influence on the analysis of precipitation records. A review by Langousis et al. (2016) found that methods of determining the threshold based on GPD asymptotic properties can lead to unrealistically high threshold and shape parameter estimates, while nonparametric methods found in the literature were generally unreliable. Much better results were obtained using the graphical Mean Residual Life Plot method (Davison and Smith, 1990). In this method, the proper threshold for the GPD analysis is obtained by plotting the mean of the excesses as a function of the threshold and identifying the lowest threshold above which the number of excesses increases linearly with the threshold value. While this method has generally been interpreted graphically, Langousis et al. (2016) provide a method for automating threshold detection from a continuous daily precipitation time series:

1. Estimate the mean value of the excesses $e(u) = E[X-u|X>u]$ above different thresholds $u_i = Xi,n$, i=1, 2, . . ., n-10, where $X_{i,n}$ denotes the ith (ascending) order statistic in a sample of size n.
2. For each u_i (i=1, 2, . . ., n - 20) in Step 1, apply weighted least squares to fit a linear model to all points ($uj, e(uj)$) that satisfy $j \geq i$. To account for the increase of the estimation variance of $e(u)$ with increasing threshold u, the weight w_j applied to each point ($u_j, e(u_j)$) is taken to be inversely proportional to the variance of $e(u)$, assuming independence of the excesses. In this case, $w_j = (n-j)/Var[X-u_j|X > u_j]$.
3. Determine the optimal threshold u^* as the lowest threshold u_i (i=1, 2, . . ., n-20) that corresponds to a local minimum of the weighted mean square error function of the linear regression,

Once the threshold (u) of historical daily rainfall extracted from PRISM dataset is detected by the automatic method. The same threshold is applied to daily rainfall series of historical and future predicted by GCMs. Truncated historical and modeled data($X>u$) will be used to predict the changes of 90th percentile rainfall magnitude with the EQM methods. To apply the EQM method, quantiles of modeled future daily rainfall series are matched to the distribution for historical daily rainfall series.

$$\boldsymbol{Y}_{daily}^{\boldsymbol{adj1}} = \boldsymbol{H}_{\boldsymbol{o-c}}^{\boldsymbol{-1}}\left(H_{\boldsymbol{m-p}}\left(\boldsymbol{x}_{\boldsymbol{m-p}}\right)\right) = H^{-1}((\boldsymbol{H}(\boldsymbol{X}_{daily}^{\boldsymbol{GCM_{FUT}}}|\boldsymbol{\theta}^{\boldsymbol{GCM_{FUT}}}))|\boldsymbol{\theta}^{PRSIM}), \quad \text{Equation 13}$$

where the vertical bar "|" indicates conditional dependence, i.e., $H(\boldsymbol{X}_{daily}^{GCM_{FUT}}|\boldsymbol{\theta}^{GCM_{FUT}})$ indicates the cumulative distribution function (GPD with threshold u for this case) of the future GCM truncated daily rainfall series calculated at the cumulative probability corresponding to $\boldsymbol{X}_{daily}^{GCM_{FUT}}$ using the parameter set $\boldsymbol{\theta}^{GCM_{FUT}}$ calculated for that future series. $\boldsymbol{\theta}^{PRISM}$ represents the GPD parameters from fit to the PRISM daily rainfall series. To account for the difference between the CDFs for the model outputs of future and current periods, a second adjustment factor is calculated:

$$\boldsymbol{Y}_{daily}^{\boldsymbol{adj2}} = H_{\boldsymbol{m-c}}^{\boldsymbol{-1}}\left(H_{\boldsymbol{m-p}}\left(\boldsymbol{x}_{\boldsymbol{m-p}}\right)\right) = H^{-1}((\boldsymbol{H}\left(\boldsymbol{X}_{daily}^{\boldsymbol{GCM}_{\boldsymbol{FUT}}}|\boldsymbol{\theta}^{\boldsymbol{GCM}_{\boldsymbol{FUT}}}\right))|\boldsymbol{\theta}^{\boldsymbol{GCM}}) \quad \text{Equation 14}$$

The projected AMP series is then calculated as:

$$\boldsymbol{Y}_{daily}^{\boldsymbol{PRISM_FUT}} = \boldsymbol{X}_{daily}^{\boldsymbol{GCM_FUT}} + \boldsymbol{Y}_{\boldsymbol{daily}}^{\boldsymbol{adj1}} - \boldsymbol{Y}_{\boldsymbol{daily}}^{\boldsymbol{adj2}} \quad \text{Equation 15}$$

Then the derived future daily rainfall series $\boldsymbol{Y}_{daily}^{\boldsymbol{PRISM_FUT}}$ can be fit to GPD distribution. Equation 16 was used to estimate an unconditional distribution and return value:

$$\boldsymbol{Prob}(\boldsymbol{Y} > \boldsymbol{y}) = \boldsymbol{Prob}(\boldsymbol{y} > \boldsymbol{u}) * (\boldsymbol{1} - \boldsymbol{H}(\boldsymbol{y} - \boldsymbol{u}; \boldsymbol{\sigma}, \boldsymbol{\xi})) \quad \text{Equation 16}$$

where $Prob(y > u)$ could be estimated using the ratio between length of rainfall records above threshold and the full rainfall records. After the probabilities and amounts of rainfall from unconditional distribution were derived using Equation5. The 90th percentile rainfall amount estimated by each GCM was calculated using linear interpolation:

$$\boldsymbol{Y}_{\boldsymbol{90}} = \frac{\boldsymbol{Prob}_{\boldsymbol{90}} - \boldsymbol{Prob}_{\boldsymbol{90-}}}{\boldsymbol{Prob}_{\boldsymbol{90+}} - \boldsymbol{Prob}_{\boldsymbol{90-}}} * (\boldsymbol{Y}_{\boldsymbol{90+}} - \boldsymbol{Y}_{\boldsymbol{90-}}) \quad \text{Equation 17}$$

where Y_{90+} and Y_{90-} are the observations closest above and below the 90th percentile in the rainfall series.

The POT analysis addresses 24-hr events only, so sub-daily analysis is not needed. We do the analysis using daily rainfall depths without constraint correction [adjustment for events that pass through the day boundary] as this is the method commonly used in practice to estimate water quality volumes.

We tested the method through preliminary applications to NOAA Atlas 14 station in Maryland. A major challenge was that the automated selection of the threshold followed by GPD fitting did not always work properly and sometimes yielded unreasonable results, especially when a very high threshold was selected. We found that this problem could be solved by providing initial guesses for the parameters of the GPD distribution that are in the reasonable range for what is obtained for stations with more stable distributions.

An example of applying the code is shown for Pocomoke City (station 18-7140). The threshold detection method (Figure 2-1) shows the algorithm successfully estimated the rainfall magnitude at the first local minimum of weighted mean square error (WMSE). Figure 2-2 is an example of 90th percentile rainfall predictions using all archived GCMs (both rcp45 and rcp85) for 2055 and 2085.

One interesting result of screening analyses across the full set of Maryland Atlas 14 stations is that the 90th percentile event may not be predicted to increase, even while a majority of scenarios predict an increase in total precipitation volume.

While total annual precipitation volume is expected to increase across the Eastern U.S. under future climate, it is also anticipated that an increasing proportion of annual precipitation will be concentrated in larger, more intense events (Kundzewicz et al., 2007; Groisman et al., 2012). Future climate may incorporate both more extreme flood events and longer drought periods, resulting in a situation in which the 2- to 500-year storm event magnitudes increase, but the 90th percentile events decrease. This may be good news in the sense that BMPs designed to treat water quality in typical storm events (e.g., about 10 times per year) may be adequately sized to address future climate, even though flood control responses to extreme large events may be inadequate.

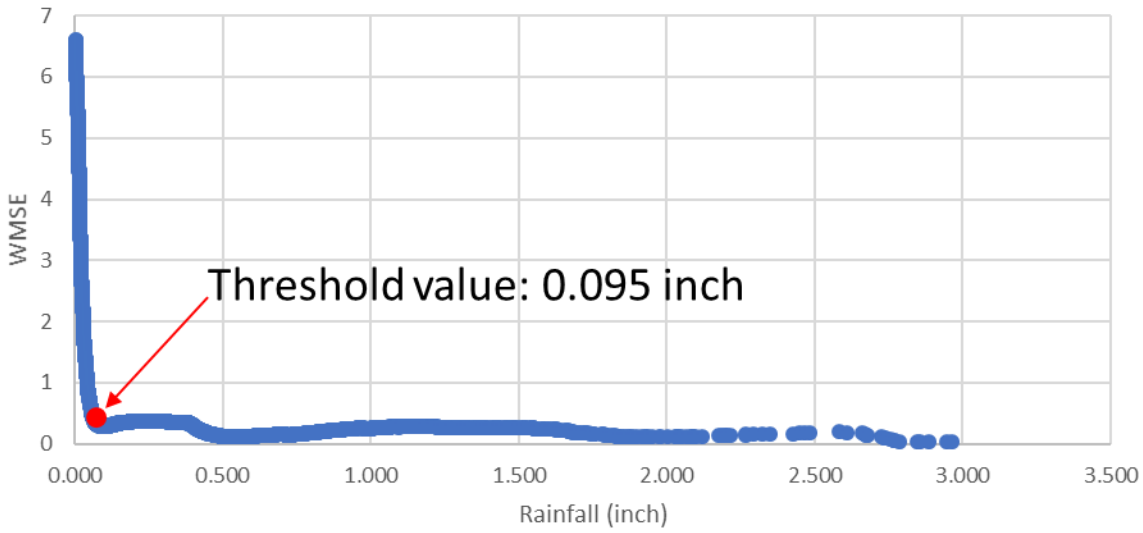


Figure 2-1. Threshold Value Detected by the Python Algorithm for Site 18-7140

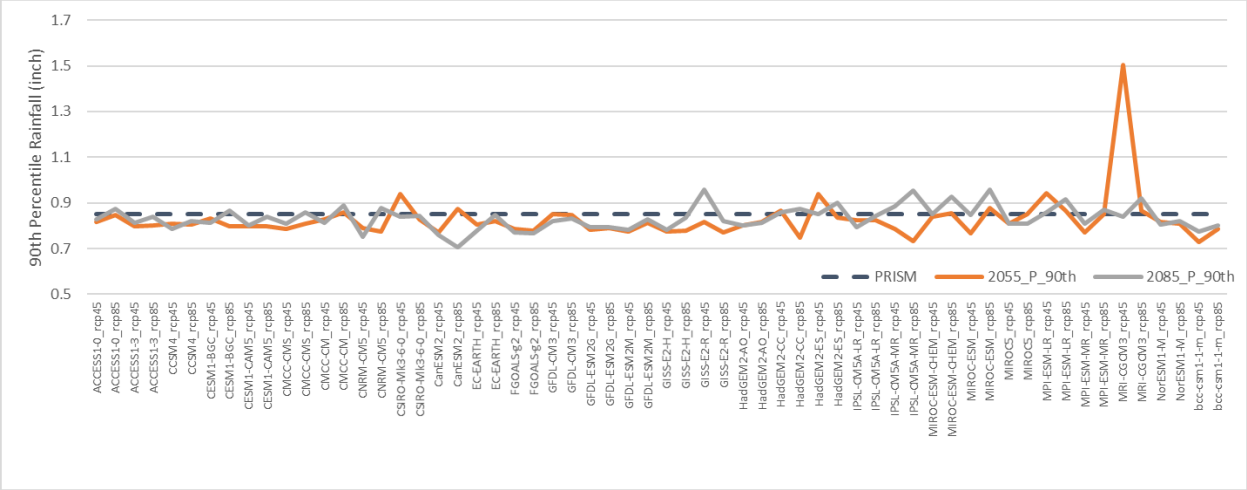


Figure 2-2. Future 90th-percentile Rainfall Event Predictions for Different GCMs at Site 18-7140

2.2 RUNOFF AND BMP SIMULATION WITH SWMM

Precipitation estimates are converted to runoff with EPA's Storm Water Management Model version 5 (SWMM5; Rossman, 2015). To evaluate potential runoff depth on a unit-area basis we route the future storms implied by the IDF curves through the SWMM model (version 5.1.013), packaged in a Python wrapper with GUI that controls input and output. The actual SWMM subbasin layout needed to accomplish this task is quite simple. We specify a single BMP catchment (<10 acres and thus not requiring time of concentration adjustments) for which the user can specify impervious and pervious acreage, roughness, depression storage, and soil/slope properties. The resulting runoff timeseries can

be analyzed directly or routed through a variety of gray and green stormwater BMPs, which are explicitly set up using SWMM input templates.

The IDF curve results are converted into design storm precipitation events for use by SWMM by applying the appropriate 24-hr rainfall distribution type identified for the Soil Conservation Service TR-55 method (SCS, 1986). Other, more sophisticated methods of rainfall disaggregation could be used, but we chose this older method because it is the approach of choice for many local stormwater design manuals.

The linkage between the IDF simulations and SWMM is summarized schematically in Figure 2-3. The IDF analysis portion of the tool appears on the right side. After identification of bounding climate scenarios (described in Section3.2), the program queries various data servers and retrieves historic and future climate model output for a user-identified location of interest, along with the AMP series for the NOAA Atlas 14 station closest to the user location.

All the components of the system are implemented in Python 3. The simulation code is provided in the Appendix.

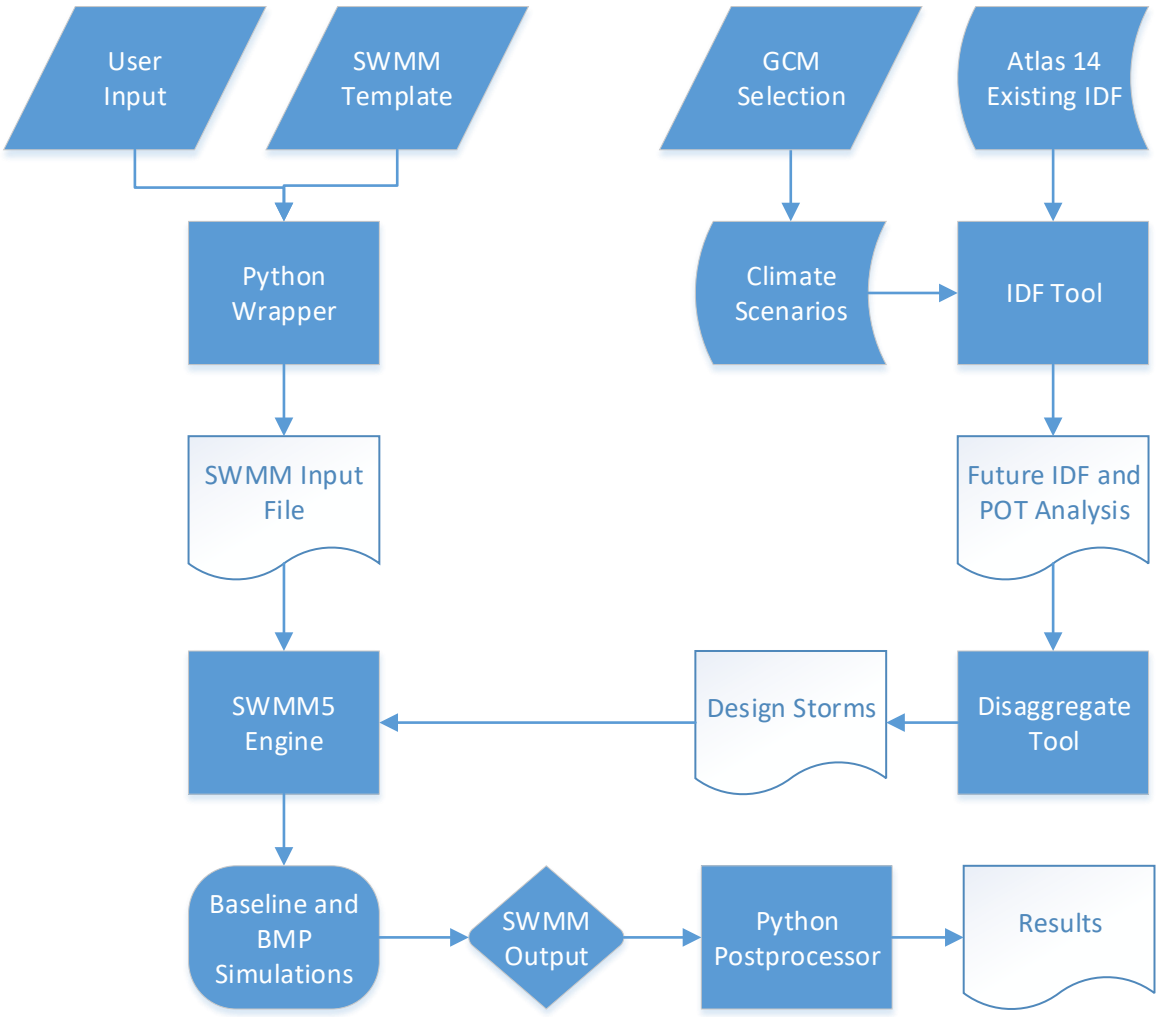


Figure 2-3. Schematic of IDF Analysis Tool

For the project we built BMP templates to address a stormwater extended wet detention basin (representative of a “gray” engineered storage-based management component), and a planted

bioretention cell (representative of a “green” stormwater infrastructure component that relies on infiltration and evapotranspiration of stormwater). The next two subsections outline the specifications for representation of these BMPs:

2.2.1 Bioretention

The generic specification for bioretention includes a 9-inch surface ponding depth, 24 inches of growing media, and 12 inches of stone drainage layer. The system is assumed to have an underdrain (4-inch pipe in the middle of drainage layer that controls outflow. The growing media consists of 25% compost and 75% sandy soil with a porosity of 0.529 (Fassman-Beck et al., 2015). The drainage layer has a void ratio of 0.54 and a drainage coefficient of 0.18 fir a drain height of 41 inches and drain time of 72 hours.

Storage volume includes the ponding depth and the storage in the media (taking porosity into account). The depth of storage is thus 0.75 ft ponding + 2 ft media x 0.529 porosity = 1.808 ft.

Maryland uses pre-calculated estimates of WQv and specifies two “rainfall zones” – a western zone and eastern zone that use a 0.9 in storm and 1.0 in storm respectively for the WQv calculation. As a result, the assumed bioretention footprint for a given percent impervious area varies by rainfall zone. This was incorporated by assigning each of the 79 Atlas 14 weather station locations to its corresponding rainfall zone, and the bioretention footprints were adjusted accordingly.

In addition, we follow Maryland guidance relative to the following:

- Footprint relative to the design treatment volume
- Ponding depth, media depth, and underdrain stone storage layer depth
- Media composition, which influences porosity, infiltration rate, and hydrologic performance
- Underdrain offset from the bottom of the stone storage layer
- Drain time from a completely full state

2.2.2 Extended Wet Detention Basin

The Maryland design for wet ponds assumes that untreated runoff will flow into the pond and displace “clean” water from the previous storm which has been stored long enough to allow settling and some nutrient uptake to take place. The untreated runoff enters the pond at one end, and the treated water exits the other end with minimal mixing of the two (an assumption often referred to as “plug flow”). While the validity of the plug flow assumption is open to debate, the concept is incorporated into numerous pond design specifications throughout the U. S. Maryland requires that the permanent pool volume is at least as large as the treatment volume. In addition to having a WQv requirement, Maryland also specifies a recharge volume requirement (REv), a relatively smaller fraction of the WQv that must be infiltrated onsite. Since wet ponds cannot be used to address the REv, we assume the REv has been addressed on the site upstream of the wet pond. As a result, the wet pond pool volume is assumed to be the difference between the WQv and the REv. We then increased the pool volume by 10%, in part to be conservative and also because we did not include any recharge BMPs in the simulation upstream of the wet ponds.

Our wet pond representation incorporates design guidance for side slopes, including within the pool, safety and aquatic benches, and the storage basin. An average slope of 34% (run/rise 2.9) was used to simplify volume calculations. We used pyramid sections to develop the stage-area curves used by SWMM for the dynamic stage-volume-discharge simulation.

Maryland also specifies a Channel Protection Volume (CPv), which is specified as extended detention of the 1-yr 24-hr storm event. Maryland defines extended detention as 12 hours or 24 hours depending on the Water Use classification of the receiving water. The stormwater manual provides a specific method for calculating the CPv, the allowable peak discharge for the CPv, and the orifice diameter for the allowable peak discharge. We incorporated all elements of the specifications for each of the 79 Atlas 14 locations, including WQv Rainfall Zone, Water Use classification, and 1-yr 24-hr storm depth (provided in the manual by county). The wet pond design also incorporates an emergency spillway to safety pass the peak flow from the 100-yr 24-hr storm event without overtopping the storage basin.

2.2.3 BMP Sizing with Maryland Environmental Site Design

Implicit assumptions about climate are built into guidance and regulations for both systems of BMPs and the design of individual BMP types. Maryland Department of the Environment's (MDE) 2000 Stormwater Design Manual presented calculations for a Water Quality volume (WQv) and a channel protection volume (CPv) for the design of stormwater BMPs. With the 2009 revisions to the Design Manual, MDE moved to the more holistic approach of Environmental Site Design (ESD), which combines the WQv and CPv objectives to produce a unified approach to stormwater design and management based on the net effects of all stormwater controls present on a site (MDE, 2009, Chapter 5).

The general concept of ESD is to control runoff from a developed site in response to the 1-year 24-hour storm so that it is no greater than the runoff that would be expected for the same site with a cover of undeveloped woods in good condition, considering the distribution of hydrologic soil groups on the site. ESD does not require detailed simulation modeling of developed and undeveloped conditions. Rather, it provides a simplified approach based on the relative change in Curve Number used in the National Resources Conservation Service TR-55 method (NRCS, 1986). The difference in responses to the 1-yr 24-hr event determines the excess runoff that needs to be treated (Q_E). In units of depth, $Q_E = P_E \times R_V$. R_V is the surface runoff fraction, defined as $R_V = 0.005 + 0.009 \times I$, where I is the impervious fraction expressed as a percentage. P_E is then the excess rainfall amount that needs to be treated. Rather than calculating P_E, simple lookup tables are provided (one for each of the four hydrologic soil groups, A, B, C, and D). P_E is listed in the table in increments of 0.2 inches and imperviousness in increments of 5% and incorporates a single assumption about the 1-yr 24-hr storm across all of Maryland, so the answer is not exact, but is sufficient to achieve the desired level of control on average, especially when weighted across multiple subareas of a site with differing soil and development characteristics.

The approach of controlling site runoff to levels expected for woods in good condition is in theory climate agnostic because both developed and woods runoff will change if climate changes. However, the table that is used to determine P_E is rooted in specific assumptions about the magnitude of the 1-yr 24-hr storm event that may not hold under future climate conditions.

We investigated this issue by examining the changes in precipitation and the resulting difference in runoff between developed and good condition woods, as predicted by TR-55, under future climate scenarios for the 79 NOAA Atlas 14 stations for which we have developed estimates of the future 1-yr 24-hr event.

The TR-55 method (NRCS, 1986) predicts runoff (Q, inches) via the curve number equation as

$$Q = \frac{(P - 0.2\,S)^2}{P + 0.8\,S}$$

where P is the 24-hr precipitation depth (inches) and S = 1000/CN – 10, where CN is the Curve Number. CN assumptions for ESD are shown in Table 2-1. CNs for developed land were calculated as a weighted mixture of the CN for connected impervious area (98) and that for open space in good condition.

Table 2-1. Curve Numbers for Environmental Site Design Simulations (MDE, 2009)

Land Use	Hydrologic Soil Group			
	A	B	C	D
Woods, good condition	38	55	70	77
Developed, 25% Impervious	54	70	80	85
Developed, 50% Impervious	69	80	86	89
Developed, 80% Impervious	86	91	93	94

The runoff predicted by the CN method as well as the difference between runoff for developed land and good condition woods for a given hydrologic soil group and impervious percentage is an exact second-order polynomial function of P (Figure 2-4). This allows direct calculation of the implications of both spatial variability and magnitude change in the 1-yr 24-hr event.

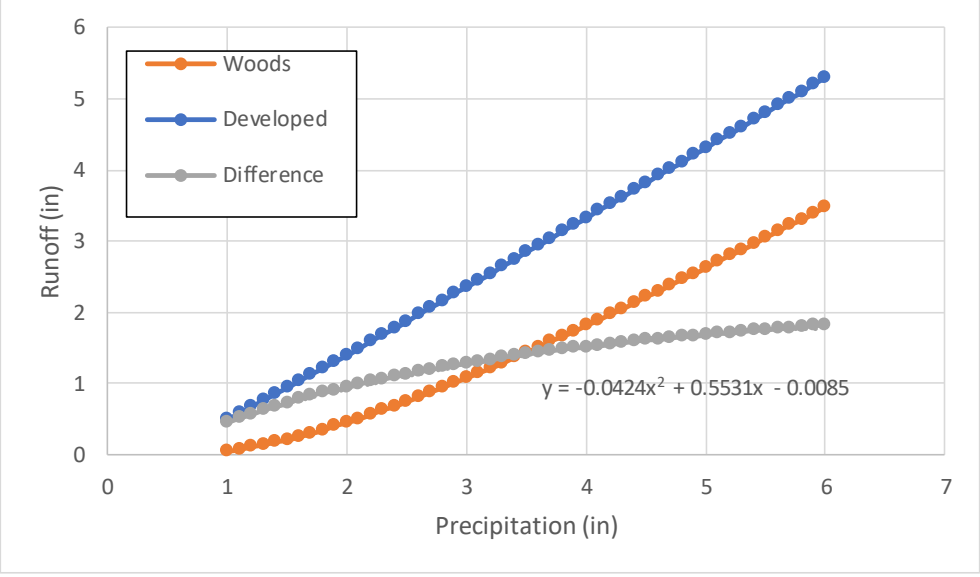


Figure 2-4. Curve Number Prediction of Runoff as a Function of Precipitation for Hydrologic Group D Soils, Developed Land at 80% Imperviousness

Note: Polynomial equation represents the difference between runoff from developed land and runoff from woods in good condition.

3.0 DATA

3.1 NOAA IDF CURVE STATIONS IN MARYLAND

Potential precipitation IDF curves are developed for potential mid-century (ca. 2055) and late-century (ca. 2085) climate scenarios at all 79 Atlas 14 sites within the state of Maryland (Figure 3-1 and Table 3-1). In addition to the IDF results, we retrieved the AMS series from the NOAA ftp server.

For stations without hourly data, we developed a lookup that identifies the nearest hourly station, which is used as a surrogate for sub daily precipitation at the station of interest. (Note that the nearest station can be in an adjoining state.) The results at the surrogate station are then scaled by the average ratio of the daily total at the station of interest to the total at the surrogate station.

This scaling approach is conceptually similar to that used in Atlas 14 vol, 2, v. 3.0 (Bonnin et al., 2006) to correct for potential discrepancies between daily totals and the sum of hourly precipitation amounts within a day. In Atlas 14, the 1-hour through 12-hour duration data are already adjusted by the ratio between the daily and sum of hourly totals. As the last step of our process applies the estimated change ratio between historic and future conditions this ratio adjustment procedure does not need to be reapplied here.

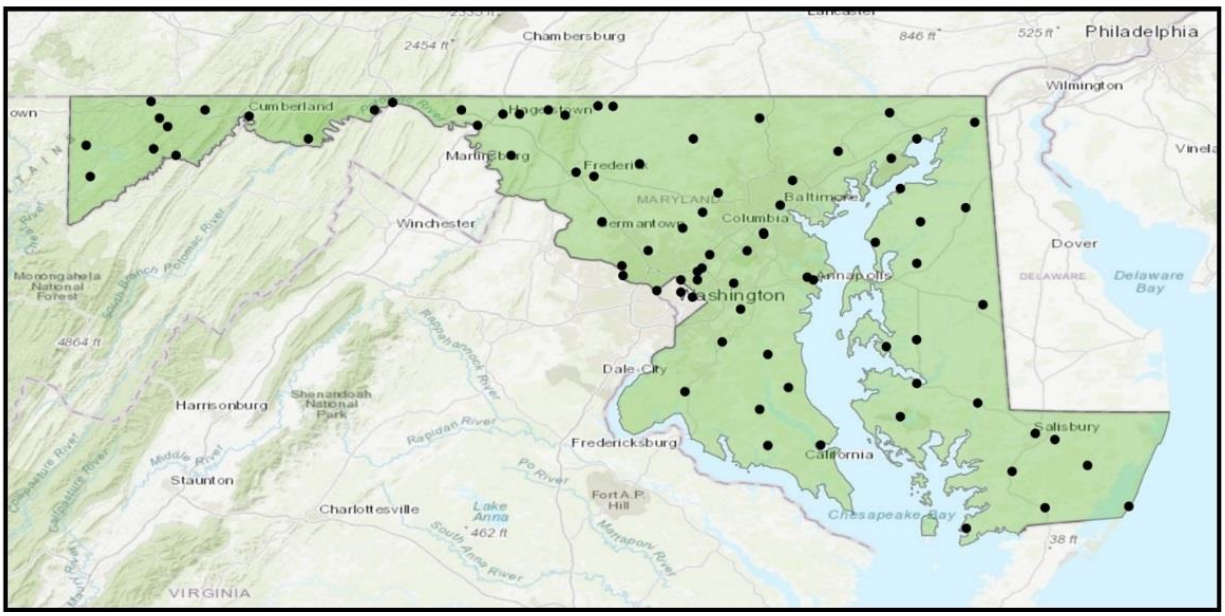


Figure 3-1. NOAA Atlas 14 Sites in Maryland and the District of Columbia

Table 3-1. Key to NOAA Atlas 14 Sites

18-0185	ANNAPOLIS US NAVAL ACA, MD
18-0193	ANNAPOLIS POLICE BRKS, MD
18-0335	ASSATEAGUE IS NATL SEA, MD
18-0465	BALTIMORE WSO ARPT, MD
18-0470	BALTIMORE WSO CITY, MD
18-0700	BELTSVILLE, MD
18-0705	BELTSVILLE PLANT STN 5, MD
18-0732	BENSON POLICE BARRACKS, MD
18-0915	BLACKWATER REFUGE, MD
18-1032	BOYDS 2 NW, MD
18-1125	BRIGHTON DAM, MD
18-1385	CAMBRIDGE WATER TRMT P, MD
18-1530	CATOCTIN MOUNTAIN PARK, MD
18-1627	CENTREVILLE, MD
18-1710	CHELTENHAM 1 NW, MD
18-1750	CHESTERTOWN, MD
18-1790	CHEWSVILLE-BRIDGEPOR, MD
18-1862	CLARKSVILLE 3 NNE, MD
18-1890	CLEAR SPRING 1 ENE, MD
18-1980	COLEMAN 3 WNW, MD
18-1995	COLLEGE PARK, MD
18-2060	CONOWINGO DAM, MD
18-2215	CRISFIELD SOMERS COVE, MD
18-2282	CUMBERLAND 2, MD
18-2325	DALECARLIA RESVR DC, MD
18-2523	DENTON 2 E, MD
18-2700	EASTON POLICE BARRACKS, MD
18-2770	EDGEMONT, MD
18-2860	ELKTON, MD
18-2905	EMMITSBURG, MD
18-2906	EMMITSBURG 2 SE, MD
18-3230	FORT GEORGE G MEADE, MD
18-3348	FREDERICK POLICE BRKS, MD
18-3355	FREDERICK 3 E, MD
18-3415	FROSTBURG 2, MD
18-3675	GLENN DALE BELL STN, MD
18-3795	GRANTSVILLE, MD
18-3855	GREAT FALLS, MD
18-3975	HAGERSTOWN, MD
18-4030	HANCOCK, MD
18-4780	KEEDYSVILLE, MD
18-5080	LA PLATA 1 W, MD
18-5111	LAUREL 3 W, MD
18-5201	LEONARDTOWN 3 NW, MD
18-5865	MECHANICSVILLE 5 NE, MD
18-5894	MERRILL, MD
18-5985	MILLINGTON 1 SE, MD
18-6350	NATIONAL ARBORETUM DC, MD
18-6408	NEW GERMANY, MD
18-6620	OAKLAND 1 SE, MD
18-6770	OWINGS FERRY LANDING, MD
18-6844	PARKTON 2 SW, MD
18-6980	PERRY POINT, MD
18-7010	PICARDY, MD
18-7140	POCOMOKE CITY, MD
18-7272	POTOMAC FILTER PLANT, MD
18-7325	PRINCE FREDERICK 1 N, MD
18-7330	PRINCESS ANNE, MD
18-7700	ROCK HALL, MD
18-7705	ROCKVILLE 1 NE, MD
18-7806	ROYAL OAK 2 SSW, MD
18-8000	SALISBURY, MD
18-8005	SALISBURY FAA ARPT, MD
18-8065	SAVAGE RIVER DAM, MD
18-8315	SINES DEEP CREEK, MD
18-8380	SNOW HILL 4 N, MD
18-8405	SOLOMONS, MD
18-8720	TAKOMA PARK BALT AVE, MD
18-8855	TONOLOWAY, MD
18-8877	TOWSON, MD
18-9030	UNIONVILLE, MD
18-9035	U S SOLDIERS HOME DC, MD
18-9070	UPPER MARLBORO 3 NNW, MD
18-9140	VIENNA, MD
18-9409	WESTERNPORT UPRC, MD
18-9440	WESTMINSTER POLICE BRK, MD
18-9570	WILLIAMSPORT, MD
18-9750	WOODSTOCK, MD

3.2 CLIMATE MODEL SELECTION

Archives of statistically downscaled climate model output from the 5th round Coupled Model Intercomparison Project (CMIP5) include output from 32 or more Global Climate Models/General Circulation Models (GCMs) for two or more Representative Concentration Pathways (RCPs) of greenhouse gas accumulation. While it is possible to estimate IDF curves and 90th percentile precipitation estimates from all GCMs, it is often more useful to identify a smaller set of GCMs that bound the most likely range of predicted future conditions. Future climate projections are uncertain and are best used to describe a probability envelope of potential future conditions (an "ensemble of opportunity") to which adaptation may be needed. Specifically, climate scenarios that approximate smaller, median, and larger range of potential changes in precipitation intensity are useful to frame the problem.

Different GCM runs provide differing predictions of future temperature and precipitation. Temperature is expected to increase under RCP 8.5 versus RCP 4.5 in most locations, but precipitation may increase or decrease. A typical LASSO biplot of average annual changes in precipitation and temperature from statistically downscaled GCM runs is shown for Durham, NC in Figure 3-2.

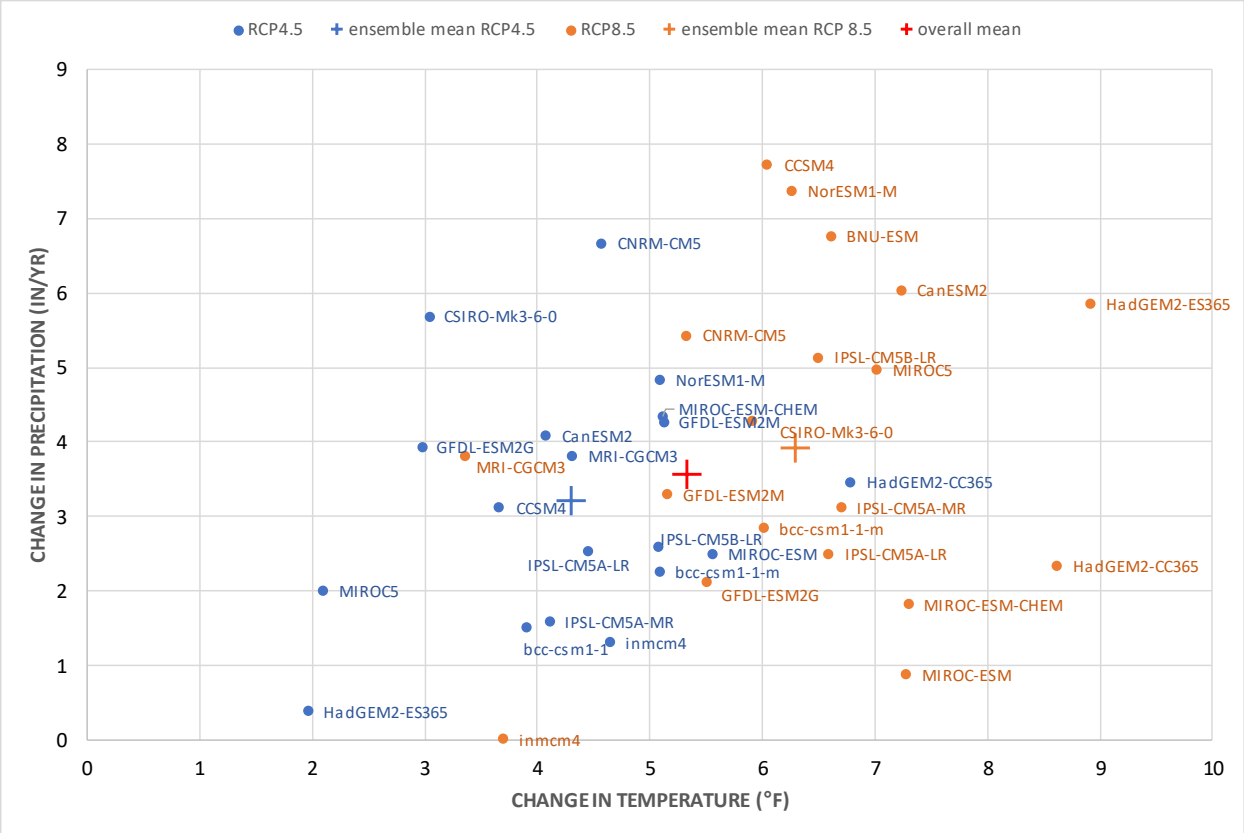


Figure 3-2. Example Biplot of Forecast Changes in Average Annual Precipitation and Air Temperature for Durham North Carolina for 2050 - 2080 vs. 1950 – 2005

Multiple GCM runs are available from the CMIP5 experiments (approximately 32 GCMs applied to two or more Representative Concentration Pathway (RCP) greenhouse gas scenarios). We selected downscaled GCMs from the RCP 4.5 and RCP 8.5 experiments that approximate the 10th percentile of the distribution of predicted change in future rainfall volume, the 90th percentile, and the model ensemble

median from each of the two RCPs. This approach helps to approximate the potential risk envelope of future conditions (which are inherently unknowable as they depend on human mitigation actions in the interim and are also subject to considerable model uncertainty) while rejecting the most extreme outliers among the population of models. We do not advocate selecting individual GCMs based on their skill in predicting historic climate for a given area because past performance is not a reliable guide to future prediction under a changing climate (Dixon et al., 2016).

Because the focus of the work described here is on storm events (whether moderate or extreme), selection of central and bounding GCM scenarios can be based on the precipitation axis only. For example, we can select GCM runs from the joint distribution of RCP 4.5 and RCP 8.5 CMIP5 simulations near the 10th, 50th, and 90th percentiles of the distribution of projected precipitation volume. The analysis uses the 10th and 90th percentiles, rather than the most extreme outliers, as it is well recognized that some individual GCMs may provide unrealistic results for a given area. It is therefore standard practice to ignore the most extreme outliers and use a model at approximately the 90th percentile of the distribution of a characteristic of interest from the complete set of models as a reasonable upper bound. Use of such an upper percentile is generally considered appropriate for engineering/hydrologic design planning purposes.

Philip Morefield of U.S. EPA developed Python code for screening climate scenarios as part of the "Locating and Selecting Scenarios Online" (LASSO) tool that scans the downscaled GCM output archive monthly data to identify annual and seasonal changes in precipitation volume (lasso.epa.gov). We adapted code from the LASSO tool to do initial screening for our project on precipitation. However, there are numerous ways to do this. For instance, one could select based on total annual precipitation volume or volume in seasons most likely to be associated with floods. Total annual precipitation volume appears to be a sufficient criterion for extreme event IDF analysis but may not be sufficient for analysis of the 90th percentile event. In some cases, GCMs predict that total precipitation volume increase will be largely confined to the largest events, with longer intervening drought periods, so an increase in total precipitation volume does not necessarily translate to an increase in the 90th percentile event. Therefore, we ranked scenarios separately relative to the 90th percentile event using the following approach:

1. Calculate the sum of rain events that are greater than or equal to the 90th percentile historical rainfall event for each site for each scenario (historical and future).
2. Convert to the large rain event (>=90th percentile) depth per day
3. Calculate the relative change rate of the large rain depth per day (rpd): (rpd_gcm-rpd_hist)/rpd_hist
4. Rank the relative changes from all GCMs and get the 10th, RCP4.5 median, RCP85 median, and 90th GCMs by value.

This simplified screening procedure does not guarantee that the selected scenarios will always approximate the 10th to 90th percentile range, which would require an analysis of all GCMs. It does, however, help to ensure that a selection of GCMs with relatively different precipitation predictions will be chosen for more detailed analysis.

Evaluation of downscaled GCM output from the LOCA archive for each MD/DC Atlas 14 station location yields selections for IDF analysis based on relative change in annual precipitation volume. Table 3-2 shows the 60 LOCA-downscaled GCM and RCP combinations that are evaluated in subsequent tables. Table 3-3 then shows the selected scenarios for evaluation of mid-century conditions, while Table 3-4 shows results for late-century conditions.

The method selects a wide number of different GCM scenarios but does contain some patterns. For the 90th percentile event, the low-end (10th percentile of increases) is associated with the lower greenhouse gas forcing or cooler scenario (RCP 4.5) 70 percent of the time, while the high-end (90th percentile) is

associated with the higher greenhouse gas forcing or warmer scenario (RCP 8.5) 75 percent of the time for mid-century conditions in Maryland. For late-century conditions, the results are 80 and 53 percent, respectively. The reduction in the correlation of the wetter scenarios with warmer conditions may result competing effects of the greater moisture-holding capacity of warmer air versus an increase in the likelihood of drought.

Systematic differences among GCMs across Maryland are also evident. For instance, for the mid-century conditions, the 90th percentile is represented in 13 out of 60 cases by the MIROC-rcp8.5 scenario, while the 10th percentile is represented in 10 out of 60 cases by the MIROC-ESM_rcp4.5, with no overlap between the summary statistics for the two GCMs.

Table 3-2. Key to CMIP5 GCM Scenarios in the LOCA Downscaled Climate Data Archive

1	ACCESS1-0_rcp45	21	CSIRO-Mk3-6-0_rcp45	41	HadGEM2-ES_rcp45
2	ACCESS1-0_rcp85	22	CSIRO-Mk3-6-0_rcp85	42	HadGEM2-ES_rcp85
3	ACCESS1-3_rcp45	23	EC-EARTH_rcp45	43	IPSL-CM5A-LR_rcp45
4	ACCESS1-3_rcp85	24	EC-EARTH_rcp85	44	IPSL-CM5A-LR_rcp85
5	bcc-csm1-1-m_rcp45	25	FGOALS-g2_rcp45	45	IPSL-CM5A-MR_rcp45
6	bcc-csm1-1-m_rcp85	26	FGOALS-g2_rcp85	46	IPSL-CM5A-MR_rcp85
7	CanESM2_rcp45	27	GFDL-CM3_rcp45	47	MIROC5_rcp45
8	CanESM2_rcp85	28	GFDL-CM3_rcp85	48	MIROC5_rcp85
9	CCSM4_rcp45	29	GFDL-ESM2G_rcp45	49	MIROC-ESM_rcp45
10	CCSM4_rcp85	30	GFDL-ESM2G_rcp85	50	MIROC-ESM_rcp85
11	CESM1-BGC_rcp45	31	GFDL-ESM2M_rcp45	51	MIROC-ESM-CHEM_rcp45
12	CESM1-BGC_rcp85	32	GFDL-ESM2M_rcp85	52	MIROC-ESM-CHEM_rcp85
13	CESM1-CAM5_rcp45	33	GISS-E2-H_rcp45	53	MPI-ESM-LR_rcp45
14	CESM1-CAM5_rcp85	34	GISS-E2-H_rcp85	54	MPI-ESM-LR_rcp85
15	CMCC-CM_rcp45	35	GISS-E2-R_rcp45	55	MPI-ESM-MR_rcp45
16	CMCC-CM_rcp85	36	GISS-E2-R_rcp85	56	MPI-ESM-MR_rcp85
17	CMCC-CMS_rcp45	37	HadGEM2-AO_rcp45	57	MRI-CGCM3_rcp45
18	CMCC-CMS_rcp85	38	HadGEM2-AO_rcp85	58	MRI-CGCM3_rcp85
19	CNRM-CM5_rcp45	39	HadGEM2-CC_rcp45	59	NorESM1-M_rcp45
20	CNRM-CM5_rcp85	40	HadGEM2-CC_rcp85	60	NorESM1-M_rcp85

Table 3-3. Bounding Scenarios for Analysis of Changes in Precipitation Volume, ca. 2056

Site	10th Percentile	RCP4.5 Median	RCP8.5 Median	90th percentile
18-0015	50	5	30	60
18-0185	49	3	14	52
18-0193	17	3	14	32
18-0335	15	3	2	34
18-0465	49	23	4	32
18-0470	43	41	4	19
18-0700	40	23	16	11
18-0705	49	39	16	11
18-0732	44	23	14	34
18-0915	45	13	4	48
18-1032	37	1	20	9
18-1125	57	51	20	9
18-1385	17	13	30	60
18-1530	29	59	36	12
18-1627	40	3	38	48
18-1710	57	39	16	60
18-1750	58	23	4	10
18-1790	35	53	22	18
18-1862	57	55	22	11
18-1890	44	1	8	11
18-1980	17	13	38	56
18-1995	57	41	24	11
18-2060	58	7	30	20
18-2215	49	19	2	11
18-2282	29	7	58	48
18-2325	43	39	24	60
18-2523	49	39	46	56
18-2700	50	33	6	32
18-2770	29	3	20	12
18-2860	49	51	16	6

Site	10th Percentile	RCP4.5 Median	RCP8.5 Median	90th percentile
18-2905	50	25	20	48
18-2906	50	25	4	48
18-3230	40	23	20	60
18-3348	35	1	36	9
18-3355	35	1	16	18
18-3415	45	7	8	14
18-3675	44	1	24	48
18-3795	43	51	36	34
18-3855	40	3	16	47
18-3975	35	7	22	48
18-4030	37	39	8	52
18-4780	29	1	8	48
18-5080	17	19	4	60
18-5111	54	15	56	60
18-5201	45	3	4	48
18-5865	44	39	8	32
18-5894	29	15	12	34
18-5985	40	13	30	56
18-6350	57	3	18	10
18-6408	2	3	8	14
18-6620	37	11	12	47
18-6770	57	7	24	48
18-6844	58	15	2	48
18-6980	29	1	22	60
18-7010	45	25	58	32
18-7140	17	31	30	21
18-7272	40	53	24	6
18-7325	44	55	4	9
18-7330	38	3	12	36
18-7700	17	23	2	56
18-7705	57	35	8	11

Site	10th Percentile	RCP4.5 Median	RCP8.5 Median	90th percentile
18-7806	57	15	46	22
18-8000	20	29	36	41
18-8005	38	7	2	34
18-8065	17	3	36	18
18-8315	37	39	12	34
18-8380	49	39	2	34
18-8405	45	25	6	48
18-8720	17	39	24	10
18-8855	37	51	58	60
18-8877	49	1	24	6
18-9030	49	13	22	32
18-9035	17	33	20	10
18-9070	37	3	18	21
18-9140	45	7	46	11
18-9409	1	3	8	32
18-9440	49	41	8	48
18-9570	44	7	10	11
18-9750	57	1	16	9

See Table 3-1 for site indices; Table 3-2 for identification of GCM scenarios.

Table 3-4. Bounding Scenarios for Analysis of Changes in Precipitation Volume, ca. 2085

Site	10th Percentile	RCP4.5 Median	RCP8.5 Median	90th percentile
18-0015	5	29	16	60
18-0185	43	15	52	22
18-0193	43	15	24	22
18-0335	16	33	6	58
18-0465	17	31	48	34
18-0470	49	33	58	18
18-0700	41	7	6	60
18-0705	5	29	6	60
18-0732	41	1	6	34
18-0915	41	55	46	11
18-1032	41	23	40	11
18-1125	37	1	32	11
18-1385	37	23	40	21
18-1530	44	1	16	11
18-1627	37	55	24	22
18-1710	41	3	24	60
18-1750	57	15	42	34
18-1790	17	1	32	11
18-1862	41	19	16	11
18-1890	41	53	10	21
18-1980	44	53	48	56
18-1995	5	15	6	11
18-2060	49	53	6	11
18-2215	25	1	60	24
18-2282	44	7	6	27
18-2325	43	1	36	11
18-2523	17	53	36	22
18-2700	5	3	36	21
18-2770	5	1	6	34
18-2860	37	15	20	40

Site	10th Percentile	RCP4.5 Median	RCP8.5 Median	90th percentile
18-2905	25	55	32	11
18-2906	17	1	40	11
18-3230	44	59	32	60
18-3348	5	59	32	21
18-3355	2	15	16	56
18-3415	38	35	10	33
18-3675	44	33	6	22
18-3795	43	7	6	21
18-3855	43	15	24	34
18-3975	39	9	32	11
18-4030	57	9	16	33
18-4780	41	53	8	21
18-5080	43	15	18	10
18-5111	41	1	36	56
18-5201	44	3	40	11
18-5865	44	3	48	10
18-5894	43	57	16	4
18-5985	37	23	32	34
18-6350	5	7	18	11
18-6408	43	19	8	21
18-6620	5	19	8	56
18-6770	41	31	24	27
18-6844	37	39	14	11
18-6980	44	29	16	60
18-7010	44	19	8	21
18-7140	19	59	42	11
18-7272	5	49	6	11
18-7325	41	7	40	11
18-7330	17	23	36	4
18-7700	43	31	48	54
18-7705	44	3	32	10

Site	10th Percentile	RCP4.5 Median	RCP8.5 Median	90th percentile
18-7806	5	9	24	56
18-8000	25	55	6	14
18-8005	5	57	10	4
18-8065	25	7	10	33
18-8315	39	19	14	6
18-8380	8	31	6	47
18-8405	44	23	24	22
18-8720	57	1	32	11
18-8855	43	9	8	34
18-8877	44	53	36	34
18-9030	5	13	52	22
18-9035	57	15	52	11
18-9070	43	29	6	56
18-9140	41	31	36	54
18-9409	43	7	10	4
18-9440	41	19	20	11
18-9570	41	55	32	21
18-9750	49	13	16	21

See Table 3-1 for site indices; Table 3-2 for identification of GCM scenarios.

GCM scenarios for the analysis of changes in the 90th percentile 24-hour precipitation event were screened on the basis of percentage of events greater than the historic 90th percentile event. The selected bounding scenarios are summarized in Table 3-5 (for ca. 2055 conditions based on 2040-2069 GCM output) and in Table 3-6 (for ca. 2085 conditions based on 2070-2099 GCM output). Identities of the GCM scenarios are shown in Table 3-2.

For the 90th percentile event, the low-end (10th percentile of increases) is associated with the lower greenhouse gas forcing scenario (RCP 4.5) 71 percent of the time, while the high-end (90th percentile) is associated with the higher greenhouse gas forcing scenario (RCP 8.5) 68 percent of the time for ca. 2056 conditions across Maryland. For ca. 2085 predictions, the results are 82 and 94 percent, respectively.

Table 3-5. Bounding Scenarios for Analysis of the 90th Percentile 24-hour Precipitation Event, ca. 2056

Site	10th Percentile	RCP4.5 Median	RCP8.5 Median	90th percentile
18-0015	49	35	4	48
18-0185	14	9	28	15
18-0193	29	9	12	15
18-0335	45	21	32	56
18-0465	29	55	40	52
18-0470	14	23	10	48
18-0700	33	19	56	22
18-0705	33	55	10	16
18-0732	13	59	20	38
18-0915	9	31	24	22
18-1032	59	41	12	36
18-1125	26	5	20	38
18-1385	6	7	10	39
18-1530	8	31	18	56
18-1627	17	1	30	34
18-1710	7	3	46	21
18-1750	29	7	6	39
18-1790	13	7	32	21
18-1862	50	19	2	21
18-1890	8	19	32	11
18-1980	45	9	18	40
18-1995	26	51	18	48
18-2060	55	33	30	19
18-2215	60	15	34	54
18-2282	29	13	14	48
18-2325	45	1	20	22
18-2523	45	31	46	48
18-2700	59	7	38	22
18-2770	45	13	20	38
18-2860	17	51	4	22

Site	10th Percentile	RCP4.5 Median	RCP8.5 Median	90th percentile
18-2905	49	25	48	28
18-2906	49	25	46	18
18-3230	29	59	4	56
18-3348	57	29	22	40
18-3355	26	59	10	21
18-3415	57	19	10	21
18-3675	7	53	2	10
18-3795	29	45	12	52
18-3855	35	3	2	47
18-3975	57	41	10	28
18-4030	23	39	2	56
18-4780	23	41	2	40
18-5080	7	9	28	56
18-5111	49	19	2	21
18-5201	17	29	24	39
18-5865	14	25	18	38
18-5894	17	3	10	27
18-5985	50	1	32	46
18-6350	26	1	4	15
18-6408	8	45	10	60
18-6620	50	37	4	27
18-6770	33	55	46	39
18-6844	33	5	18	27
18-6980	7	43	18	40
18-7010	26	41	14	27
18-7140	19	59	32	54
18-7272	14	57	2	38
18-7325	43	37	18	22
18-7330	9	1	52	56
18-7700	29	3	6	39
18-7705	44	59	24	36

Site	10th Percentile	RCP4.5 Median	RCP8.5 Median	90th percentile
18-7806	49	9	30	21
18-8000	45	17	8	28
18-8005	29	17	24	56
18-8065	43	37	22	18
18-8315	51	39	36	60
18-8380	19	3	4	34
18-8405	57	1	10	36
18-8720	50	55	18	15
18-8855	45	33	2	36
18-8877	33	3	4	36
18-9030	59	9	12	21
18-9035	33	1	46	22
18-9070	54	37	44	38
18-9140	17	51	28	21
18-9409	5	23	40	32
18-9440	50	43	48	28
18-9570	26	41	18	40
18-9750	8	51	48	56

See Table 3-1 for site indices; Table 3-2 for identification of GCM scenarios.

Table 3-6. Bounding Scenarios for Analysis of the 90th Percentile 24-hour Precipitation Event, ca. 2085

Site	10th Percentile	RCP4.5 Median	RCP8.5 Median	90th percentile
18-0015	17	33	52	16
18-0185	17	55	2	42
18-0193	19	33	2	56
18-0335	9	13	32	12
18-0465	57	47	24	12
18-0470	14	19	52	36
18-0700	13	23	60	58
18-0705	17	23	36	12
18-0732	17	53	52	16
18-0915	5	33	52	42
18-1032	43	19	2	15
18-1125	57	31	36	18
18-1385	5	33	2	54
18-1530	19	23	10	48
18-1627	5	11	36	12
18-1710	19	55	18	54
18-1750	5	33	18	12
18-1790	14	53	18	12
18-1862	8	23	2	22
18-1890	19	7	42	22
18-1980	25	23	58	22
18-1995	13	5	28	56
18-2060	17	19	6	28
18-2215	60	39	18	46
18-2282	29	53	42	28
18-2325	49	9	52	54
18-2523	25	29	36	16
18-2700	25	11	58	4
18-2770	29	55	6	46
18-2860	47	33	24	3

Site	10th Percentile	RCP4.5 Median	RCP8.5 Median	90th percentile
18-2905	19	7	18	56
18-2906	19	31	58	12
18-3230	43	39	24	42
18-3348	43	35	18	22
18-3355	26	31	18	54
18-3415	7	35	16	6
18-3675	14	29	6	16
18-3795	7	59	60	22
18-3855	25	27	2	34
18-3975	31	9	18	12
18-4030	39	53	28	52
18-4780	59	39	6	40
18-5080	17	23	32	12
18-5111	13	9	12	40
18-5201	7	5	18	56
18-5865	17	31	18	54
18-5894	7	1	40	54
18-5985	25	27	10	56
18-6350	25	5	18	21
18-6408	19	37	40	6
18-6620	7	9	30	16
18-6770	17	29	18	16
18-6844	59	33	24	12
18-6980	47	33	2	22
18-7010	29	23	42	34
18-7140	26	51	4	46
18-7272	57	37	12	15
18-7325	17	51	36	16
18-7330	44	13	32	46
18-7700	8	23	2	22
18-7705	13	33	24	48

Site	10th Percentile	RCP4.5 Median	RCP8.5 Median	90th percentile
18-7806	25	11	10	4
18-8000	31	15	18	48
18-8005	9	15	18	34
18-8065	29	37	58	4
18-8315	26	13	30	4
18-8380	25	1	4	45
18-8405	59	31	28	34
18-8720	43	23	58	16
18-8855	59	13	6	54
18-8877	5	39	6	4
18-9030	25	29	54	56
18-9035	26	29	60	16
18-9070	25	9	36	12
18-9140	30	47	12	56
18-9409	7	53	36	46
18-9440	26	23	10	16
18-9570	19	23	6	40
18-9750	8	47	52	54

See Table 3-1 for site indices; Table 3-2 for identification of GCM scenarios.

(This page left intentionally blank.)

4.0 RESULTS – EXTREME PRECIPITATION

The methods described in Section 2.1 were applied to the four GCMs selected for each of two future time periods and the historic time period at the 79 Maryland Atlas 14 stations (Section 3.0). Results are provided electronically in two databases, one for the IDF analysis and one for the peaks-over-threshold analysis of the 90th percentile 24-hour event. The two databases (IDF-db.xlsx and 90th%le-db.xlsx) are provided in Microsoft Excel™ format. Each database contains three tabs.

The results of the analyses are contained on the IDFdb tab. For each station, time horizon, and GCM combination, the *IDFdb* tab in the 90th%le-db.xlsx database provides a single result (the estimated 24-hour 90th percentile event). The *IDFdb* tab in the IDF-db.xlsx database provides, for each station, time horizon, and GCM combination, sets of 10 durations (5-minute to 24-hour) for 10 difference recurrence intervals.

To aid the user in exploring the databases, each contains a *Graph* tab for visualization. On this tab, the user can select a station from a drop-down list. For the IDF-db, the user can also select a recurrence interval. The workbook will then retrieve the requested data and display it in both tabular and graphical form (see examples below).

Results of the IDF analysis suggest a widespread risk of increase under future conditions in Maryland for the intensity of extreme precipitation events of a given duration and recurrence. However, this increase is not consistent among GCM scenarios downscaled by LOCA. At many stations, the future results suggest more of an increase in the cone of uncertainty than a unimodal increase in intensity – implying a risk of more intense events, but not always a consensus. For some GCM simulations the predicted intensity of low recurrence events decreases, presumably due to drier conditions predicted during the convective storm season. The method also assumes that relative bias between historical LOCA-downscaled GCM performance and observed data will be retained into the future – which in some cases where the fit to historic conditions is poor can lead to extreme future predictions that may not be physically realistic. It does appear that LOCA fails to provide a strong match to the distribution of historic high precipitation events, especially for stations near the land-water interface, even though the developers claim that "LOCA produces better estimates of extreme days" (Pierce et al., 2014). A newly released pre-print of Wang et al. (2020) appears to show that LOCA tends to under-estimate the magnitude of extreme precipitation events due to the way in which the historic training data set was constructed.

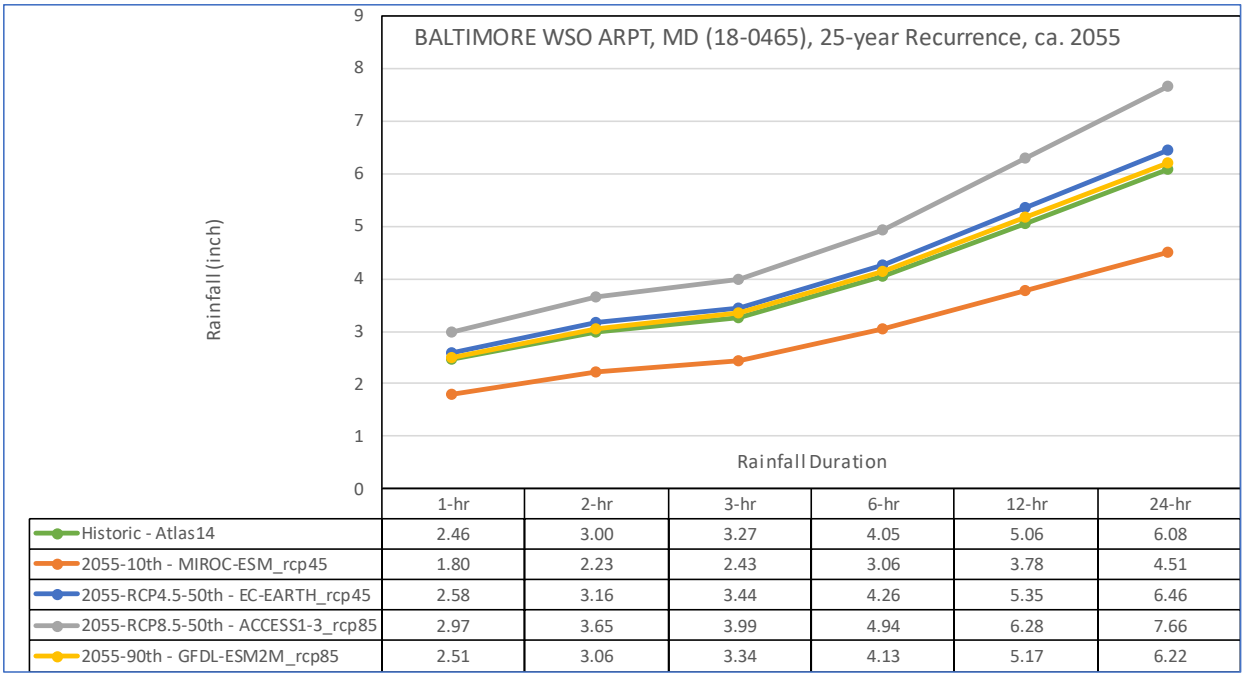
We also noted that the selection of GCMs that have higher or lower total annual precipitation volume often does not guarantee a similar alteration in the intensity of low-recurrence storm events. This could be associated with GCMs that predict a higher frequency of moderate intensity events and/or a seasonal shift away from the convective storm season.

A careful look at the results reveals instances where projected results for a given GCM do not increase monotonically across recurrence interval – especially for events with greater than 100-yr recurrence intervals. These anomalies occur due to the statistical nature of the analysis and the last step of the analysis in which the projected results are renormalized against the published IDF curve ordinates. This can result in some crossing behavior if the shape of the relationship between intensity and recurrence interval for a given duration is substantially different between historical AMS data and the GCM output and is exacerbated where results are extrapolated beyond the 30-yr time window for future climate output (e.g., predicting change in a 500-year event from statistical fit to a 30-year sample). These small

discrepancies should not interfere with the intended use of the results to investigate the potential range of risk for which adaptation may be required under further climate.

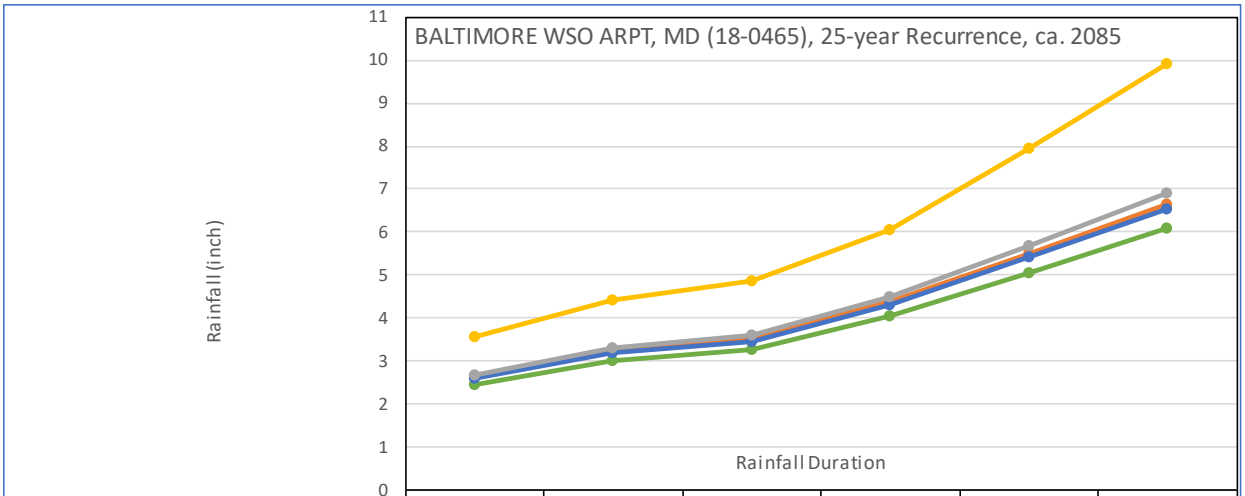
The predicted intensity of the 90th percentile 24-hour event does not show a consistent increase at most stations under future conditions. This is in line with studies that suggest total annual precipitation volume will most likely increase under future climate, but that much of this increase will be associated with more extreme, low-recurrence events (Easterling et al., 2017). The 90th percentile results thus appear to be "good news" as they suggest that many water quality BMPs that are optimized to capture and treat pollutants associated with sub-yearly recurrence events are likely to continue to provide expected services under future climate.

Representative figures from the reporting databases are shown in Figure 4-1 through Figure 4-3.



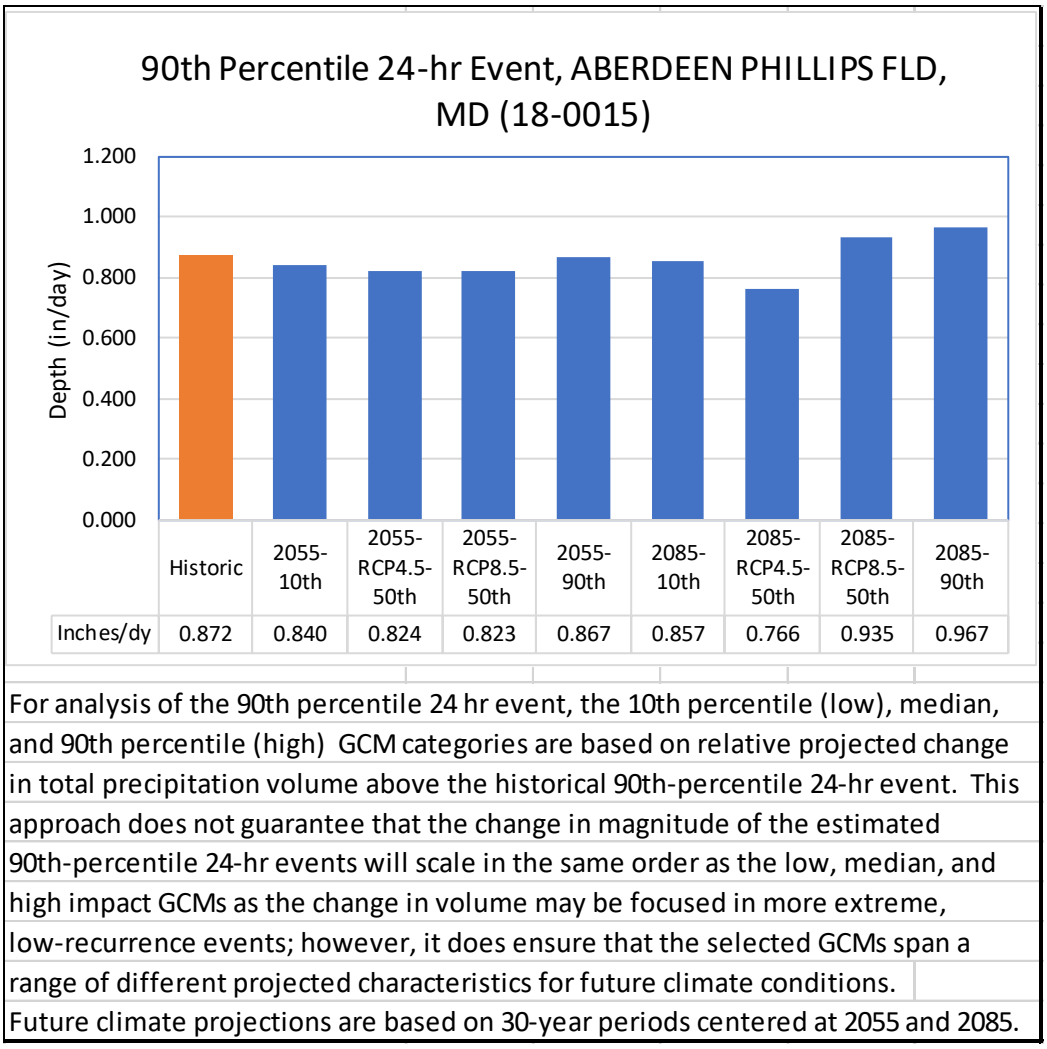
	1-hr	2-hr	3-hr	6-hr	12-hr	24-hr
Historic - Atlas14	2.46	3.00	3.27	4.05	5.06	6.08
2055-10th - MIROC-ESM_rcp45	1.80	2.23	2.43	3.06	3.78	4.51
2055-RCP4.5-50th - EC-EARTH_rcp45	2.58	3.16	3.44	4.26	5.35	6.46
2055-RCP8.5-50th - ACCESS1-3_rcp85	2.97	3.65	3.99	4.94	6.28	7.66
2055-90th - GFDL-ESM2M_rcp85	2.51	3.06	3.34	4.13	5.17	6.22

Figure 4-1. Projected 25-year IDF Curves for Baltimore WSO Airport ca. 2055



	1-hr	2-hr	3-hr	6-hr	12-hr	24-hr
Historic - Atlas14	2.46	3.00	3.27	4.05	5.06	6.08
2085-10th - CMCC-CMS_rcp45	2.66	3.24	3.54	4.37	5.49	6.63
2085-RCP4.5-50th - GFDL-ESM2M_rcp45	2.60	3.18	3.47	4.30	5.41	6.53
2085-RCP8.5-50th - MIROC5_rcp85	2.70	3.31	3.62	4.49	5.69	6.90
2085-90th - GISS-E2-H_rcp85	3.55	4.43	4.87	6.07	7.94	9.90

Figure 4-2. Projected 25-year IDF Curves for Baltimore WSO Airport ca. 2085



For analysis of the 90th percentile 24 hr event, the 10th percentile (low), median, and 90th percentile (high) GCM categories are based on relative projected change in total precipitation volume above the historical 90th-percentile 24-hr event. This approach does not guarantee that the change in magnitude of the estimated 90th-percentile 24-hr events will scale in the same order as the low, median, and high impact GCMs as the change in volume may be focused in more extreme, low-recurrence events; however, it does ensure that the selected GCMs span a range of different projected characteristics for future climate conditions. Future climate projections are based on 30-year periods centered at 2055 and 2085.

Figure 4-3. Projected Results for 90th Percentile 24-hour Precipitation Event, Aberdeen-Phillips Field

5.0 RESULTS – EVENT RUNOFF AND BMP SIMULATIONS

The SWMM simulations are performed at all 79 Atlas 14 stations in Maryland. Each station is evaluated for two future periods centered at 2055 and 2085). For each time period, results are generated for four GCMs representing the 10th, median RCP 4.5, median RCP 8.5, and 90th percentile in terms of predicted change in future total precipitation volume. Simulations are run for the 1, 2, 10, and 100-yr 24-hour storm events, plus the 90th percentile 24-hour event. The two BMPs are simulated with three levels of imperviousness (25%, 50%, and 80%). This provides a database of 20,574 simulations.

Because of the large number of runs completed, results are provided in four separate electronic databases:

- SWMM_BIORETENTION_IDF_OUTPUT_SUMMARY.xlsx
- SWMM_BIORETENTION_POT_OUTPUT_SUMMARY.xlsx
- SWMM_WETPOND_IDF_OUTPUT_SUMMARY.xlsx
- SWMM_WETPOND_POT_OUTPUT_SUMMARY.xlsx

Within each database, the first tab provides the raw results from each individual simulation. These are results for a 48-hour simulation (with storm event on the first day) for a drainage area (nominal 1 acre for bioretention and 25-acre for extended wet detention). Results are generated as total runoff in cubic feet (per two days) with peak flow in cfs. The second tab contains summaries of the first tab at varying levels of aggregation.

5.1 RUNOFF

SWMM5 simulated runoff prior to entering the BMP is equivalent to the unmanaged runoff from the site and can be used to build intensity-frequency relationships for future runoff events. The frequency is the same as the frequency of the underlying rain event. Summary results for the 1-acre bioretention simulation produce estimates of peak flow as cfs/ac as well as estimates for total storm flow. Results for peak flow (averaged across all sites) are shown in Figure 5-1, separated by recurrence interval and impervious percentage. By the end of the century, peak runoff rates are predicted to increase, on average, about 13 – 14 percent, with slightly higher increases for longer recurrence intervals and lower impervious percentages.

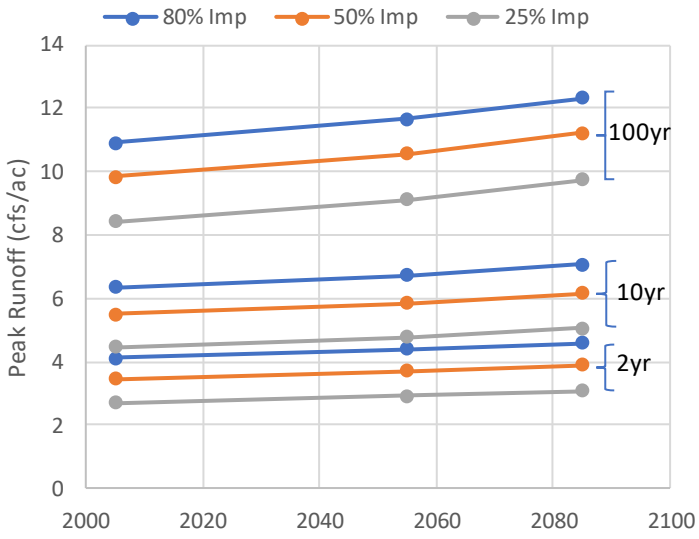


Figure 5-1. Historic and Future Peak Flow Averages by Recurrence

5.2 BIORETENTION BMP

Raw output for the bioretention simulations is displayed in the following format. Columns A through I provide the run identification information, such as the following:

SWMM Output----------								
StationName	StationID	Year	GCM_RCP	BMP_Type	ANALYSIS_Type	WQ_Depth	EVENT_Type	P_IMPERV
ABERDEEN PHILLIPS FLD, MD	18-0015	Historic	Atlas14	Bioretention	IDF	2.67	1-yr 24-hr	25

Here, "Year" can be Historic, 2055, or 2085 and "GCM_RCP" can be either Atlas 14 or the name of a future climate GCM. "ANALYSIS_Type" is either IDF or POT, where POT represents the 90th percentile analysis. "WQ_Depth" is the design requirement water quality depth in inches, and "P_Imper" is impervious percentage. The other variables are self-explanatory.

Columns J through M provide the SWMM hydraulic output. The volumes are totals over the 48-hour simulation period:

PeakFlow_cfs	Overflow_cf	Underdrain_outflow_cf	TotalOutflow
2.10	3,792	1,820	5,612

Finally, columns O through R summarize the change relative to Atlas 14 (historic) design conditions:

Change ----------			
PeakFlow_cfs%	Overflow_cf%	Underdrain_outflow_cf%	TotalOutflow%
12.05%	16.65%	3.77%	12.47%

Bioretention cells are designed to provide water quality treatment for the 90th percentile 24-hour rainfall event. We noted in Section 4.0 that the 90th percentile event under future climate conditions was frequently predicted to be smaller than historic, with overall increases in total precipitation volume concentrated in more extreme events. This is borne out in the analysis of bioretention response to this event (the "POT" database). Taking the average of the median change across all sites, the peak flow and total outflow decline by -17 and -18%, respectively, for 2055, and by -11 and -12% for 2085 (Table 5-1. On average, bioretention produces no bypass overflow under historic or future conditions for the 90th-percentile event. There is, however, a wide range in predicted responses between sites and an even larger range between individual site and climate scenario combinations.

Table 5-1. Summary of Response of Bioretention to 90th-percentile Event

Average of median change across all sites				
	Peak Flow (cfs)	Overflow (ft^3)	Underdrain (ft^3)	Total Outflow (ft^3)
2055	-17.26%	0%	-18.02%	-18.02%
2085	-11.33%	0%	-11.93%	-11.93%
Range of median change over sites				
2055	-57.10% to 12.29%	0%	-58.57% to 18.91%	-58.57% to 18.91%
2085	-50.48% to 13.56%	0%	-51.49% to 15.56%	-51.49% to 15.56%
Range over all individual scenarios				
2055	-75.69% to 392.4%	0% to 21.44%	-79.00% to 87.80%	-79.00% to 101.8%
2085	-73.35% to 1724%	0% to 82.41%	-76.29% to 110.5%	-76.29% to 141.7%
Median change versus impervious %				
I=25	-17.72%	0%	-21.42%	-21.42%
I=50	-15.14%	0%	-16.32%	-16.32%
I=80	-12.05%	0%	-12.51%	-12.51%

Bioretention is not designed to fully treat larger low-recurrence events with longer return periods. Averaging over the medians of all sites and future scenarios (incorporating 1-year through 100-year 24-hour events) the peak flow, bypass (overflow), and total outflow increase by 8, 11, and 7%, respectively for 2055 and by 16, 21, and 14% by 2085.

Table 5-2. Summary of Responses of Bioretention to Future 1-year through 100-year Events

Average of median change across all sites				
	Peak Flow (cfs)	Overflow (ft^3)	Underdrain (ft^3)	Total Outflow (ft^3)
2055	8.43%	11.13%	1.73%	7.30%
2085	15.71%	20.76%	2.97%	13.54%
Range of median change over sites				
2055	-1.29% to 22.31%	-1.44% to 29.56%	-0.20% to 4.24%	-1.23% to 20.65%
2085	2.31% to 34.65%	3.58% to 42.29%	0.44% to 6.45%	1.96% to 27.30%
Range over all individual scenarios				
2055	-48.28% to 201.0%	-58.59% to 264.7%	-10.72% to 12.68%	-48.35% to 228.6%
2085	-43.36% to 139.4%	-52.48% to 173.8%	-10.66% to 12.02%	-44.96% to 151.1%
Median change versus impervious %				
I=25	10.51%	12.75%	2.21%	10.13%
I=50	11.15%	15.33%	2.23%	9.73%
I=80	12.87%	18.87%	2.32%	9.46%

The bioretention results for outflows by different pathways for all scenarios in all areas of Maryland are summarized graphically in Figure 5-2 and Figure 5-3. The left side of these figures shows the low-range responses (based on the 90th-percentile event simulations) while the right side shows the high-range responses (based on the IDF simulations) at varying levels of imperviousness. Results for the 25% impervious case look somewhat anomalous because the Simple Method sizing rule tends to undersize bioretention when imperviousness is low. For larger, low-recurrence events, the bioretention response becomes approximately linear.

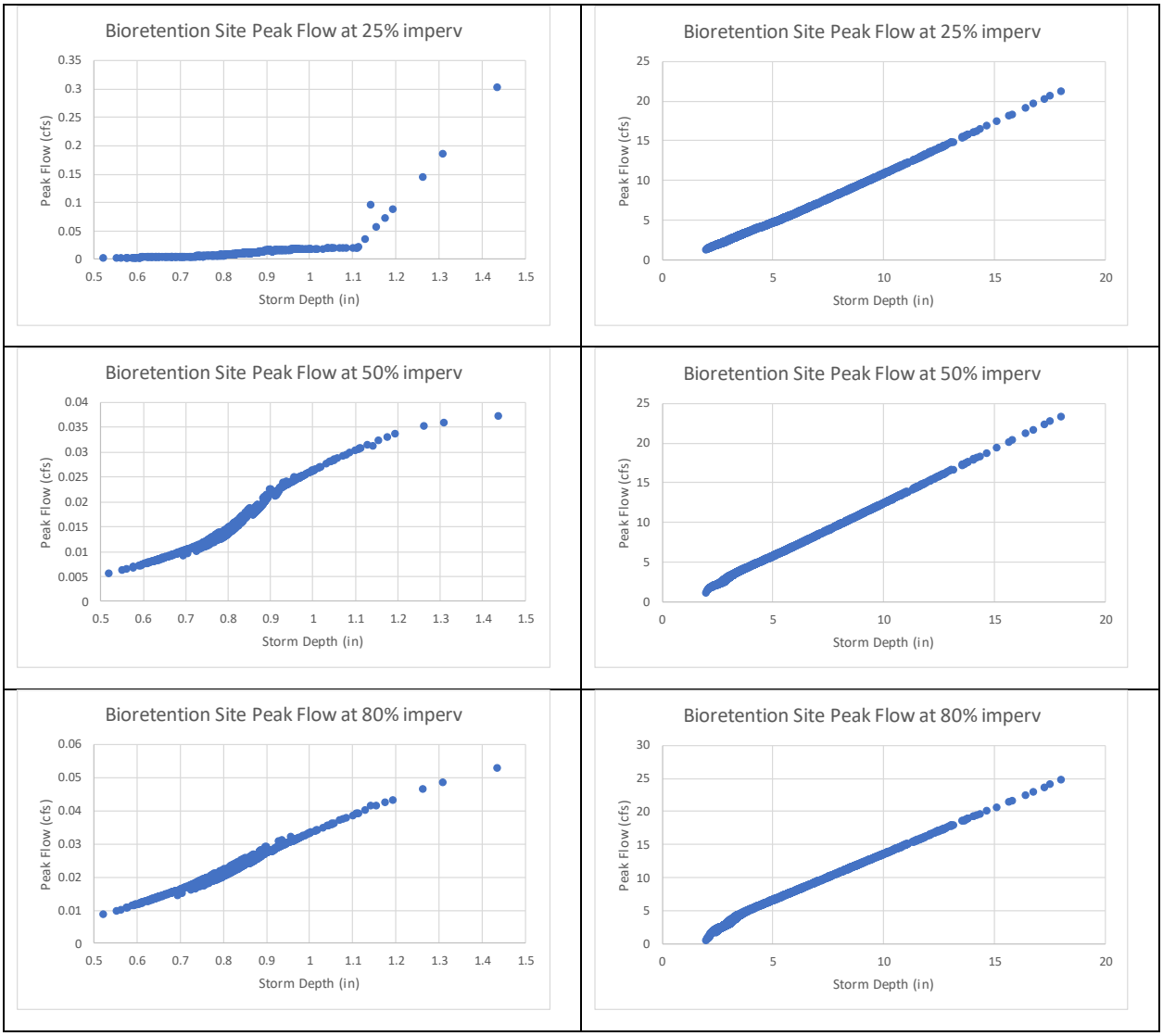


Figure 5-2. Bioretention Simulation Results for Peak Outflow as a Function of Total Storm Depth

Note: Figures on left side show closeup of responses to higher frequency, lower volume peak events; figures on right side show responses to lower frequency extreme events.

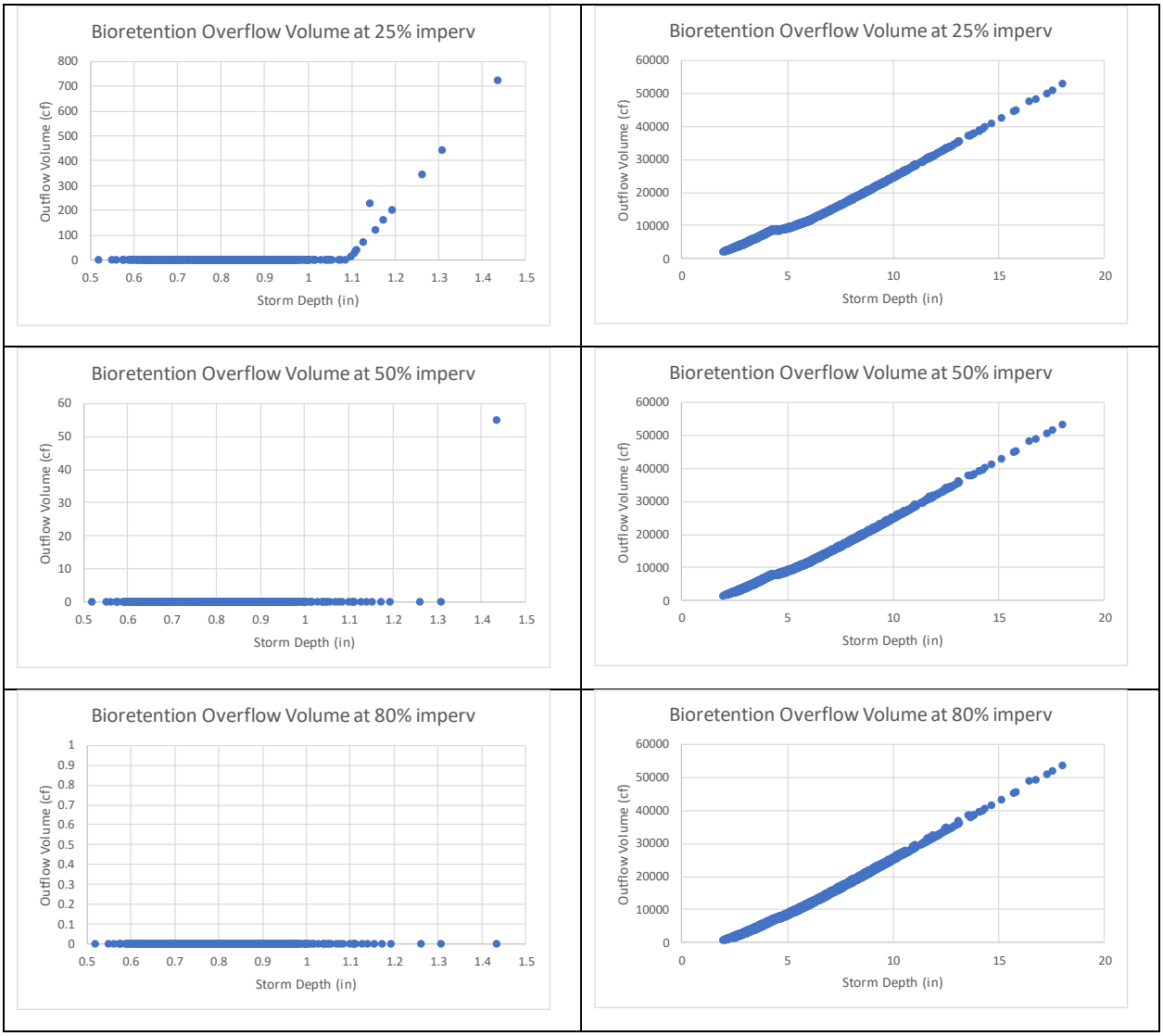


Figure 5-3. Bioretention Simulation Results for Overflow Volume as a Function of Total Storm Depth

Note: Figures on left side show closeup of responses to higher frequency, lower volume peak events; figures on right side show responses to lower frequency extreme events.

5.3 EXTENDED WET DETENTION BMP

Raw output for the extended wet detention simulations is displayed a format similar to bioretention. Columns A through J provide the run identification information. This differs from bioretention in adding the scenario rainfall (column H) and the channel protection volume stage for the design (column J).

Columns K through M provide the SWMM hydraulic output. "Site_peak_flow_cfs" is the instantaneous peak output from the BMP, including both the from the orifice and flow over the weir. "Site_volume_cf" is the total outflow from the wet pond (in cubic feet) over the 48-hour simulation period. For this BMP, "TotalOutflow" is the same as Site_volume_cf but is included for consistency with the bioretention output format.

Site_peak_flow_cfs	Site_volume_cf	TotalOutflow
30.952	147,229	147,229

Finally, columns O and R summarize the change relative to Atlas 14 (historic) design conditions:

PeakFlow_cfs%	TotalOutflow%
11.31%	12.17%

As was noted for bioretention, the 90th percentile event under future climate conditions was frequently predicted to be smaller than historic, with overall increases in total precipitation volume concentrated in more extreme events. Accordingly, the wet pond simulations also tend to show a decline in outflow for the 90th percentile event, but with substantial variability among scenarios (Table 5-3). Peak flow is relatively insensitive to impervious percentage for the 90th-percentile event as releases from the pond are controlled by the orifice.

Table 5-3. Summary of Response of Extended Wet Detention to 90th-percentile Event

Average of median change across all sites		
	Peak Flow	Total Outflow
2055	-5.97%	-10.70%
2085	-3.95%	-7.06%
Range of median change over sites		
2055	-20.74% to 5.36%	-36.15% to 10.96%
2085	-18.10% to 4.82%	-31.83% to 9.35%
Range over all individual scenarios		
2055	-30.13% to 33.88%	-51.27% to 72.73%
2085	-28.15% to 44.88%	-48.82% to 111.09%
Median change versus impervious %		
25	-6.81%	-12.26%
50	-5.09%	-9.19%
80	-3.94%	-7.15%

For larger low recurrence events, averaging over the medians of all sites and future scenarios (incorporating 1-year through 100-year 24-hour events) the peak flow and total outflow increase by 22 and 7%, respectively for 2055 and by 41 and 13% by 2085 for extended wet detention (Table 5-4).

Table 5-4. Summary of Responses of Extended Wet Detention to Future 1-year through 100-year Events

Average of median change across all sites		
	Peak Flow	Total Outflow
2055	21.89%	6.89%
2085	41.44%	12.81%
Range of median change over sites		
2055	-1.84% to 58.99%	-1.23% to 20.17%
2085	6.21% to 108.62%	1.93% to 25.58%
Range over all individual scenarios		
2055	-75.39% to 607.22%	-48.65% to 232.77%
2085	-70.79% to 778.38%	-45.28% to 152.61%
Median change versus impervious %		
25	28.15%	10.13%
50	32.26%	9.20%
80	27.08%	8.61%

The extended wet detention basin results for all scenarios in all areas of Maryland are summarized graphically in Figure 5-4 and Figure 5-5. The left side of these figures shows the low-range responses (based on the 90th-percentile event simulations) while the right side shows the high-range responses (based on the IDF simulations) at varying levels of imperviousness. The separate lines in the peak flow responses reflect the differing design criteria in eastern and western Maryland.

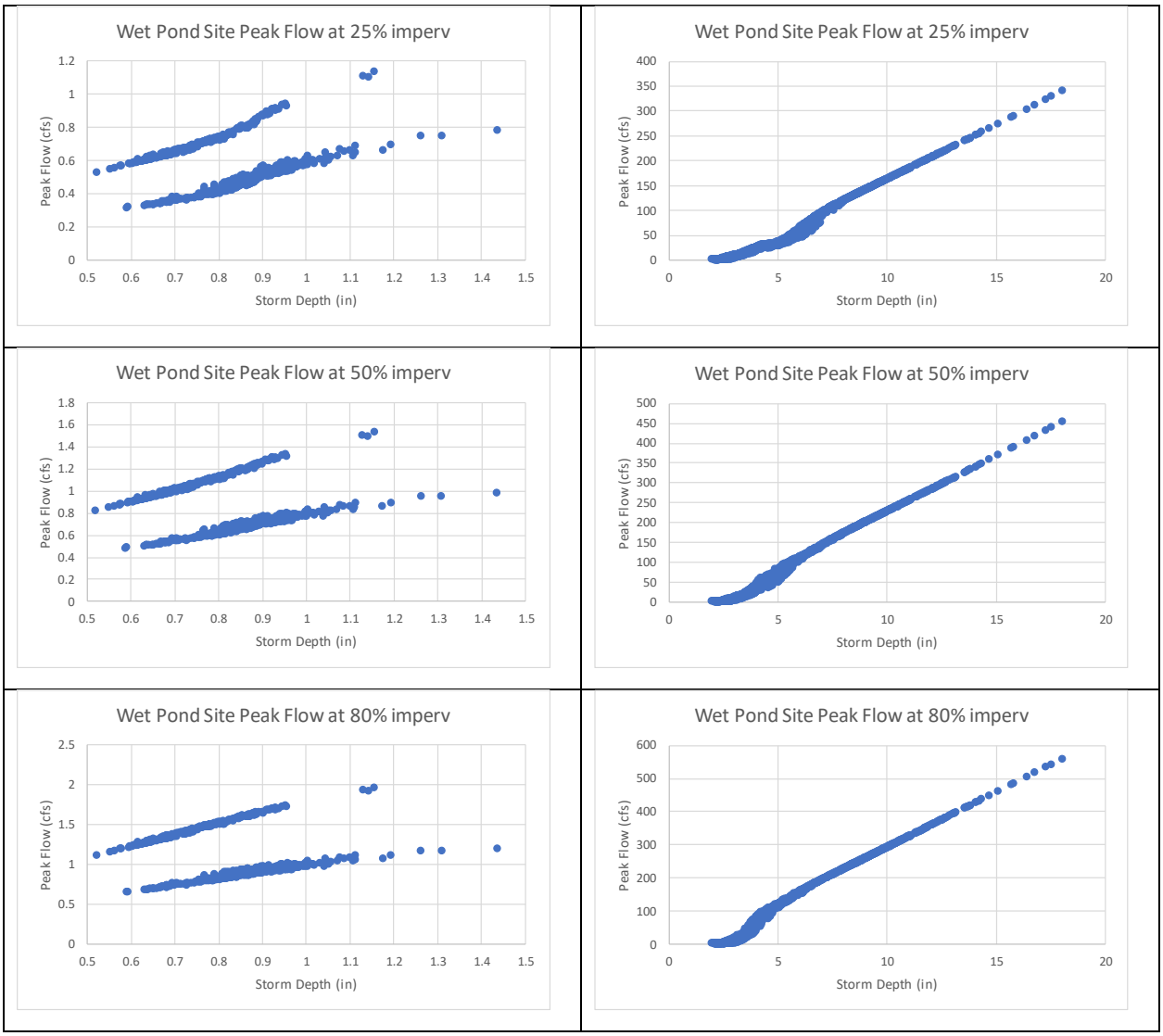


Figure 5-4. Extended Wet Detention Basin Simulation Results for Peak Outflow as a Function of Total Storm Depth

Note: Figures on left side show closeup of responses to higher frequency, lower volume peak events; figures on right side show responses to lower frequency extreme events.

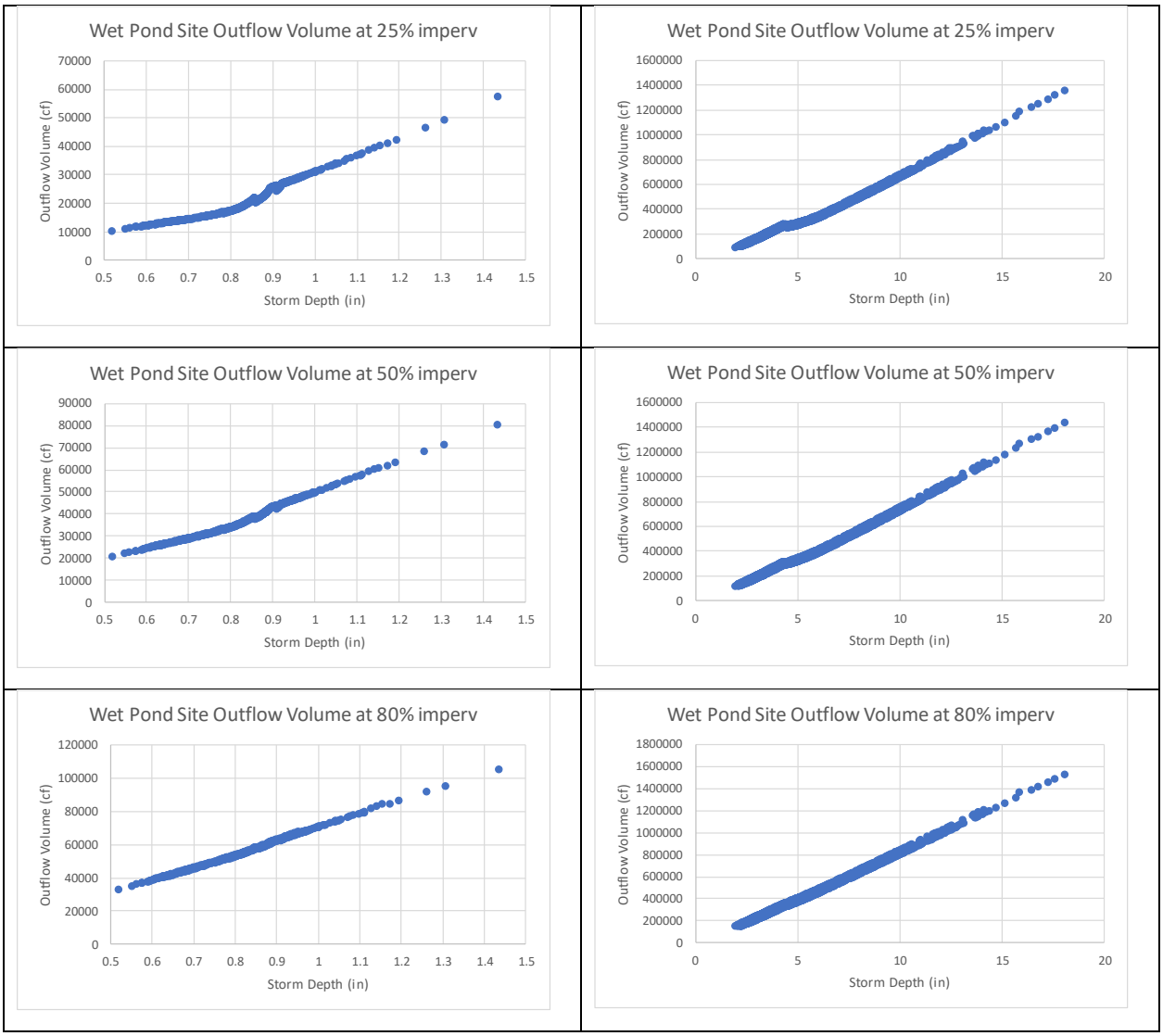


Figure 5-5. Extended Wet Detention Simulation Results for Overflow Volume as a Function of Total Storm Depth

Note: Figures on left side show closeup of responses to higher frequency, lower volume peak events; figures on right side show responses to lower frequency extreme events.

6.0 IMPLICATIONS FOR DESIGN

This section builds upon the previous material to provide a quantitative evaluation of the potential impacts of changes in storm IDF relationships in three areas: channel stability, risk of road flooding, and the general performance efficiency of urban stormwater BMPs.

6.1 CHANNEL STABILITY

The structure of a stream channel adjusts over time as it attempts to reach an approximate equilibrium between flow energy and sediment supply. If these inputs change, then the channel will also change. For example, in urbanizing areas where impervious surface increases, resulting in increased runoff and greater flow energy, channels often respond by first incising and then widening, losing connection with the floodplain, and generating large quantities of mobile sediment. These changes result in degraded habitat and poor biology (Walsh et al., 2005).

The morphologic response of stream channels is closely related to the effective discharge or channel-forming flow (Wolman and Miller, 1960), which integrates the sediment-carrying capacity and probability of occurrence to evaluate the flow that, over time, transports the largest mass of sediment. Effective discharge is closely related to bankfull discharge and is typically associated with flows that have a recurrence frequency of once in from one to two years (Simon, 2004). One of the functions of urban BMPs is to limit erosive flows and maintain channel stability by retaining enough water to achieve a specified channel protection volume; in Maryland, this is based on a one-year 24-hour runoff event (MDE, 2009). Similarly, Palmer et al. (2005) state that ecologically successful stream restoration designs must be self-sustaining systems with the ability to maintain equilibrium despite changes; thus, restoration designs seek to ensure that the redesigned channel is consistent with expected channel-forming flows.

Current practice for both BMP and restoration design typically relies on the historic record to estimate design flows. If future climate brings more intense precipitation and runoff at recurrence intervals corresponding to channel-forming flows, then sediment transport capacity will increase and channel adjustments of incision or widening can be expected as the system attempts to reach a new equilibrium. Thus, changes in IDF relationships could threaten the resilience of stream restoration efforts, while BMPs to control runoff might not achieve channel protection goals.

Changes in the one-year 24-hour (or 1.5-year 24-hour) flow give an indication of potential risks to stream channel resilience but are not a direct measure of stream stability. On the other hand, a full analysis of stability is a site-specific exercise that needs to incorporate the geometry, slope, and external sediment supply to a stream reach in addition to the flow. As a middle way, simplified semi-quantitative tools are useful to provide broad-scale screening of the potential effects of changes in IDF relationships on stream stability.

The GeoTools package (Bledsoe et al., 2007; Raff et al., 2007) is designed to aid in the estimation of erosion potential and associated risk indices. The use of these methods is demonstrated in Bledsoe and Watson (2001) and Bledsoe (2002), among others.

The GeoTools effective discharge analysis provides two summary measures of channel stability.

- The **Mobility Index** (*MI*) is defined as $MI = S\sqrt{\frac{Q}{d_{50}}}$, where *Q* is discharge (m^3/s), *S* is slope (dimensionless), and d_{50} is the median grain size (m [mm x 10-3]; Chang, 1985; Bledsoe and Watson, 2001). *MI* was developed in part as a measure of channel form and stability in cases where channel width data are unavailable.
- **Specific Stream Power** (ω) is defined as $\omega = \frac{\Omega}{w} = \frac{\gamma_m Q S}{w}$, where Ω is total stream power, γ_m is the specific weight of the water and sediment mixture (kg), and *w* is the channel width (m). This measure has also been used as an index of channel form and response (Bledsoe and Watson, 2001).

Section 4.0 developed estimates of precipitation IDF relationships under future climate in Maryland, while Section 5.1 provided SWMM5-predicted runoff associated with future precipitation events of specified recurrence and duration. The runoff simulations use a unit-area representation of a generic urban landscape at varying levels of effective imperviousness. Because channel width is not explicitly specified for each location, analysis with *MI* is more useful than ω for evaluating potential changes in stream stability.

Bledsoe and Watson (2001) used *MI* to develop logistic regressions to predict whether a stream channel was stable (meandering) or unstable (incising). Their model #45, which uses the base-10 logarithm of *MI* and defines *MI* based on annual (1-year recurrence) 24-hour flow magnitude rather than bankfull flow, classified stable meandering and incising channels with sand beds with over 95% accuracy over a sample of 77 well-studied streams. The resulting logistic model of the probability of incision (*p*) is:

$$p = \frac{exp(\beta_0 + \beta_1 X)}{1 + exp(\beta_0 + \beta_1 X)},$$

$$\beta_0 = 7.89, \qquad \beta_1 = 22.11,$$

$$X = log_{10} MI = log_{10}\left(S\sqrt{\left[Q_{1-yr}/d_{50}\right]}\right)$$

The logistic model results in an S-shaped curve. As *MI* approaches 0, *p* also asymptotes toward zero; as *MI* approaches 1, *p* asymptotes towards 1. The rate of change of *p* relative to *MI* is steepest in the middle of the range, where a small change in *MI* can result in a large change in *p*. A similar type of relationship is expected for Maryland streams, although the regression coefficients may differ, and an equation of this form is useful for exploring relative risk of stream instability due to climate change.

To apply the logistic model to the IDF analysis, we use for *Q* the peak runoff response to the 1-year precipitation event on a 1-acre drainage area predicted by the SWMM model (bioretention setup without presence of BMP). We use the 1-acre peak rather than daily average flow for comparative purposes because it is the shear stress associated with the peak flow rate that determines sediment mobility during the event; however, it is evident that the analysis of real streams with multiple contributing areas is much more complex.

Note that *Q* scales with the drainage area with an approximately linear response until significant variations in time of concentration manifest and *MI* thus scales approximately as the square root of the drainage area. This indicates that as area and/or *Q* increases then either *S* must decrease or $\sqrt{d_{50}}$ must increase by a proportional amount to maintain the same probability of channel stability. Results are presented here on a 1-acre basis to explore the potential relative changes in stability under future climate.

The logistic model probability representation is a function of $S/\sqrt{d_{50}}$. Setting $p = 0.5$ defines the point of transition from likely stable to likely incising conditions (for sand-bed streams). This occurs when

$$\frac{S}{\sqrt{d_{50}}} = \frac{10^{-\beta_0/\beta_1}}{\sqrt{Q}}$$

The resulting transition frontier is shown in Figure 6-1. As Q increases above the transition curve the predicted probability of incision increases above 50%.

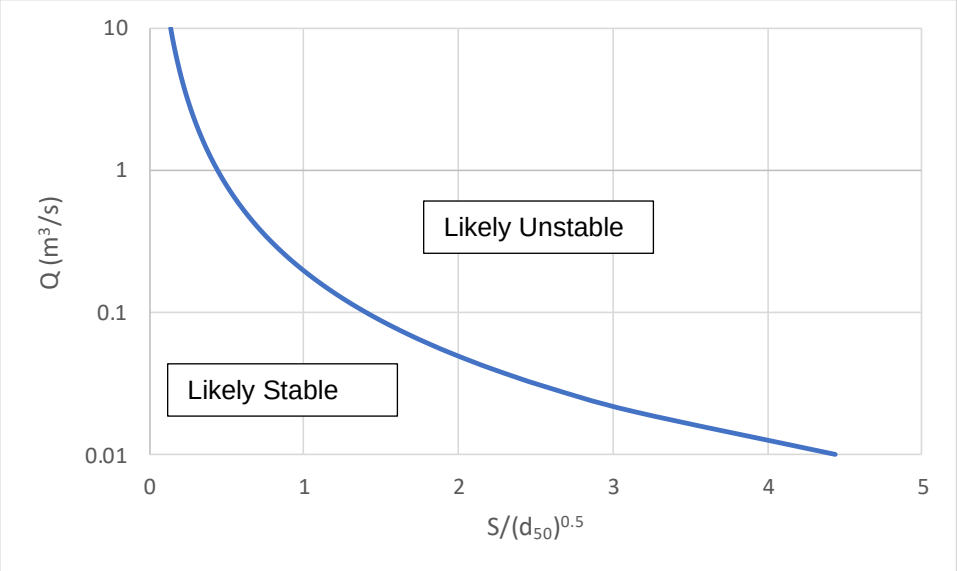


Figure 6-1. Stability Transition Frontier for Sand Bed Stream with 1-acre Drainage

The probability of instability increases with longer recurrence frequency and increased imperviousness, both of which increase peak runoff. We explore results without BMPs (also applicable to stream restoration design), with runoff control by bioretention cells, and with extended wet detention basins.

Figure 6-2, showing results without BMPs, compares predicted *MI* for runoff from 1 acre at 25% and 80% imperviousness (average across all sites, with $S/\sqrt{d_{50}} = 1.75$, where $p = 50\%$ corresponds to $MI = 0.443$.) Each chart shows nine lines, representing historic conditions, the four selected GCMs for ca. 2055 conditions, and the four selected GCMs for ca. 2085 conditions, $S/\sqrt{d_{50}} = 1.75$ is taken as an example of a headwater stream or drainage channel at conditions near the stability limit, corresponding to, for instance, a channel with a slope of 1.5% and a d_{50} of 0.073 mm or a slope of 2.77% and a d_{50} of 0.25 mm. Most future climate scenarios show an increase in *MI* that grows larger at longer return intervals.

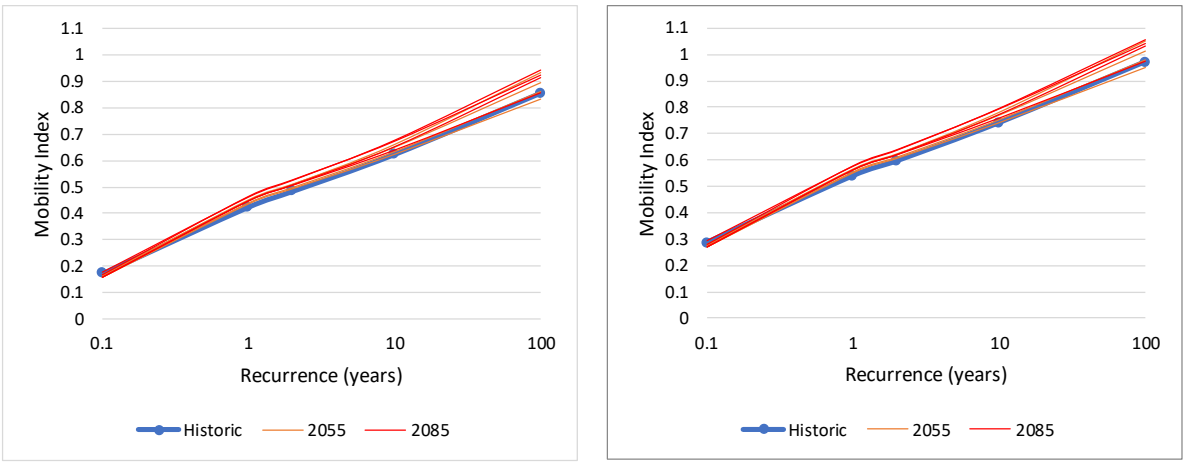


Figure 6-2. Average Mobility Index for 25% (left) and 80% (right) Impervious Cover 1-acre Parcel, $S/\sqrt{d_{50}}$ = 1.75 $m^{-0.5}$

For the logistic regression of Bledsoe and Watson, the 1-year 24-hr event flow results provide the prediction of potential channel instability. Maintaining the ratio of $S/\sqrt{d_{50}}$ = 1.75 $m^{-0.5}$ (other ratios provide similar, but shifted results), simulation of the probability of instability based on the 1-year recurrence peak runoff calculated using SWMM from historic and potential future IDF curves yields the average results across all 79 Maryland Atlas 14 stations at 25% imperviousness shown in Figure 6-3 and summarized (for three levels of imperviousness) on the left side of Table 6-1. These probabilities increase with both percent imperviousness and time into the future, with only historic climate conditions at 25% imperviousness falling below the 50% target for these site conditions.

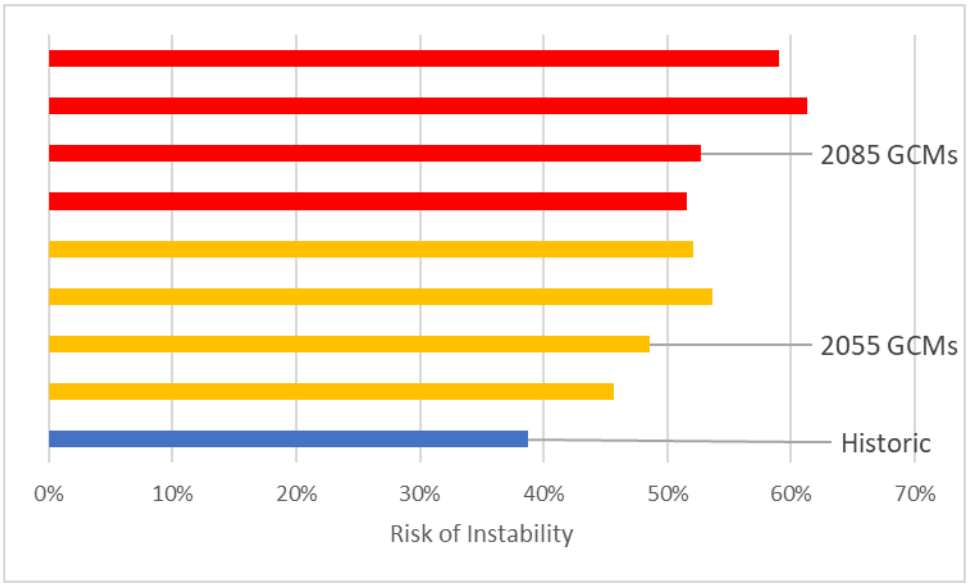


Figure 6-3. Predicted Probability of Channel Instability at 25% Imperviousness for Runoff from a 1 Acre Site with $S/\sqrt{d_{50}}$ = 1.75 using the Logistic Regression of Bledsoe and Watson (2001)

Table 6-1. Probability of Channel Instability for Runoff from 1 Acre with $S/\sqrt{d_{50}}$ = 1.75, with and without Bioretention BMPs

	No BMP			Bioretention		
Imperviousness	25%	50%	80%	25%	50%	80%
Historic	38.73%	71.59%	86.79%	34.39%	49.41%	44.78%
2055	50.01%	78.76%	90.21%	45.57%	64.51%	63.32%
2085	56.16%	82.06%	91.73%	52.04%	71.72%	71.76%

Note: Results are averages across 79 sites. Results for 2055 and 2085 are averaged across four GCMs for each site.

The right side of Table 6-1 shows the results for the same conditions but with treatment of runoff by bioretention cells designed to current Maryland standards. Bioretention cell sizing varies with Simple method predictions of runoff amount, which suppresses variability across percent imperviousness. For historic climate, the probability of incision is less than 50% for all three levels of imperviousness (which appears to corroborate the design standards); however, the probability of instability increases under predicted future climate conditions.

Channels with lower values of $S/\sqrt{d_{50}}$ (e.g., with a lower slope or larger particle size) will have lower predicted risk of instability. Results for an individual site are sensitive to the value of $S/\sqrt{d_{50}}$, although the pattern remains the same (Table 6-2). For a fine sand bed with d_{50} = 0.25 mm, the $S/\sqrt{d_{50}}$ range corresponds to slopes from 1.58% to 3.16%.

Table 6-2. Probability of Channel Instability for Runoff from 1 Acre Parcel with Alternative $S/\sqrt{d_{50}}$ at 80% Imperviousness

	No BMP				Bioretention			
$S/\sqrt{d_{50}}$	1.0	1.5	1.75	2.0	1.0	1.5	1.75	2.0
Historic	2.96%	59.92%	86.79%	95.95%	0.37%	15.58%	44.78%	74.51%
2055	4.13%	67.75%	90.21%	97.08%	0.82%	28.53%	63.32%	86.03%
2085	4.96%	71.69%	91.73%	97.56%	1.24%	37.34%	71.76%	90.02%

Results shown above represent averages across 79 sites for which there are varying predictions of change in the 1-year 24-hour flow. Results for individual sites are highly variable, reflecting genuine geographic variations, statistical, and potential anomalies in the LOCA downscaling process, as well as the effective impervious area of the drainage.

Figure 6-4 gives an illustration of the spread among individual results in the form of a histogram versus probability bins for predicted instability (again using $S/\sqrt{d_{50}}$ = 1.75 as an example). All time periods have examples that span most of the possible probability range; however, the future time periods predict a reduction in low probability categories and an increase in high probability categories. The shift associated with future climate is more clearly seen in a histogram that shows the percentage of cases that are greater than a given level of probability (Figure 6-5).

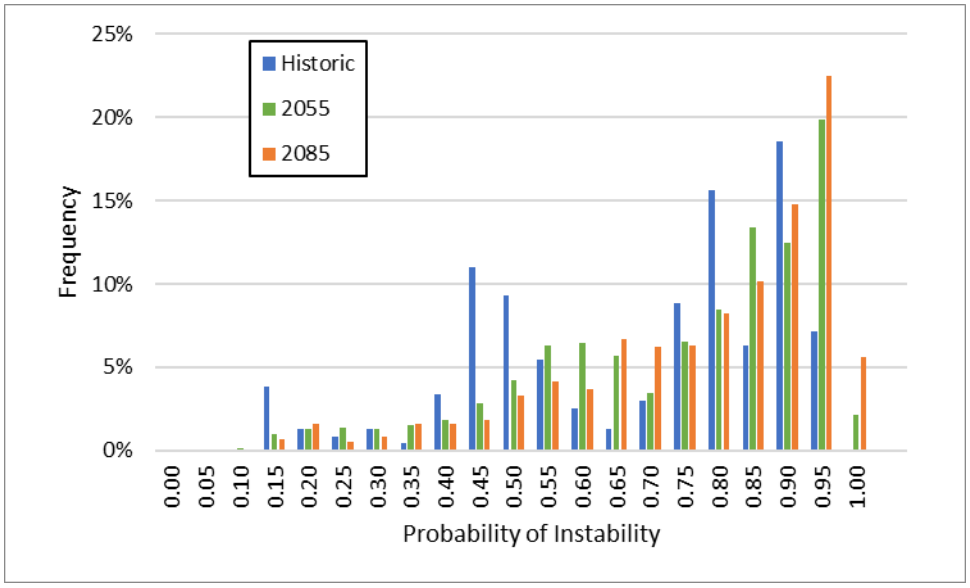


Figure 6-4. Histogram of Individual Station/GCM/Imperviousness for Probability of Channel Instability with $S/\sqrt{d_{50}}$ = 1.75, 1 Acre Drainage, and no BMP

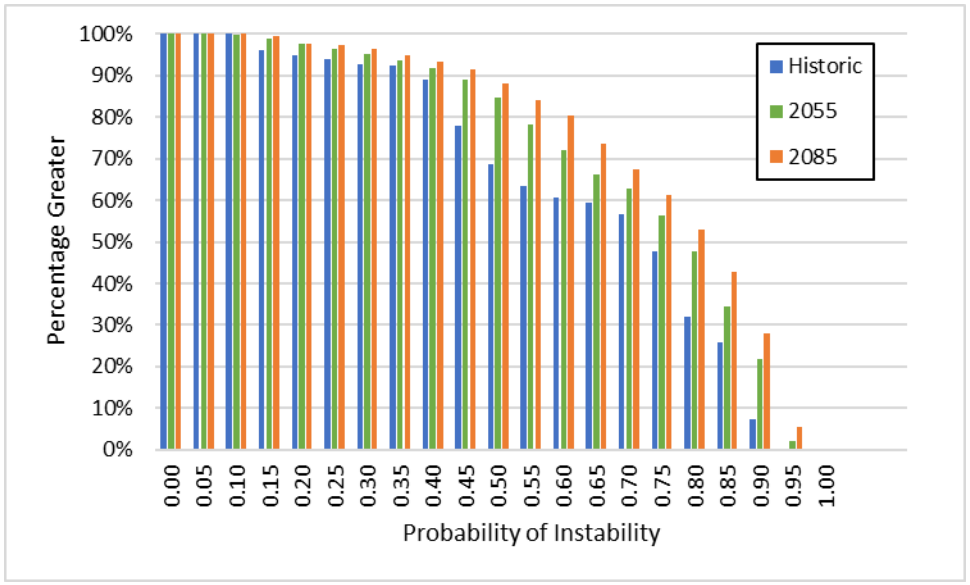


Figure 6-5. Inverse Cumulative Distribution Function (Percentage Greater than Specified Level) of Individual Station/GCM/Imperviousness for Probability of Channel Instability with $S/\sqrt{d_{50}}$ = 1.75, 1 Acre Drainage, and no BMP

An extended wet detention pond is assumed to treat a larger drainage area than a bioretention cell and the SWMM simulations of flow through the pond use a contributing area of 25 acres, which results in higher runoff volume. Accordingly, the value of $S/\sqrt{d_{50}}$ must shift to a lower value to maintain stability. To provide comparability with the bioretention example we scale the ratio by the square root of the drainage area. Dividing the previous example value of this ratio of 1.75 by $\sqrt{25}$ yields $S/\sqrt{d_{50}}$ = 0.35, which results in an *MI* diagram similar to that shown above in Figure 6-2. For example, a ratio of 0.35 might correspond to a slope of 0.55% at a d_{50} of 0.25 mm.

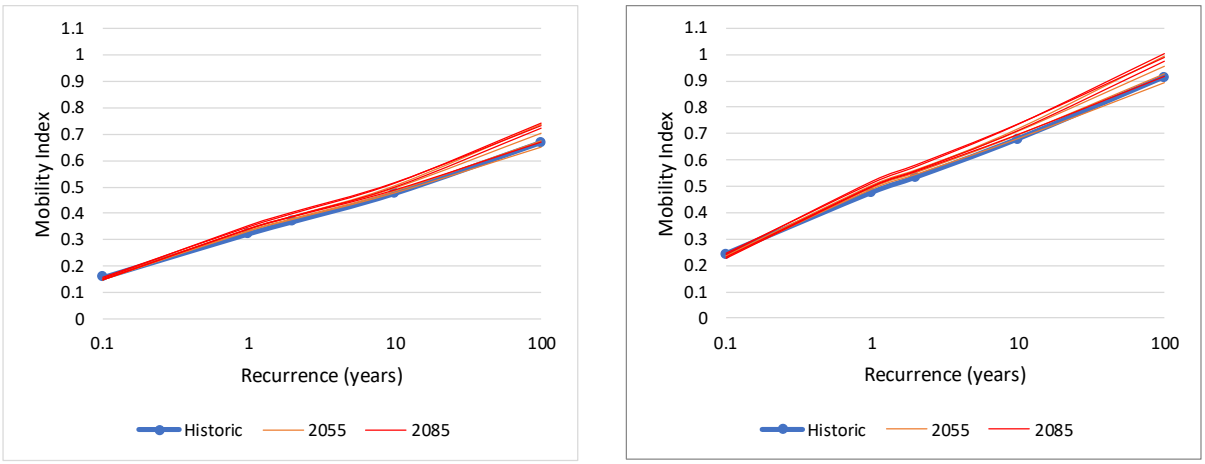


Figure 6-6. Average Mobility Index for 25% (left) and 80% (right) Impervious Cover, 25-acre Parcel, $S/\sqrt{d_{50}} = 0.35$ m$^{-0.5}$

The wet detention pond is designed to provide protection to the channel through the 10-year event, with a margin of safety. It is thus not surprising that the *MI* remains low for the 1-year event at $S/\sqrt{d_{50}} =$ 0.35 m$^{-0.5}$ or even when $S/\sqrt{d_{50}}$ is increased to 1.0 due to a higher slope or decreased median particle size (Figure 6-7). Estimated average probability of instability is summarized in Table 6-3.

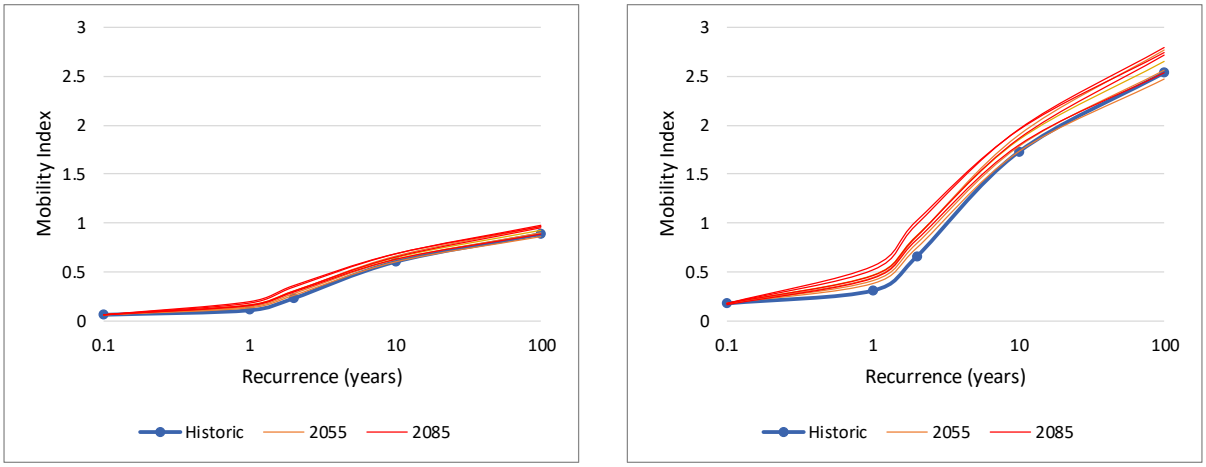


Figure 6-7. Average Mobility Index for 80% Impervious Cover, 25-acre Parcel, $S/\sqrt{d_{50}} = 0.35$ m$^{-0.5}$ (left) and $S/\sqrt{d_{50}} = 1.0$ m$^{-0.5}$ (right)

Table 6-3. Probability of Channel Instability for Runoff from 25-Acre Parcel based on 1-yr 24-hr Event with Alternative Values of $S/\sqrt{d_{50}}$

	No BMP		Wet Detention Pond	
$S/\sqrt{d_{50}}$	0.35	1.0	0.35	1.0
25% Impervious				
Historic	4.38%	99.91%	0.00%	2.53%
2055	6.76%	99.99%	0.00%	18.48%
2085	8.58%	100.00%	0.00%	37.73%
50% Impervious				
Historic	31.05%	99.99%	0.00%	2.94%
2055	40.55%	99.99%	0.00%	26.53%
2085	46.16%	100.00%	0.01%	51.59%
80% Impervious				
Historic	66.58%	100.00%	0.00%	2.91%
2055	74.64%	100.00%	0.00%	38.42%
2085	78.46%	100.00%	0.02%	69.33%

The analyses presented in this section indicate that relatively small increases in the magnitude of the runoff associated with the 1-year 24-hour storm event could result in a strong increase in the risk of channel instability. This implies that BMPs and restoration designs may not function as intended to protect stream channels if the intensity and frequency of large storm events continues to increase. However, the geomorphic impact on individual stream reaches will vary according to site-specific characteristics and cannot be predicted through a generic analysis, although *MI* curves and estimates of stability risk similar to those presented above could be developed for a specific site using GeoTools (Bledsoe et al., 2007). How predictions of increased risk should be addressed also depends on other factors, such as the useful lifespan of a design and the ability of the stream to adjust to changes as discussed further in Section 7.0.

6.2 ROADWAY FLOODING RISK

Roadway flooding is an important public safety concern associated with changing rainfall patterns. In many cases, road overtopping occurs when culvert capacity is exceeded. Overloaded culverts can also result in increased exit velocities that affect stream stability. By definition, culverts are structures that have low flexibility: once installed they are difficult and expensive to replace. It is therefore important to include a margin of safety in culvert design, which should attempt to account for potential changes in runoff over the design life.

The Maryland Department of Transportation, State Highway Administration (MDOT-SHA) provides guidelines for culvert design (MDOT-SHA, 2009) and refers to the Federal Highway Administration HDS 5 (FHWA, 2012) for hydraulic calculations. MDOT-SHA (2009) establishes different levels of service depending on road type. Culverts are designed for various storm recurrences, ranging from the 10-year

storm (peak runoff) for local streets to the 100-year storm for expressways; however, the performance of all regulated culverts must also be examined for the 100-year flood. The Froude number, for which a value of 1.0 would represent the point of conversion from sub-critical to critical turbulent flow at the outlet, must not exceed 0.9 or the pre-existing Froude number, whichever is higher, as a result of the 100-year storm. Culverts are to have a minimum diameter of 18”; 24” if the length is over 60 feet.

MDOT-SHA (2009) is not very clear on the target freeboard to be maintained between the headwater elevation and the road surface, but references HDS 5, which calls for a freeboard of 2 feet at the design flow. Calculation of flow through a culvert is complicated because culverts are generally a significant constriction to watercourse cross-sectional area and are subject to a range of gradually varied and rapidly varied flow types influenced by geometric characteristics of the culvert and those immediately upstream and downstream. Further, culvert flow may be categorized as outflow controlled (in which the tailwater elevation has a significant influence) or inlet control (in which the headwater depth at the culvert has the major influence). Culvert design calculations must simultaneously address both possibilities, leading to complex calculations. HDS 5 recommends the use of the Federal Highway Administration program HY8 (http://www.fhwa.dot.gov/engineering/hydraulics/software/hy8/), based on Schall et al. (2012), for this purpose.

For our analysis, we consider two designs for example. One is for a minor arterial road (which is designed for the 50-year event) and one is for a local road (which is designed for the 10-year event). The minor arterial representation is selected to match the Design Guideline 1 example given in FHWA (2012). The example 50-year storm peak (from a moderate sized [125-acre] watershed) is 200 cfs; the 10-year storm peak (from a smaller [75-acre] local watershed) is 24 cfs.

Both examples assume a 1% culvert slope and use of a concrete round culvert with a non-projecting end, and both have an upstream invert elevation of 100 ft and road surface at a crest elevation of 110 ft. The design must thus achieve a maximum headwater elevation of 108 ft or less after accounting for 2 feet of freeboard. A headwater elevation just below 108 ft is obtained with a 4.5 ft diameter culvert for the minor arterial example and a diameter of 1.5 ft for the local road. Figure 6-8 and Figure 6-9 show the full HY-8 specifications for these designs.

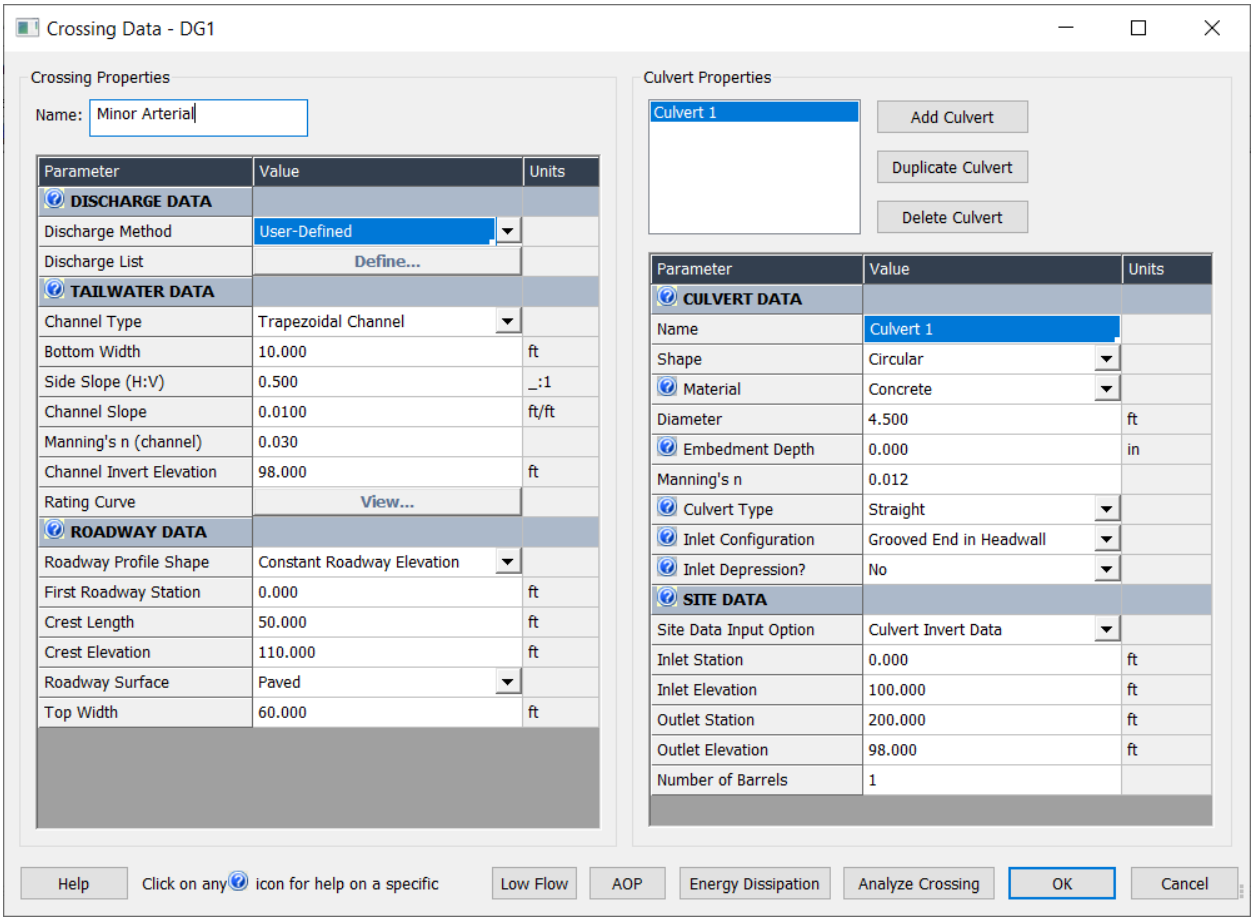


Figure 6-8. Minor Arterial Road Culvert, HY-8 Specifications

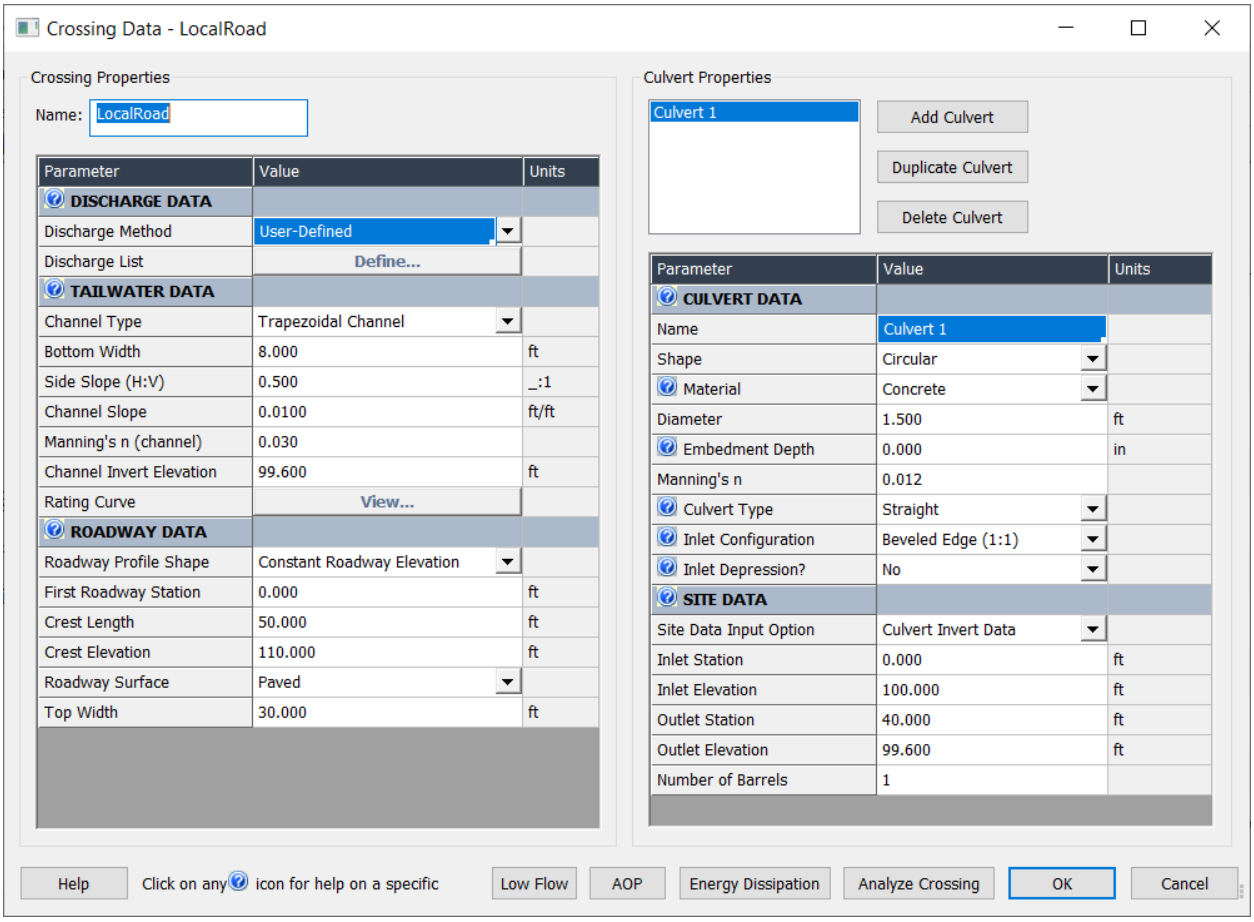


Figure 6-9. Local Road Culvert HY-8 Specifications

The two culverts described above meet requirements based on historic climate. We now examine performance under potential future climate. Section 5.0 provides predictions of runoff from a unit area urban site (at various levels of imperviousness) both with and without BMPs under present and potential future climate regimes for 79 Maryland stations. We report here on the 80% impervious simulations – using this extreme case for clarity of exposition. Similar relationships would be found at lower levels of imperviousness because the imperviousness controls the peak runoff used for both current condition design and future condition predictions.

To test culvert performance, it is necessary to convert the unit-area flows to actual flow amounts. To do this, note that for the flows of interest (10-year recurrence and above) and high imperviousness, the runoff flow peak is a linear function of the 24-hour rainfall event (Figure 6-10). This implies that it is reasonable to scale the unit-area runoff results to the magnitude of the event flows used in the culvert simulations. (Note, this ignores dissipation of the flood peak relative to variable time of concentration across the contributing watershed, but the effect is expected to be small for a highly impervious area and errs on the side of conservatism. We also assume that the *n*-year recurrence 24-hr flood event is synonymous with the runoff from the *n*-year recurrence 24-hr rainfall event, ignoring potential contributions from snowmelt.)

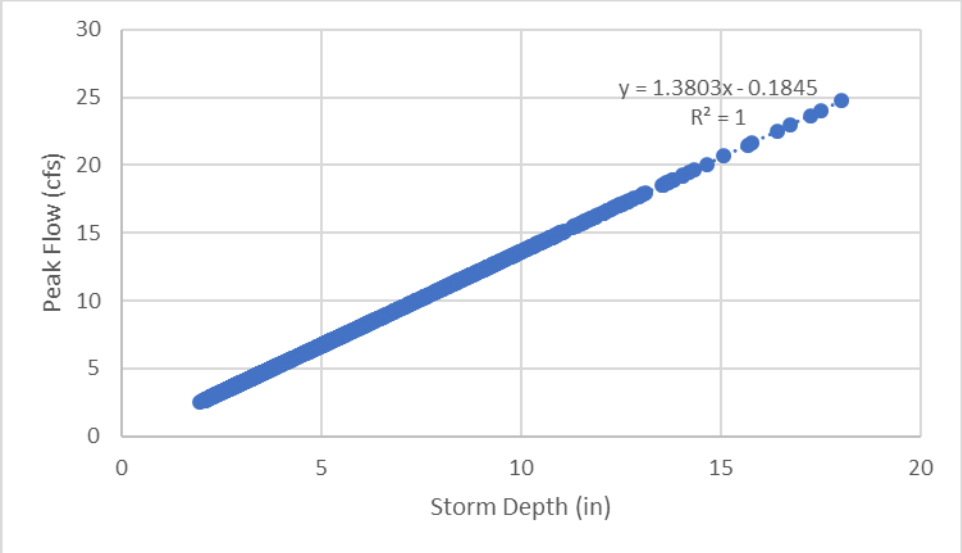


Figure 6-10. Relationship between Peak Flow from 1-acre (80% Impervious) and 24-hour Precipitation Depth

We ran HY-8 at multiple flow levels ranging from 50% to 200% of the design flow (10-year for the local road culvert and 50-year flow for the arterial culvert). Table 6-4 and Table 6-5 summarize the HY-8 results.

Table 6-4. HY-8 Results, Local Road Culvert

Total Discharge (cfs)	Culvert Discharge (cfs)	Headwater Elevation (ft)	Inlet Control Depth (ft)	Outlet Control Depth (ft)	Tailwater Depth (ft)	Outlet Velocity (ft/s)	Tailwater Velocity (ft/s)	Depth on Road (ft)	% Design Flow
12.0	12.0	102.64	2.64	2.31	0.50	7.31	2.92	0	50%
14.4	14.4	103.35	3.35	2.93	0.56	8.42	3.12	0	60%
16.8	16.8	104.15	4.15	3.63	0.61	9.77	3.30	0	70%
19.2	19.2	105.13	5.13	4.43	0.67	10.87	3.46	0	80%
21.6	21.6	106.30	6.30	5.32	0.72	12.22	3.61	0	90%
24.0	**24.0**	**107.60**	**7.60**	**6.31**	**0.76**	**13.58**	**3.75**	**0**	**100%**
26.4	26.4	109.04	9.04	7.40	0.81	14.94	3.88	0	110%
28.8	27.9	110.03	10.03	8.16	0.85	15.81	4.00	0.03	120%
31.2	28.0	110.08	10.08	8.19	0.90	15.85	4.12	0.08	130%
33.6	28.1	110.11	10.11	8.22	0.94	15.88	4.22	0.11	140%
36.0	28.1	110.14	10.14	8.24	0.98	15.90	4.33	0.14	150%
38.4	28.1	110.17	10.17	8.26	1.02	15.93	4.42	0.17	160%
40.8	28.2	110.19	10.19	8.28	1.06	15.95	4.52	0.19	170%
43.2	28.2	110.22	10.22	8.30	1.10	15.97	4.61	0.22	180%
45.6	28.3	110.24	10.24	8.31	1.13	15.98	4.69	0.24	190%
48.0	28.3	110.26	10.26	8.33	1.17	16.00	4.78	0.26	200%

Table 6-5. HY-8 Results, Minor Arterial Culvert

Total Discharge (cfs)	Culvert Discharge (cfs)	Headwater Elevation (ft)	Inlet Control Depth (ft)	Outlet Control Depth (ft)	Tailwater Depth (ft)	Outlet Velocity (ft/s)	Tailwater Velocity (ft/s)	Depth on Road (ft)	% Design Flow
100	100.00	104.29	4.29	2.11	1.60	12.66	5.81	0	50%
120	120.00	104.86	4.86	2.92	1.79	13.20	6.17	0	60%
140	140.00	105.49	5.49	4.29	1.97	13.69	6.49	0	70%
160	160.00	106.20	6.21	5.11	2.13	14.14	6.77	0	80%
180	180.00	107.01	7.01	6.00	2.30	14.54	7.03	0	90%
200	**200.00**	**107.90**	**7.90**	**6.97**	**2.45**	**14.89**	**7.27**	**0**	**100%**
220	220.00	108.88	8.88	8.01	2.60	15.10	7.49	0	110%
240	240.00	109.94	9.94	9.11	2.75	15.45	7.69	0	120%
260	244.98	110.22	10.22	9.43	2.88	15.73	7.88	0.22	130%
280	247.53	110.36	10.36	9.58	3.02	15.88	8.06	0.36	140%
300	249.67	110.48	10.48	9.71	3.15	16.00	8.23	0.48	150%
320	251.57	110.59	10.59	9.83	3.28	16.11	8.38	0.59	160%
340	253.33	110.69	10.69	9.94	3.40	16.21	8.54	0.69	170%
360	254.97	110.78	10.78	10.04	3.53	16.31	8.68	0.78	180%
380	256.52	110.87	10.87	10.14	3.65	16.40	8.82	0.87	190%
400	257.99	110.96	10.96	10.23	3.76	16.48	8.95	0.96	200%

HY-8 predictions of headwater depth and outlet velocity as a function of discharge are exactly fit by two second-order polynomials of the form $Y = \beta_2 X^2 + \beta_1 X + \beta_0$, with a break at the elevation where the road is overtopped (Figure 6-11 and Table 6-6). This allows prediction for any discharge within the polynomial fitting range (i.e., from 50% to 200% of the design flow).

The bottom portion of Figure 6-11 shows how the outlet and tailwater velocities, which may impact downstream channel stability, increase with flow.

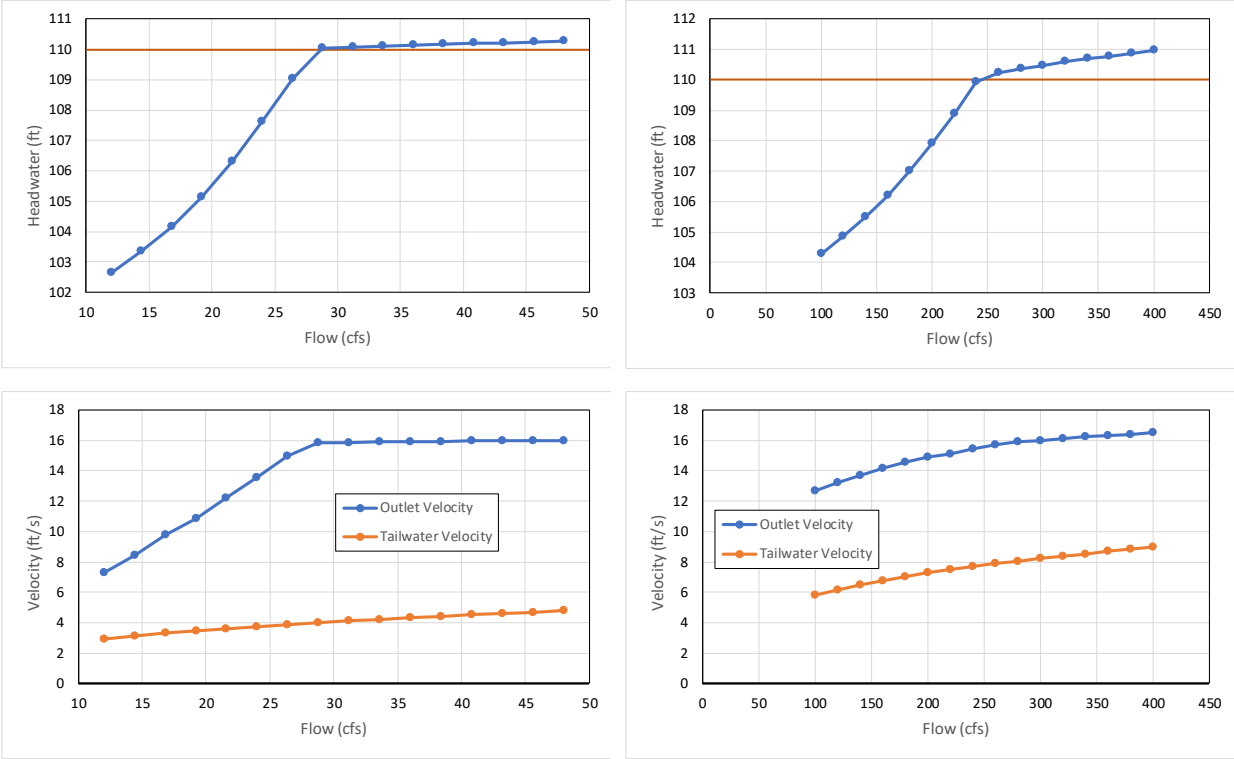
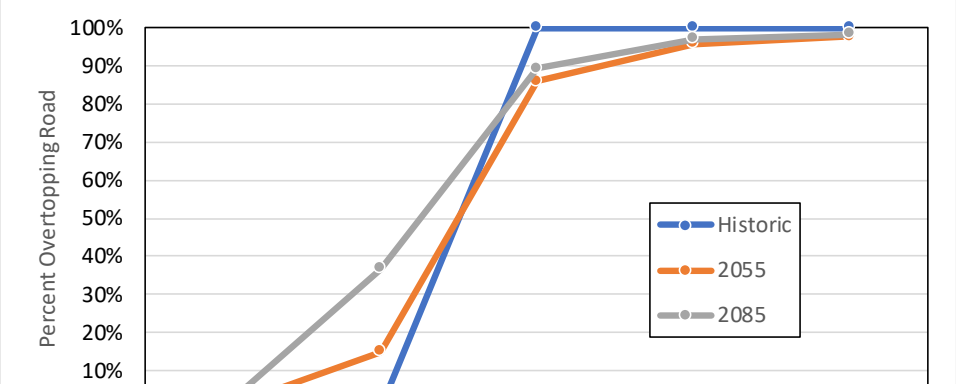


Figure 6-11. Relationship of Headwater Elevation and Outlet Velocity to Flow for Local Road (Left) and Minor Arterial (Right) Culvert Designs

Table 6-6. Polynomial Coefficients for Relationship of Headwater Elevation and Outlet Velocity to Flow

Design	Range	β_2 (X^2)	β_1 (X)	β_0
Headwater Elevation				
Local Road	Below Road	1.3496E-02	-0.0741	101.5943
	Above Road	-2.4238E-04	0.0302	109.3666
Minor Arterial	Below Road	1.0610E-04	0.0042	102.8152
	Above Road	-1.0268E-05	0.0120	107.8073
Outlet Velocity				
Local Road	Below Road	3.7781E-03	0.3856	2.1323
	Above Road	-2.1833E-04	0.0265	15.2324
Minor Arterial	Below Road	-4.4243E-05	0.0343	9.7418
	Above Road			

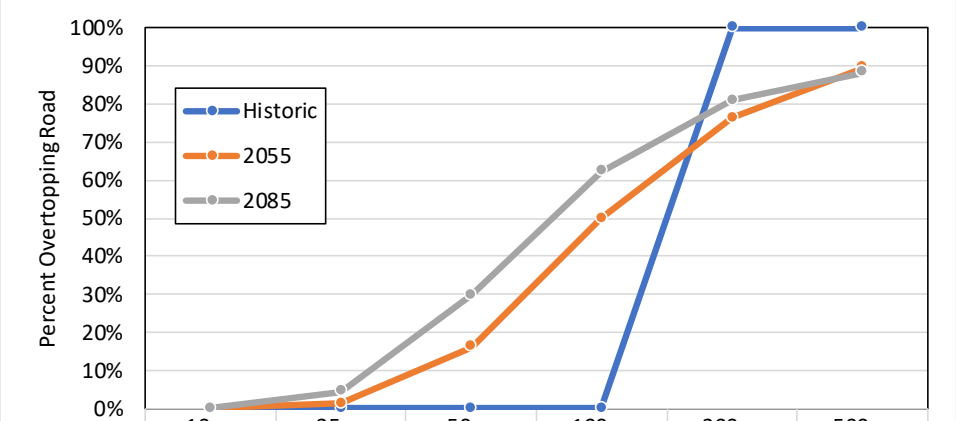
The polynomial relationships in Table 6-6 allow prediction of response to future runoff events of different recurrence frequencies (Figure 6-12 and Figure 6-13). Results are averages for all 79 Atlas 14 stations. The historic simulations are based directly on Atlas 14 IDF results, while the future climate percentages summarize results from four different downscaled GCMs per station and time.



	5-yr	10-yr	25-yr	50-yr	100-yr
Historic	0.00%	0.00%	100.00%	100.00%	100.00%
2055	0.00%	14.87%	86.08%	95.89%	97.78%
2085	0.63%	36.71%	89.24%	97.15%	98.42%

Figure 6-12. Predicted Frequency of Road Overtopping under Future Climate, Local Road Culvert

Note: Design of local road culvert is based on the 10-year event.



	10-yr	25-yr	50-yr	100-yr	200-yr	500-yr
Historic	0.00%	0.00%	0.00%	0.00%	100.00%	100.00%
2055	0.00%	1.27%	16.14%	50.00%	76.27%	89.56%
2085	0.00%	4.43%	29.75%	62.34%	81.01%	88.29%

Figure 6-13. Predicted Frequency of Road Overtopping under Future Climate, Minor Arterial Culvert

Note: Design of the minor arterial culvert is based on the 50-year event,

As expected, the culverts do not result in road overtopping at their design storm recurrence under historic climate (10-year recurrence for the local road culvert and 50-year recurrence for the minor arterial culvert.) The local road culvert results in road flooding at all stations for the 25-year event under historic climate, whereas the minor arterial culvert exceeds the target freeboard elevation (2 feet below the road surface) for the 100-year event but does not cause road flooding until flows are greater than the 100-year event.

The predicted future climate results never reach 100% overtopping because they are based on a statistical analysis of multiple GCMs that includes some instances where future extreme flows are not predicted to increase. The key result is the predicted future response to the design event for each culvert. For the local road culvert designed for the 10-year event, the risk of road overtopping during such an event is nearly 15% by 2055 and 37% by 2085. For the minor arterial culvert designed for the 50-year event, the risk of overtopping during such an event is 16% by 2055 and 30% by 2085.

Per MDOT-SHA (2009), all culverts have a minimum service life of 50 years and a service life of at least 75 years if the roadbed width is greater than 27 feet, so the results suggest that design criteria may need to be adjusted to account for future climate. Results for individual sites will of course vary according to the local climate and the characteristics of specific culverts and roads.

6.3 URBAN BMP PERFORMANCE

Water quality BMPs are used to mitigate existing or prospective impacts of land-use change and other human activities on water quality. BMPs are typically implemented through regulations and design guidance based on observations and assessment of existing problems (e.g., flooding, or bacterial impairment in a monitored waterbody) or on anticipation of potential problems based on experience with similar sites (e.g., expected impacts from new urban development). These decisions generally assume that BMPs will function as observed under historical climate, weather, and hydrological conditions. For instance, design requirements for water quality BMPs are typically based on achieving a level of control

for a design rainfall event with a given probability of occurrence, based on the past record of observed rainfall. This approach assumes that the underlying statistical properties of historical climate (e.g., average and variability) will remain unchanged in the future. From a statistical perspective, this is known as a stationary system. If the underlying conditions change, then the assumptions built into design criteria may be inappropriate, and the performance of BMPs may be less protective of waterbodies than intended.

Implicit assumptions about climate are built into guidance and regulations for both systems of BMPs and the design of individual BMP types. We consider first how future climate may affect systems of BMPs and then discuss design guidance for individual BMPs. Ultimately, it is the net effect of systems of BMPs that control impacts on water quality.

Maryland Department of the Environment's (MDE) 2000 Stormwater Design Manual presented calculations for a Water Quality volume (WQv) and a channel protection volume (CPv) for the design of stormwater BMPs. With the 2009 revisions to the Design Manual, MDE moved to the more holistic approach of Environmental Site Design (ESD), which combines the WQv and CPv objectives to produce a unified approach to stormwater design and management based on the net effects of all stormwater controls present on a site (MDE, 2009, Chapter 5).

6.3.1 BMP Systems: Environmental Site Design

The general concept of ESD is to control runoff from a developed site in response to the 1-year 24-hour storm so that it is no greater than the runoff that would be expected for the same site with a cover of undeveloped woods in good condition, considering the distribution of hydrologic soil groups on the site. ESD does not require detailed simulation modeling of developed and undeveloped conditions. Rather, it provides a simplified approach based on the relative change in Curve Number used in the National Resources Conservation Service TR-55 method (NRCS, 1986). The difference in responses to the 1-yr 24-hr event determines the excess runoff that needs to be treated (Q_E). In units of depth, $Q_E = P_E \times R_V$. R_V is the surface runoff fraction, defined as $R_V = 0.005 + 0.009 \times I$, where I is the impervious fraction expressed as a percentage. P_E is then the excess rainfall amount that needs to be treated. Rather than calculating P_E simple lookup tables are provided (one for each of the four hydrologic soil groups, A, B, C, and D). P_E is listed in the table in increments of 0.2 inches and imperviousness in increments of 5% and incorporates a single assumption about the 1-yr 24-hr storm across all of Maryland, so the answer is not exact, but is sufficient to achieve the desired level of control on average, especially when weighted across multiple subareas of a site with differing soil and development characteristics.

The approach of controlling site runoff to levels expected for woods in good condition is in theory climate neutral because both developed and woods runoff will change if climate changes. However, the table that is used to determine P_E is rooted in specific assumptions about the magnitude of the 1-yr 24-hr storm event that may not hold under future climate conditions.

We investigated how climate change might affect design criteria by examining the changes in precipitation and the resulting difference in runoff between developed and good condition woods, as predicted by TR-55, under future climate scenarios for the 79 NOAA Atlas 14 stations for which we have developed estimates of the future 1-yr 24-hr event.

The TR-55 method (NRCS, 1986) predicts runoff (Q, inches) via the curve number equation as

$$Q = \frac{(P - 0.2\,S)^2}{P + 0.8\,S}$$

where P is the 24-hr precipitation depth (inches) and S = 1000/CN – 10, where CN is the Curve Number. CN assumptions for ESD are shown in Table 2-1. CNs for developed land were calculated as a weighted mixture of the CN for connected impervious area (98) and that for open space in good condition.

Table 6-7. Curve Numbers for Environmental Site Design Simulations

Land Use	Hydrologic Soil Group			
	A	B	C	D
Woods, good condition	38	55	70	77
Developed, 25% Impervious	54	70	80	85
Developed, 50% Impervious	69	80	86	89
Developed, 80% Impervious	86	91	93	94

The runoff predicted by the CN method as well as the difference between runoff for developed land and good condition woods for a given hydrologic soil group and impervious percentage is an exact second-order polynomial function of P, as shown in Figure 2-4. This allows direct calculation of the implications of both spatial variability and magnitude of change in the 1-yr 24-hr event.

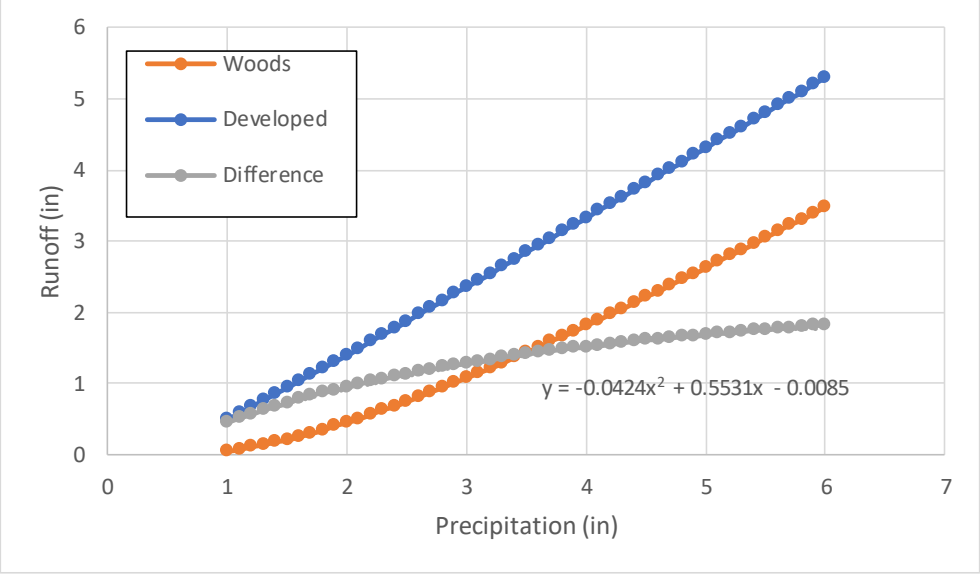


Figure 6-14. Curve Number Prediction of Runoff as a Function of Precipitation for Hydrologic Group D Soils, Developed Land at 80% Imperviousness

Note: Polynomial equation represents the difference between runoff from developed land and runoff from woods in good condition.

The 1-yr 24-hr event is predicted to increase, on average, over the course of the 21st century. The magnitude of the difference between runoff from developed land and woods in good condition (the *theoretical* Q_E) will also tend to increase, as shown for example in Table 6-8. (The statistics are based on 79 stations and four climate scenarios for each future time.) This suggests a possible need to adjust ESD P_E table in MDE (2009) in the future; however, the predicted changes in Q_E are small.

Table 6-8. Treatment Volume (Q_E, inches) for Historic and Predicted Future Climate for Hydrologic Group D Soils, Developed Land at 80% Imperviousness

Time	Minimum	Maximum	Average	Median
Historic	0.94	1.24	1.13	1.16
2055	0.91	1.42	1.19	1.21
2085	0.94	1.43	1.22	1.24

Of more relevance than how the theoretical Q_E may change over time with runoff from both undisturbed woods and developed sites calculated under a non-stationary climate is how the predicted future excess runoff compares to the Q_E that would be calculated using the tables in MDE (2009). This provides an indication of the extent to which existing ESD regulations may be sufficient to achieve the desired level of protection in the future. These results are provided in Table 6-9 through Table 6-12. In these tables a positive result means that the calculated treatment volume (the difference between runoff from developed land and good condition woods) is greater than the Q_E as calculated from the methods in Chapter 5 of MDE (2009) leading to a shortfall in treatment, while a negative result means that Q_E provides a margin relative to the site-specific target. The "Percent Exceeding" column is the percentage of trials (combinations of GCMs and stations) where the site-specific need for volume control is greater than Q_E.

Table 6-9. Relationship of Excess Stormwater Volume to Q_E Calculated using Environmental Site Design Procedure from 2009 Design Manual (MDE, 2009) – Hydrologic Soil Group A

Time	Minimum	Maximum	Average	Median	Percent Exceeding
80% Impervious, Q_E =1.85					
Historic	-0.94	-0.25	-0.51	-0.45	0.00%
2055	-1.00	0.28	-0.36	-0.33	4.50%
2085	-0.93	0.31	-0.28	-0.24	14.00%
50% Impervious, Q_E =0.90					
Historic	-0.63	-0.25	-0.40	-0.37	0.00%
2055	-0.66	0.07	-0.31	-0.30	1.10%
2085	-0.62	0.08	-0.27	-0.25	1.80%
25% Impervious, Q_E = 0.44					
Historic	-0.40	-0.26	-0.32	-0.31	0.00%
2055	-0.41	-0.12	-0.29	-0.28	0.00%
2085	-0.40	-0.12	-0.27	-0.26	0.00%

Table 6-10. Relationship of Excess Stormwater Volume to Q_E Calculated using Environmental Site Design Procedure from 2009 Design Manual (MDE, 2009) – Hydrologic Soil Group B

Time	Minimum	Maximum	Average	Median	Percent Exceeding
80% Impervious, Q_E =1.69					
Historic	-0.53	0.10	-0.13	-0.07	19.50%
2055	-0.59	0.53	0.00	0.03	59.10%
2085	-0.52	0.55	0.07	0.11	67.50%
50% Impervious, Q_E =0.90					
Historic	-0.33	0.10	-0.05	-0.02	28.00%
2055	-0.37	0.41	0.03	0.06	66.80%
2085	-0.32	0.42	0.08	0.11	74.10%
25% Impervious, Q_E = 0.44					
Historic	-0.19	0.05	-0.04	-0.02	22.90%
2055	-0.22	0.23	0.01	0.02	63.60%
2085	-0.19	0.24	0.04	0.06	72.20%

Table 6-11. Relationship of Excess Stormwater Volume to Q_E Calculated using Environmental Site Design Procedure from 2009 Design Manual (MDE, 2009) – Hydrologic Soil Group C

Time	Minimum	Maximum	Average	Median	Percent Exceeding
80% Impervious, Q_E =1.54					
Historic	-0.47	-0.06	-0.20	-0.17	0.00%
2055	-0.51	0.21	-0.12	-0.10	13.20%
2085	-0.47	0.22	-0.08	-0.05	30.50%
50% Impervious, Q_E =0.90					
Historic	-0.29	0.01	-0.10	-0.07	3.10%
2055	-0.32	0.21	-0.04	-0.02	35.50%
2085	-0.29	0.21	-0.01	0.01	55.00%
25% Impervious, Q_E = 0.33					
Historic	0.00	0.18	0.12	0.13	98.40%
2055	-0.02	0.31	0.15	0.16	99.50%
2085	0.00	0.31	0.17	0.19	99.60%

Table 6-12. Relationship of Excess Stormwater Volume to Q_E Calculated using Environmental Site Design Procedure from 2009 Design Manual (MDE, 2009) – Hydrologic Soil Group D

Time	Minimum	Maximum	Average	Median	Percent Exceeding
80% Impervious, Q_E =1.39					
Historic	-0.45	-0.15	-0.26	-0.23	0.00%
2055	-0.48	0.04	-0.20	-0.18	1.20%
2085	-0.45	0.05	-0.16	-0.14	1.80%
50% Impervious, Q_E =0.90					
Historic	-0.32	-0.10	-0.18	-0.16	0.00%
2055	-0.35	0.04	-0.14	-0.13	1.60%
2085	-0.32	0.05	-0.11	-0.10	4.70%
25% Impervious, Q_E = 0.33					
Historic	0.02	0.17	0.11	0.13	100.00%
2055	0.00	0.26	0.14	0.15	100.00%
2085	0.02	0.27	0.16	0.17	100.00%

The calculations reveal a few anomalies. For historic conditions for D soils and 25% impervious the calculated difference between runoff from developed land and good conditions woods is always greater than Q_E, and this is also almost always the case for C soils at 25% impervious, although the magnitude of the difference is small. This is primarily due to the coarse resolution of the simplified statewide tables in Chapter 5 of MDE (2009) that yields approximate P_E values only in 0.2-inch increments. For example, this results in P_E and Q_E being identical for A, B, C, and D soils at 50% impervious.

The percent of cases in which Q_E calculated under current design guidance does not provide sufficient control volume to match forest conditions does tend to increase for future climate, but, except for B soils, the change in percentage is generally small. Perhaps the most important result is that the magnitude of the difference between the calculated treatment need and Q_E is small, even under 2085 conditions. The largest average difference (2085 for C soils at 25% impervious) is 0.17 inches. Further, the biggest estimates of untreated runoff depth are associated with instances in which the statewide method already tends to underestimate the need. Where the 2085 average is greater than zero, the largest increase relative to the larger of the calculated need and Q_E is only 0.08 inches.

6.3.2 Design of Individual Practices

While the focus of urban stormwater management in Maryland has changed to ESD, MDE (2009) also provides design guidance for individual BMPs based on WQv and CPv – although the net effect of all practices on a site must still meet ESD objectives. Meeting ESD objectives will typically occur through a mix of BMPs of different types, each of which will have its own hydrologic and pollutant removal characteristics.

Unlike ESD, the design guidance for individual practices such as bioretention continues to recognize a separate WQv. The WQv is defined as the storage needed to capture and treat runoff from the 90th percentile (24-hr) rainfall event. MDE (2009) defines this event as equivalent to 1 inch in the eastern part of Maryland and 0.9 inches in the western four counties. Thus, the guidelines for BMP design are also tied to specific assumptions about historic climate, which may or may not be appropriate in the future.

Storm event runoff in excess of the WQv can bypass treatment altogether (as in BMPs based on infiltration) or be subject to reduced treatment efficiency due to less contact time (as in BMPs based on filtration or retention). Incomplete water quality treatment of runoff in excess of the WQv is expected; however, if the fraction of annual runoff that exceeds the WQv increases then the total pollutant removal efficiency will be less than expected.

As noted above in Section 4.0, we found no consistent prediction of an increase in the magnitude of the 90th percentile event across Maryland. In many cases, the future 90th percentile event was predicted to be less than the historic event. Simulations of the response of bioretention (designed for the historic WQv) to future 90th percentile events and found that the median change across all sites and scenarios resulted in a decline of 18% in total outflow by 2055 and 12% by 2085 (Section 5.2). (All these results are conditional on the LOCA statistical downscaling process and may differ using other approaches.)

The projected future results suggest that the bioretention BMP is likely to maintain (or even improve) pollutant removal efficiency in future for the majority of individual storm events. However, most climate simulations indicate that annual average total precipitation volume will increase in future, even where there is no consistent increase in the 90th percentile event. That indicates a situation where a greater fraction of annual precipitation is packed into the more extreme events above the 90th percentile. Runoff simulations suggest that the magnitude of these lower frequency events will increase over time and that the change will be greater for more extreme events. This will result in an increase in treatment bypass under such events, which could decrease the long-term average water quality performance of BMPs.

The extended wet detention results in Section 5.3 also show that, on average, the volume of the 90th percentile WQv event is predicted to decline under future climate, which would result in longer detention time and potentially greater pollutant removal. However, for larger events with recurrence intervals of one year or greater the predicted total flow through and the peak outflow from extended wet detention ponds tends to increase, resulting in reduced treatment times. The predicted changes in the performance of wet detention ponds and bioretention are thus similar. Bioretention does have an advantage of more flexibility if climate forecasts turn out to be incorrect as it is generally easier and less expensive to expand bioretention than to rebuild detention basins.

(This page left intentionally blank.)

7.0 DISCUSSION

7.1 POTENTIAL USE OF CONTINUOUS SIMULATION

A comprehensive analysis of the implications of future changes in the cumulative distribution function of rainfall events on BMP performance may require the use of continuous simulation, not just analysis of the response to events of a specified occurrence. Continuous simulation is outside the scope of the current work, which is focused on the IDF analysis. A detailed analysis should also represent the full details of realistic site layouts.

An example of such a study (in which the author of this report was a participant) is provided by Job et al. (2018). Job et al. used continuous model simulations to evaluate site conditions and BMP performance under future climate conditions in five U.S. locations, including Harford County, MD. The analysis provides insights into the potential impacts of changes in the characteristics of precipitation time series (rather than just extreme events) on stormwater infrastructure performance and allows comparison of how the responses may differ between conventional stormwater detention and GI practices.

Job et al. used the Hydrologic Simulation Program – FORTRAN (HSPF) model (Bicknell et al., 2004) to simulate hourly unit-area time series of runoff and pollutant loads (total suspended solids, total nitrogen, and total phosphorous) from pervious and impervious land. Future climate scenarios were developed from the current time series using dynamically downscaled GCMs. Realistic site layouts and associated stormwater management infrastructure were simulated using the System for Urban Stormwater Treatment and Analysis Integration (SUSTAIN) model (Shoemaker et al., 2009), a decision support system and modeling tool. Hourly output is provided by SUSTAIN for each individual BMP and at the site outlet.

The SUSTAIN stormwater management scenarios considered five types of developed land use: residential, commercial, mixed-use, ultra-urban, and green street areas combined with a variety of stormwater BMPs, ranging from gray storage infrastructure to GI designs consistent with local design standards, requirements, and guidance.

Each stormwater management approach was modeled under current and various projected future climate scenarios for the mid-21st century and evaluated for pollutant removal and ability to match pre-development hydrology. The site's practices were then modified to achieve the same or better performance as under current climate using SUSTAIN's optimization function to identify the lowest cost alternative. For the Harford County, MD study area, Job et al. modified the initial designs using two different management strategies – increasing the size of the structural storage practices and addressing water quality performance gaps by incorporating additional distributed GI practices into the site.

Gray and green BMP systems generally removed more total runoff volume and pollutant mass under future increases in precipitation and runoff compared to current conditions. However, overall site export rates of runoff volume and pollutant mass still increased (i.e., BMPs did not remove 100% of the additional runoff/pollutant load resulting from increased precipitation) despite better volume/mass removal. Changes in large storm event runoff show that BMPs designed for current conditions will likely not mitigate increases in stormwater runoff and associated downstream channel erosion and flooding impacts under projected future conditions. Thus, there may be a need for adapting site stormwater infrastructure to future precipitation conditions to protect downstream water resources. Sites may also need to be configured to be adaptable in the first place to allow for the placement of additional stormwater treatment if needed in the future.

Job et al. found that increasing BMP size/volume can mitigate the potential increases in flow, runoff volume, and pollutant loads, but larger BMPs result in increased costs. The most difficult performance measure to mitigate was usually control of large flooding event outflows, suggesting that site designs will need greater temporary volume storage and/or reconfiguration of outlet structures to mitigate flooding and channel erosion risk in locations where the magnitude of extreme events is expected to increase.

Overall, approaches to stormwater management that combined both conventional and GI elements tended to have the best combined cost resiliency. GI also provides an advantage in flexibility, because it typically has a shorter design life before rehabilitation is required – so it would be possible to commit less investment now and use an adaptive, incremental approach as the climate evolves. There is an ongoing need for additional detailed, site-specific continuous simulation studies to fully understand the ways in which BMPs, stormwater conveyance infrastructure, and receiving streams may respond to potential future climate conditions.

7.2 ADAPTATION OF BMPS IN A CHANGING CLIMATE

Stormwater management attempts to ensure desirable outcomes in the face of uncertain conditions. The presence of uncertainty is typically addressed through a risk analysis approach in which an attempt is made to minimize the probability of adverse outcomes. Traditional engineering risk assessment is based on a summary of the environmental conditions the project is likely to face (based on an implicit assumption that the past is an adequate guide to the future) accompanied by the addition of a margin of safety to protect against failure.

Climate change introduces a new level of complexity. Despite significant advances in climate science and modeling, and clearer understanding of many key aspects of climate, it is not currently possible to forecast long-term, local-scale changes in climate with accuracy. Key challenges include differing levels of confidence in projections of future climate changes at spatial and temporal scales relevant to resource managers, variability in projecting the effects of climate change and management activities on the environment, and potential nonlinear or abrupt changes (Dessai and Hulme, 2004; West et al., 2012). These uncertainties must be acknowledged, together with the recognition that climate change impacts will present an evolving, moving target throughout the coming century. It is common for managers to cite the high uncertainties associated with climate change projections as an obstacle to making adaptation decisions (Weaver et al. 2013; Hoffman et al. 2014). A key realization is that, while decision-making under large climate change uncertainties can be difficult, uncertainty is not equivalent to knowing nothing (Hoffman et al. 2014). There is a lot we know, and a large body of research and case studies that can be drawn upon to inform adaptation planning.

At the watershed/neighborhood scale, water quality protection plans typically involve a mix of gray and green practices specified to achieve a desired level of performance, with varying degrees of resilience and adaptability to change. It is important to evaluate the resilience of individual practices; however, what really matters is the resilience of the overall water quality protection plan. A typical plan will combine BMPs with varying degrees of resilience. BMPs that have low resilience and/or adaptability may well have a significant role in a water quality protection plan, but should be incorporated primarily to address short-term issues that must be addressed now and for which changing circumstances in the future are not a major concern (for example, containing and controlling runoff from a contaminated industrial site).

Uncertainty in future IDF relationships introduces uncertainty into assessment of risk and vulnerability associated with engineering designs. One approach used to minimize potential future risk is conservative

design criteria. For instance, New York City's climate resiliency guidelines suggest that the current 50-year IDF curve should be used as a proxy for the future 5-year storm for the 2080s and on-site detention/retention systems should be designed to retain the volume associated with the current 50-year curve (NYC MORR 2019). The Federal Highway Administration (FHWA) has proposed a tiered framework with five levels of analysis depending on the analysis of the risks of a project and its hydrologic service life (Kilgore et al. 2016). Where risk is high (based on asset criticality, vulnerability, and cost) and anticipated service life is long, an analysis of potential hydrologic responses to changes in both land use and climate with associated confidence intervals is needed (e.g., 68% confidence interval for service life between 30 and 75 years). Multiple types of model and data uncertainty contribute to uncertainty in estimating runoff; however, a key source of uncertainty for prospective analysis is the difference between different climate models and greenhouse gas emission scenarios. FHWA recommends evaluation over multiple climate models/scenarios to address this source of uncertainty, focusing on the potential change in the NOAA Atlas 14 analysis of 24-hour duration precipitation amounts (and associated confidence intervals) for appropriate recurrence intervals.

In general, climate-smart strategies must address both how change will affect stressors of concern and how change may alter the functionality of management actions (e.g., West et al., 2018). A key component of climate-smart strategies is implementing BMPs that will function as intended under future conditions. In practice, assessing resilience involves selecting an appropriate range of potential climate futures (hazards) and assessing the associated vulnerabilities and risks of the BMPs incorporated in a plan. While many lines of evidence can be assembled as to the likely response of BMPs to climate change, future climate conditions are subject to uncertainty. Further, the performance of BMPs may change in unexpected ways. It is therefore important to both select BMP strategies that appear to be robust under the range of likely future climate conditions and to monitor their effectiveness over time. Flexibility and adaptive management are hallmarks of sound adaptation planning and decision making under high degrees of uncertainty regarding future conditions. Three general principles applicable to BMPs and climate change are:

- **Remain as flexible as possible**—Managing under uncertainty can be a major impediment to implementing adaptation, making the flexibility of candidate strategies a recommended criterion for selection (Hoffman et al. 2014). For BMPs, flexibility and adaptability are key considerations.
- **Look for no-regrets opportunities**—Low-regret or no-regret strategies and options are widely recommended. They benefit resource management regardless of whether and how climate changes or provide a wide array of benefits (Wilby et al. 2010; Hallegatte 2009; Hoffman et al. 2014). A related principle is to consider safety-margin strategies that build in additional capacity to accommodate future climate changes because the cost of doing so now is relatively small (mainly a design change), while the cost of increasing capacity after implementation can be high.
- **Look for robust solutions**—Adaptation strategies should be implemented in a way that explicitly acknowledges future uncertainties and hedges the success of the adaptations against a wide range of plausible but uncertain future climatic conditions. Options designed based on only one climate future have a higher risk of failure if the realized climate future differs substantially from that climate future. A variety of approaches and decision tools such as traditional adaptive management and Robust Decision-Making (Groves and Lempert 2007; Fischbach et al. 2015) incorporate this principle.

7.3 STREAM RESTORATION DESIGN CONSIDERATIONS

Stream restoration designers can make use of data from predicted IDF curves as one of many factors that must be considered in developing restoration designs that will be resilient in the face of projected future climate change. Mamuye and Kebebewu (2018) cite the following changes to hydrologic conditions expected with changing climate, relevant to stream restoration and stormwater management:

- Changes in precipitation patterns
- Changes in stream flow characteristics
- Groundwater recharge and availability
- Changes in vegetation composition affecting interception process
- Changes in evapotranspiration process

Mamuye and Kebebewu (2018) also note that catchments may vary greatly in their response to changing hydrology, based on differences in local climate and catchment characteristics. Therefore, additional modeling of impacts over time, locally and regionally, will be needed to inform restoration design.

In one local example, Baran et al. (2019) quantified hydrological impacts of climate change for a portion of the Occoquan watershed in Northern Virginia. Modeling results showed a general increase in median flows in the mid- and late-21st century. Low flows were projected to decrease, while high flows were projected to increase, creating a larger range between low flows and high flows.

Johnson (2019) suggests raising the priority of climate change resilience in stream restoration design through several means. First, including resilience as an explicit planning objective may increase the long-term the success of restoration projects. Considering the ecological context and scale of a restoration action will recognize that not every site will have same potential. Biological diversity and connectivity are considered to confer resilience in restoration because they apply to a wide variety of species and ecosystems. This will include connectivity of adjacent floodplains. When biological improvements are not possible (due to water quality or watershed constraints), physical resilience may be most important.

Johnson's (2019) review of literature showed that connectivity was found to enhance the capacity for stream self-organization and recovery at multiple scales. In stream design, connectivity can be improved through restoring floodplain access to streamflow, habitat connections in floodplain and riparian area, as well as within the channel, and also barrier/dam removal that restores linear connectivity. These types of design approaches offer potential for increasing resilience.

According to Johnson (2019), success criteria for building resilience into ecological restoration may include

- Planning and monitoring for resilience, to identify sources of adaptive capacity within restored and natural ecosystems and to define actions that foster resilience
- Restoration approaches that promote natural sources of resilience are more likely to be successful than those that focus on creating optimal steady states.

Johnson notes that past trends in climate and streamflow make it clear that stationarity of the physical environment is no longer a valid assumption in restoration planning. Implications for successful design include:

- Critical importance of designing for a changing flow regime – not just increases in precipitation and flow, but also greater uncertainty
- There may be limitations on floodplain access and well-established vegetation, pointing to the need for multiple components that work together as a resilient system

- Developing appropriate long-term monitoring and success criteria, i.e., for mitigation sites
- Need to consider to physical channel characteristics, including in-depth review of watershed condition and acknowledgement of existing or potential instabilities upstream
- Need to consider soils and the role of temperature on soil erodibility
- Need to plan for expected frequent periods of inundation, changes in effects of saturation on bank stability, and altered sediment transport
- Vegetation survivability may be compromised due to drought conditions or frequent inundation of floodplain

Doll et al. (2020) present a case study from North Carolina, showing that stream and floodplain restoration can be used effectively to reduce flooding under a changing climate regime. Restoration that functions to address future flows can be an important component in a comprehensive watershed approach, providing both ecological and economic benefits.

Stream restoration guidance developed by the State of Washington and U.S. Fish and Wildlife Service (Cramer, 2012) emphasizes the need to consider strategies of resistance, resilience, and response in addressing climate change impacts. Design considerations include designing for future condition, including hydrological, sediment, and vegetation regimes. Minimizing constraints imposed on physical or ecological processes will help address inherent uncertainties, as will providing sufficient room for the stream channel and floodplain to adjust over time.

While designing a restored stream channel that is inadequately sized to accommodate future channel forming flows is an obvious concern, an over-sized channel can also induce instability. Further, while models can suggest the potential range of future flows, they do not provide a definitive prediction. Climate-smart planning for restoration design needs to consider potential future conditions but in the context of the expected design life of the project and the ability to adapt to unexpected changes. A resilient design should maximize the ability of the channel to adjust to altered conditions without setting off a cycle of geomorphic instability while also leaving space and opportunity to facilitate future restoration adjustments if needed.

(This page left intentionally blank.)

8.0 REFERENCES

Abatzoglou, J.T., and T.J. Brown. 2012. A comparison of statistical downscaling methods suited for wildfire applications. *International Journal of Climatology*, 32: 772-780, doi:10.1002/joc.2312.

Arnbjerg-Nielsen, K., P. Willems, J. Olsson, S. Beecham, A. Pathirana, I. Bülow Gregersen, H. Madssen, and V.T.-V. Nguyen. 2013. Impacts of climate change on rainfall extremes and urban drainage systems: A review. *Water Science & Technology*, 68: 16-28.

Balkema, A.A., and L. de Haan. 1974. Residual life time at great age. *Annals of Probability*, 2(5): 792-804.

Baran; A.A., G.E. Moglen, and A.N. Godrej. 2019. Quantifying hydrological impacts of climate change uncertainties on a watershed in Northern Virginia. *Journal of Hydrologic Engineering*, 24(12): 05019030

Berndtsson, J.C. 2010. Green roof performance towards management of runoff water quantity and quality: A review. *Ecological Engineering,* 36: 351-360.

Bicknell, B.R., J.C. Imhoff, J.L. Kittle, Jr., T.H. Jobes, A.S. Donigian, Jr. 2004. HSPF Version 12 User's Manual. National Exposure Research Laboratory, Office of Research and Development, U.S. Environmental Protection Agency, Athens, GA.

Bledsoe, B.P. 2002. Stream erosion potential and stormwater management strategies. *Journal of Water Resources Planning and Management,* 128(6):451-455.

Bledsoe, B.P., and C.C. Watson. 2001. Logistic analysis of channel pattern thresholds: meandering, braiding, and incising. *Geomorphology*, 38:281-300.

Bledsoe, B.P., M.C. Brown, and D.A. Raff. 2007. GeoTools: A toolkit for fluvial system analysis. *Journal of the American Water Resources Association*, 43(3):757-772.

Bonnin, G.M., D. Martin, B. Lin, T. Parzybok, M. Yekta, and D. Riley. 2006. NOAA Atlas 14, Precipitation-Frequency Analysis of the United States, Volume 2, Version 3.0: Delaware, District of Columbia, Illinois, Indiana, Kentucky, Maryland, New Jersey, North Carolina, Ohio, Pennsylvania, South Carolina, Tennessee, Virginia, West Virginia. National Oceanic and Atmospheric Administration, Silver Spring, MD. http://www.nws.noaa.gov/oh/hdsc/currentpf.htm.

Cannon, A. J., and S. Innocenti. 2019. Projected intensification of sub-daily and daily rainfall extremes in convection-permitting climate model simulations over North America: implications for future intensity-duration-frequency curves. *Natural Hazards and Earth System Sciences*, 19, 2, 421-440.

Castellano, C.M., and A.T. DeGaetano. 2017. Downscaling extreme precipitation from CMIP5 simulations using historical analogs. *Journal of Applied Meteorology and Climatology,* 56:2421-2439.

Chang, H.H. 1985. River morphology and thresholds. *Journal of Hydraulic Engineering*, 111: 503–519.

Cheng, L. and A. AghaKouchak. 2014. Nonstationary precipitation intensity-duration frequency curves for infrastructure design in a changing climate. *Scientific Reports*, 4:7093, doi:10.1038/srep07093.

Claytor, R.A., and T.R> Schueler. 1996. Design of Stormwater Filtering Systems. Chesapeake Research Consortium, Inc. Solomons, MD.

Cramer, M.L. (editor). 2012. Stream Habitat Restoration Guidelines. Copublished by the Washington Departments of Fish and Wildlife, Natural Resources, Transportation and Ecology, Washington State Recreation and Conservation Office, Puget Sound Partnership, and the U.S. Fish and Wildlife Service. Olympia, Washington.

Dahm, R., A. Bhardwaj, F.S. Weiland, G. Corzo, and L.M. Bouwer. 2019. A temperature-scaling approach for projecting changes in short duration rainfall extremes from GCM data. *Water,* 11, 313; doi:10.3390/w11020313.

Davison, A.C., and R.L. Smith. 1990. Models for exceedances over high thresholds. *Journal of the Royal Statistical Society*, 52(3): 393-442.

DeGaetano, A.T., and C.M. Castellano. 2017. Downscaled Projections of Extreme Rainfall in New York State. Northeast Regional Climate Center, Cornell University, Ithaca, NY.

Dessai, S., and M. Hulme. 2004. Does climate adaptation policy need probabilities? *Climate Policy*, 4(2):107-128.

Dixon, K.W., J.R. Lanzante, M.J. Nath, K. Hayhoe, A. Stoner, A. Radhakrishnan, V. Balaji, C.F. Gaitian, 2016. Evaluating the stationarity assumption in statistically downscaled climate projections: is past performance an indicator of future results? *Climatic Change*, 135, 395-408.

Doll, B.A.; J.J. Kurki-Fox, and D.E. Line. 2020. A Framework for planning and evaluating the role of urban atream restoration for improving transportation resilience to extreme rainfall events. *Water*, 12, 1620.

Dupigny-Giroux, L.A., E.L. Mecray, M.D. Lemcke-Stampone, G.A. Hodgkins, E.E. Lentz, K.E. Mills, E.D. Lane, R. Miller, D.Y. Hollinger, W.D. Solecki, G.A. Wellenius, P.E. Sheffield, A.B. MacDonald, and C. Caldwell. 2018: Northeast. Pp 669-742 *in* Impacts, Risks, and Adaptation in the United States: Fourth National Climate Assessment, Volume II [Reidmiller, D.R., C.W. Avery, D.R. Easterling, K.E. Kunkel, K.L.M. Lewis, T.K. Maycock, and B.C. Stewart (eds.)]. U.S. Global Change Research Program, Washington, DC. doi: 10.7930/NCA4.2018.CH18.

Easterling, D. R., J. R. Arnold, T. Knutson, K. E. Kunkel, A. N. LeGrande, L. R. Leung, R. S. Vose, D. E. Waliser, and M. F. Wehner. 2017. Precipitation Change in the United States. Climate Science Special Report: Fourth National Climate Assessment, Volume I. U.S. Global Change Research Program, Washington, DC.

Fassman-Beck, E., S. Wang, R. Simcock, and R. Liu. 2015. Assessing the effects of bioretention's engineered media composition and compaction on hydraulic conductivity and water holding capacity. *Journal of Sustainable Water in the Built Environment*, 1(4): 04015003. https://doi.org/10.1061/JSWBAY.0000799

FHWA. 2012. Hydraulic Design of Highway Culverts, Third Edition. Hydraulic Design Series Number 5, Publication No. FHWA-HIF-12-026. U.S. Department of Transportation, Federal Highway Administration, Washington, DC.

Fischbach, J.R., R.J. Lempert, E. Molina-Perez, A.A. Tariq, M.L. Finucane, and F. Hoss. 2015. Managing Water Quality in the Face of Uncertainty: A Robust Decision Making Demonstration for EPA's National Water Program. RAND Corporation, Santa Monica, CA.

Fowler, H. J., C.G. Kilsby, P.E., O'Connell, and A. Burton. 2005. A weather-type conditioned multi-site stochastic rainfall model for the generation of scenarios of climatic variability and change. *Journal of Hydrology,* 308 (1–4), 50–66.

Gallo, C., A. Moore, and J. Wywrot. 2012. Comparing the adaptability of infiltration based BMPs to various U.S. regions. *Landscape and Urban Planning*, 106(4): 326-335.

Galloway, G.E. 2011. If stationarity is dead, what do we do now? *Journal of the American Water Resources Association*, 47(3):563-570, doi:10.1111/j.1752-1688.2011.00550.x.

Groisman, P.Y., R.W. Knight, and T.R. Karl. 2012. Changes in intense precipitation over the central United States. *Journal of Hydrometeorology*, 13: 47−66.

Groves, D.G., and R.J. Lempert. 2007. A new analytical method for finding policy-relevant scenarios. *Global Environmental Change,* 17(1):73-85.

Hallegatte, S. 2009. Strategies to adapt to an uncertain climate change. *Global Environmental Change,* 19(2): 240-247. doi: 10.1016/j.gloenvcha.2008.12.003.

Hayhoe, K., D. Cayan, C.B> Field, P.C Frumhoff, E.P. Maurer, N.L. Miller, S.> Moser, S.H. Schneider, K.N. Cahill, E.E. Cleland, L. Dale, R. Drapek, R.M. Hanemann, L.S. Kalkstein, J. Lenihan, C.K. Lunch, R.P. Neilson, S.C> Sheridan, and J.H. Verville. 2004. Emissions pathways, climate change,

and impacts on California. *Proceedings of the National Academy of Sciences of the U.S.A.*, 101: 12,422-12,427, doi:10.1073/pnas.0404500101.

Hayhoe, K., D.J. Wuebbles, D.R. Easterling, D.W. Fahey, S. Doherty, J. Kossin, W. Sweet, R. Vose, and M. Wehner. 2018: Our changing climate. In Impacts, Risks, and Adaptation in the United States: Fourth National Climate Assessment, Volume II [Reidmiller, D.R., C.W. Avery, D.R. Easterling, K.E. Kunkel, K.L.M. Lewis, T.K. Maycock, and B.C. Stewart (eds.)]. U.S. Global Change Research Program, Washington, DC. doi: 10.7930/NCA4.2018.CH2.

Hoffman, J., E. Rowland, C. Hawkins Hoffman, J. West, S. Herrod-Julius, and M. Hayes. 2014. Decision Making Under Uncertainty. Chapter 12 in *Climate-Smart Conservation: Putting Adaptation Principles into Practice*, ed. B.A. Stein, P. Glick, N. Edelson, A. Staudt. National Wildlife Federation, Washington, DC.

Hoerling, M., J. Eischeid, J. Perlwitz, X.-W. Quan, K. Wolter, and L. Cheng. 2016. Characterizing recent trends in u.s. heavy precipitation. *Journal of Climate.* 29:2313–2332. DOI:10.1175/JCLI-D-15-0441.1.

Hollebrandse, F.A.P., S. Gillespie, and W. Asquith. 2015. lmoments3 Library Documentation, Release 1.0.2. https://buildmedia.readthedocs.org/media/pdf/lmoments3/latest/lmoments3.pdf, accessed 8/21/2019.

Hosking, J.R.M., and J.R. Wallis. 1997. *Regional Frequency Analysis, an Approach Based on L-Moments*. Cambridge University Press.

Howarth, M.E., C,D. Thorncroft, and L.F. Bosart. 2019. Changes in extreme precipitation in the Northeast United States: 1979–2014. *Journal of Hydrometeorology*, 20:673-689. DOI: 10.1175/JHM-D-18-0155.1

Huard, D., A. Mailhot,, and S. Duchesne. 2010. Bayesian estimation of intensity-duration-frequency curves and of the return period associated to a given rainfall event. *Stochastic Environmental Risk Assessment*, 24: 337-347.

Hunt, W. F., A.P. Davis, and R.G. Traver. 2012. Meeting hydrologic and water quality goals through targeted bioretention design. *Journal of Environmental Engineering*, 138(6): 698-707.

Job, S.C., M. Harris, S.H. Julius, J.B. Butcher, and J.T. Kennedy. 2018. Improving the Resilience of Best Management Practices in a Changing Environment: Urban Stormwater Modeling Studies. EPA/600/R-17/469F. National Center for Environmental Assessment, Office of Research and Development, U.S. Environmental Protection Agency, Washington, DC. http://ofmpub.epa.gov/eims/eimscomm.getfile?p_download_id=536305.

Johnson, D.W. 2019. Effects of a changing on stream form and flow regime: How this may impact sesign & long-term stability/monitoring. Blueline Environmental. Presentation at Mid-Atlantic Stream Conference, Baltimore, Maryland, November 2019.

Kadlec, R.H., and R.L. Knight. 1996. *Treatment Wetlands*. Lewis Publishers, Boca Raton, FL.

Khan, U. T., C. Valeo, A. Chu, and B. van Duin. 2012. Bioretention cell efficacy in cold climates: Part 1 — hydrologic performance. *Canadian Journal of Civil Engineering*, 39(11): 1210-1221.

Kilgore R.T., G. Herrmann, W.O. Thomas Jr., and D.B. Thompson. 2016. Highways in the River Environment – Floodplains, Extreme Events, Risk, and Resilience. Hydraulic Engineering Circular No. 17, 2nd Edition. FHWA-HIF-16-018. U.S. Department of Transportation, Federal Highway Administration, Washington, DC. https://www.fhwa.dot.gov/engineering/hydraulics/pubs/hif16018.pdf, accessed 12/13/19.

Kilsby, C. G., P.D. Jones, A. Burton, A.C. Ford, H.J. Fowler, C. Harpham, P. James, P., A. Smith, and R.L. Wilby. 2007. A daily weather generator for use in climate change studies. *Environmental Modelling & Software*, 22: 1705–1719.

Kristvik, E., B.G. Johannessen, and T.M. Muthanna. 2019. Temporal downscaling of IDF curves applied to future performance of local stormwater measures. *Sustainability*, 11, 1231; doi:10.3390/su11051231.

Kundzewicz, Z.W., L.J. Mata, N.W. Arnell, P. Döll, P. Kabat, B. Jiménez, K.A. Miller, T. Oki, Z. Sen, and I.A. Shiklomanov, 2007: Fresh water resources and their management. Chapter 3 in *Climate Change 2007: Impacts, Adaptation and Vulnerability. Contribution of Working Group II to the Fourth Assessment Report of the Intergovernmental Panel on Climate Change*, M.L. Parry, O.F. Canziani, J.P. Palutikof, P.J. van derLinden and C.E. Hanson, Eds. Cambridge University Press, Cambridge, UK

Kunkel, K.E., T.R. Karl, H. Brooks, J. Kossin, J.H. Lawrimore, D. Arndt, et al. 2013. Monitoring and understanding trends in extreme storms: State of knowledge. *Bulletin of the American Meteorological Society*, 94: 499–514, DOI: 10.1175/BAMS-D-11-00262.1.

Langousis, A., A. Mamalakis, M. Puliga, and R. Deidda. 2016. Threshold detection for the generalized Pareto distribution: Review of representative methods and application to the NOAA NCDC daily rainfall database. *Water Resources Research*, 52: 2659-2681, doi: 10.1002/2105WR018502.

Lettenmaier, D., J. Kim, and K. Wang. 2017. IDF relationships for the conterminous U.S.: Historical reconstructions and future projections. EGU General Assembly. 19 (18328).

Li, H., J. Sheffield, and E. F. Wood. 2010. Bias correction of monthly precipitation and temperature fields from Intergovernmental Panel on Climate Change AR4 models using equidistant quantile matching. *Journal of Geophysical Research: Atmospheres*, 115: D10101, doi:10.1029/2009JD012882.

Li, J., J. Evans, F. Johnson, and A. Sharma. 2017. A comparison of methods for estimating climate change impact on design rainfall using a high-resolution RCM. *Journal of Hydrology*, 547: 413-427.

Lynch, C., A. Seth, and J. Thibeault. 2016. Recent and projected annual cycles of temperature and precipitation in the northeast United States from CMIP5. *Journal of Climate*, 29 (1), 347–365. doi:10.1175/jcli-d-14-00781.1.

Mamuye, M., and Z. Kebebewu. 2018. Review on impacts of climate change on watershed hydrology. *Journal of Environment and Earth Science*, 8(1): 91-99.

Maraun, D., F. Wetterhall, A.M. Ireson, R.E> Chandler, E.J. Kendon, M. Widmann, S. Brienen, H.W. Rust, T. Sauter, M. Themeßl, V.K.C. Venema, K.P. Chen, C.M. Goodess, R.G. Jones, C. Onof,M. Vrac, and I. Thiele-Eich... 2010. Precipitation downscaling under climate change: Recent developments to bridge the gap between dynamical models and the end user. *Reviews of Geophysics*, 48, RG3003, doi:10.1029/2009RG000314.

Maurer, E.P., L. Brekke, T. Pruitt, and P. Duffy. 2007. Fine-resolution climate projections enhance regional climate change impact studies. *EOS*, 88, 504, doi: 10.1029/2007EO470006.

MDE. 2009. 2000 Maryland Stormwater Design Manual, Volumes I and II (Revised May 2009). Maryland Dept. of the Environment (MDE).

MDOT-SHA. 2009. Highway Drainage Manual Design Guidelines Culverts. Maryland Department of Transportation, State Highway Administration.

Mehran, A., A. AghaKouchak, and T.J. Philips. 2014. Evaluation of CMIP5 continental precipitation simulations relative to satellite-based gauge-adjusted observations. *Journal of Geophysical Research: Atmospheres*, 119: 1695-1707. doi:10.1002/2013JD021152

Milly, P.C.D., J. Betancourt, M. Falkenmark, R.M. Hirsch, Z.W. Kundzewicz, D.P. Lettenmaier, and R.J. Stouffer. 2008. Stationarity is dead: Whither water management? *Science*, 319: 573-574, doi:10.1126/science.1151915.

Nover, D.M., J.W. Witt, J.B. Butcher, T.E. Johnson, and C.P. Weaver. 2016. The effects of downscaling method on the variability of simulated watershed response to climate change in five U.S. basins. *Earth Interactions*. doi: 10.1175/EI-D-15-0024.1.

NRCS. 1986. Urban Hydrology for Small Watersheds. TR-55. U.S. Dept. of Agriculture, Natural Resources Conservation Service.

NYC-MORR. 2019. Climate Resiliency Design Guidelines, Version 3.0. New York City Mayor's Office of Recovery and Resilience. https://www1.nyc.gov/assets/orr/pdf/NYC_Climate_Resiliency_Design_Guidelines_v3-0.pdf, accessed 12/13/19.

Onof, C., and K. Arnbjerg-Nielsen. 2009. Quantification of anticipated future changes in high resolution design rainfall for urban areas. *Atmospheric Research*, 92(3): 350-363.

Palmer, M. A., E. S. Bernhardt, J. D. Allan, P. S. Lake, G. Alexander, S. Brooks, J. Carr, S. Clayton, C. N. Dahm, J. Follstad Shah, D.L. Galat, S. G. Loss, P. Goodwin, D. D. Hart, B. Hassett, R. Jenkinson, G. M. Kondolf, R. Lave, J. L. Meyer, T. K. O'Donnell, L. Pagano, and E. Sudduth. 2005. Standards for ecologically successful river restoration. *Journal of Applied Ecology*, 42(2): 208-217.

Panofsky, H.A. and G.W. Brier. 1968. *Some Applications of Statistics to Meteorology*. Pennsylvania State University, University Park, PA

Perica, S., D. Martin, S. Pavlovic, I. Roy, M. St. Laurent, C. Trypaluk, D. Unruh, M. Yekta, and G. Bonnin. 2013. Precipitation-Frequency Atlas of the United States. NOAA Atlas No. 14, Volume 8 Version 2.0: Midwestern States (Colorado, Iowa, Kansas, Michigan, Minnesota, Missouri, Nebraska, North Dakota, Oklahoma, South Dakota, Wisconsin). National Oceanic and Atmospheric Administration, Silver Spring, MD. http://www.nws.noaa.gov/oh/hdsc/currentpf.htm.

Pickands, J. III. 1975. Statistical inference using extreme order statistics. *Annals of Statistics*, 3(1): 119-131.

Pierce, D.W., D.R. Cayan, and B.L. Thrasher. 2014. Statistical downscaling using localized constructed analogs (LOCA). *Journal of Hydrometeorology*, 15:2558-2585. https://doi.org/10.1175/JHM-D-14-0082.1.

Prodanovic, P., and S.P. Simonovic. 2007. Development of Rainfall Intensity Duration Frequency Curves for the City of London under the Changing Climate. Report No. 058. Department of Civil and Environmental Engineering, The University of Western Ontario, London, Ontario, Canada.

Raff, D.A., B.P. Bledsoe, A.N. Flores, and M.C. Brown. 2007. GeoTools User's Manual. Engineering Research Center, Colorado State University.

Ragno, E., A. AghaKouchak, C.A. Love, L. Cheng, F. Vahedifard, and C.H.R. Lima. 2018. Quantifying changes in future intensity-duration-frequency curves using multimodel ensemble dimulations. *Water Resources Research*, 54(3): 1751-1764.

Roseen, R.M., T.P. Ballestero, J.J. Houle, P. Avellaneda, J. Briggs, G. Fowler, and R. Wildey. 2009. Seasonal performance variations for storm-water management systems in cold climate conditions. *Journal of Environmental Engineering*, 135: 128-137.

Rosenberg, E.A., P.W. Keys, D.B. Booth, D. Hartley, J. Burkey, A.C. Steinemann,·and D.P. Lettenmaier. 2010. Precipitation extremes and the impacts of climate change on stormwater infrastructure in Washington State. *Climatic Change*, doi 10.1007/s10584-010-9847-0

Rossman, L. 2015. Storm Water Management Model, User's Manual Version 5.1. EPA 600/R-14/413b. National Risk Management Laboratory, Office of Research and Development, U.S. Environmental Protection Agency, Cincinnati, OH.

Schall, J.D., P.L. Thompson, S.M. Zerges, R.T. Kilgore, and J.L. Morris. 2012. Hydraulic Design of Highway Culverts, Third Edition. Hydraulic Design Series # 5, FHWA-NHI-12-029. Federal Highway Administration, Washington, DC.

SCS. 1986. Urban Hydrology for Small Watersheds. Technical Release 55. U.S. Dept. of Agriculture, Soil Conservation Service, Washington, DC.

Serinaldi, F., and C.G. Kilsby. 2014. Rainfall extremes: Toward reconciliation after the battle of distributions. *Water Resources Research*, 50: 336-352, doi:10.1102/2013WR014211.

Simon A., W. Dickerson, and A. Heins. 2004. Suspended-sediment transport rates at the 1.5-year recurrence interval for ecoregions of the United States: Transport conditions at the bankfull and effective discharge? *Geomorphology*, 58: 243-246.

Shoemaker, L., J. Riverson Jr., K. Alvi, J.X. Zhen, S. Paul, and T. Rafi. 2009. SUSTAIN—A Framework for Placement of Best Management Practices in Urban Watersheds to Protect Water Quality. EPA/600/R-09/095. National Risk Management Research Laboratory, Office of Research and Development, U.S. Environmental Protection Agency, Cincinnati, OH.

Shrestha, A., M.S. Babel, S. Weesakul, and Z. Vojinovic. 2017. Developing Intensity-Duration-Frequency (IDF) curves under climate change uncertainty: The case of Bangkok, Thailand. *Water*, 9, 145, doi:10.3390/w9020145.

Sillmann, J., V.V. Kharin, X. Zhang, F.W. Zwiers, and D. Bronaugh. 2013. Climate extremes indices in the CMIP5 multimodel ensemble: Part 1. Model evaluation in the present climate. *Journal of Geophysical Research: Atmospheres*, 118:1716-1733. doi: 10.1002/jgrd.50203.

So, B.-J., J.-Y. Kim, H.-H. Kwon, and C.H.R. Lima. 2017. Stochastic extreme downscaling model for an assessment of changes in rainfall intensity-duration-frequency curves over South Korea using multiple regional climate models. *Journal of Hydrology*, 553: 321-337.

Srivastav, R.K., A. Schardong, and S. P. Simonovic. 2014a. Equidistance quantile matching method for updating IDF Curves under climate change. *Water Resources Management*, doi:10.1007/s11269-014-0626-y.

Srivastav, R.K., A. Schardong, and S.P. Simonovic. 2014b. Computerized Tool for the Development of Intensity-Duration-Frequency Curves under a Changing Climate. Water Resources Research Report 089, University of Western Ontario, Dept. of Civil and Environmental Engineering, London, Ontario.

Sun, Y., S. Solomon, A. Dai, A., and R. Portmann. 2006. How often does it rain? *Journal of Climate*, 19, 916–934, doi:10.1175/JCLI3672.1.

Thibeault, J. M., and A. Seth. 2014. Changing climate extremes in the Northeast United States: Observations and projections from CMIP5. *Climatic Change*, 127 (2), 273–287. doi:10.1007/s10584-014-1257-2.

Vu, M.T., S.V. Raghavan, J. Liu, and S.-Y. Liong. 2018. Constructing short-duration IDF curves using coupled dynamical-statistical approach to assess climate change impacts. *International Journal of Climatology*, 38(6): 2662-2671.

Walsh, C. J., A. H. Roy, J. W. Feminella, P. D. Cottingham, P. M. Groffman, and R. P. Morgan. 2005. The urban stream syndrome: current knowledge and the search for a cure. *Journal of the North American Benthological Society*, 24:706-723.

Wang, G., C. Kirchhoff, A. Seth, J.T. Abatzoglou, B. Livneh, D.W. Pierce, L. Fomenko, and T. Ding. 2020. Projected changes of precipitation characteristics depend on downscaling method and training data: MACA vs. LOCA using the U.S. Northeast as an example. Accepted by *Journal of Hydrometeorology*, doi: 10.1175/JHM-D-19-0275.1. http://journals.ametsoc.org/jhm/article-pdf/doi/10.1175/JHM-D-19-0275.1/4984827/jhmd190275.pdf.

Weaver, C.P., R.J. Lempert, C. Brown, J.A. Hall, D. Revell, and D. Sarewitz. 2013. Improving the contribution of climate model information to decision making: The value and demands of robust decision frameworks. *WIREs: Climate Change,* 4(1):39-60. doi: 10.1002/wcc.202.

West, J.M., C.A. Courtney, A.T. Hamilton, B.A. Parker, D.A. Gibbs, P. Bradley, and S.H. Julius. 2018. Adaptation design tool for climate-smart management of coral reefs and other natural resources. *Environmental Management*, 62: 644–664.

West, J.M., S.H. Julius, and C.P. Weaver. 2012. Assessing confidence in management adaptation approaches for climate-sensitive ecosystems. *Environmental Research Letters*, 7(1):1-8.

Wilby, R.L., H. Orr, G. Watts, R.W. Battarbee, P.M. Berry, R. Chadd, S.J. Dugdale, M.J. Dunbar, J.A. Elliott, C. Extence, D.M. Hannah, N. Holmes, A.C. Johnson, B. Knights, N.J. Milner, S.J. Ormerod, D. Solomon, R. Timlett, P.J. Whitehead, and P.J. Wood. 2010. Evidence needed to manage freshwater ecosystems in a changing climate: Turning adaptation principles into practice. *Science of the Total Environment,* 408(19):4150-4164. doi: 10.1016/j.scitotenv.2010.05.014.

Willems, P., and M. Vrac. 2011. Statistical precipitation downscaling for small-scale hydrological impact investigations of climate change. *Journal of Hydrology*, 402: 193–205.

Wolman, M.G., and J.P. Miller. 1960. Magnitude and frequency of forces in geomorphic processes. *Journal of Geology*, 68:54-74.

Wood, A. W., L. Leung, V. Sridhar, and D. P. Lettenmaier. 2004. Hydrologic implications of dynamical and statistical approaches to downscaling climate model outputs. *Climatic Change*, 62: 189-216, doi: 10.1023/B:CLIM.0000013685.99609.9e.

(This page left intentionally blank.)

APPENDIX A. PYTHON CODE

A-1. IDF UPDATES

The IDF processing code consists of six linked Python 3 scripts that must be run in order:

1. Get_Atlas14.py

```
import sys, os
import pandas as pd
import numpy as np
import urllib.request, urllib.error
from http.cookiejar import CookieJar

sites_file=r'O:\Projects\Chesapeake Bay Trust\2019 RRsc5 -
IDF\Work\IDFAnalysis\IDF_python\MD_sites_Atlas14.csv'
odir = r"O:\Projects\Chesapeake Bay Trust\2019 RRsc5 -
IDF\Work\IDFAnalysis\IDF_python\Atlas14_data"

sites_df=pd.read_csv(sites_file)

# def ATLAS14_dl(self, userLat, userLong, saveLocation, loggy):
# outf = open(loggy, "a")
# saveLocation = os.path.join(saveLocation, 'Atlas14_data')
# if not os.path.exists(saveLocation): os.makedirs(saveLocation)


for idx,site in sites_df.iterrows():
    userLat=float(site['Latitude'])
    userLong=float(site['Longitude'])
    station=site['StationID']

    # Get all IDF curve
    file = station + "_PFTabular.csv"
    outfile = os.path.join(odir, file)
    if not os.path.exists(outfile):
        try:
            url = "https://hdsc.nws.noaa.gov/cgi-bin/hdsc/new/fe_text.csv?lat=" + str(userLat) + "&lon=" +
str(userLong)
            url = url + "&type=pf&data=depth&units=english&series=pds"
            password_manager = urllib.request.HTTPPasswordMgrWithDefaultRealm()
            cookie_jar = CookieJar()
            opener = urllib.request.build_opener(
                urllib.request.HTTPBasicAuthHandler(password_manager),
                urllib.request.HTTPCookieProcessor(cookie_jar))
            urllib.request.install_opener(opener)
```

```
            request = urllib.request.Request(url)
            response = urllib.request.urlopen(request)
            body = response.read()
            with open(outfile, 'wb') as f:
                f.write(body)
            print (file + " Successfully downloaded from NOAA Atlas 14 webpage")
        except Exception as ex:
            print ("FAILURE - unable to download " + file)
    else:
        print (file + " already exists")

    # Get annual max series
    file = "MD_" + station + "_ams.txt"
    outfile = os.path.join(odir, file)
    if not os.path.exists(outfile):
        try:
            url = "https://hdsc.nws.noaa.gov/pub/hdsc/data/_TimeSeries_stations/" + "MD_" + station +
"_ams.txt"
            password_manager = urllib.request.HTTPPasswordMgrWithDefaultRealm()
            cookie_jar = CookieJar()
            opener = urllib.request.build_opener(
                    urllib.request.HTTPBasicAuthHandler(password_manager),
                    urllib.request.HTTPCookieProcessor(cookie_jar))
            urllib.request.install_opener(opener)
            request = urllib.request.Request(url)
            response = urllib.request.urlopen(request)
            body = response.read()
            with open(outfile, 'wb') as f:
                f.write(body)
            print (file + " Successfully downloaded from NOAA Atlas 14 webpage")
        except Exception as ex:
            print ("FAILURE - unable to download " + file)
            print (url)
    else:
        print (file + " already exists")


#    GET mean IDF curve
    file = station + "_existing IDF.csv"
    outfile = os.path.join(odir, file)
    if not os.path.exists(outfile):
        try:
            url = "https://hdsc.nws.noaa.gov/cgi-bin/hdsc/new/fe_text_mean.csv?lat=" + str(userLat) + "&lon="
+ str(userLong)
            url = url + "&type=pf&data=depth&units=english&series=pds"
                #state = " " + state
                #state = state.replace(' ', '%')
```

```
            #url = url + &selElevNum=" + C_elev + "&selElevSym=ft&selStaName=" + C_name.replace('
', '%20')
        password_manager = urllib.request.HTTPPasswordMgrWithDefaultRealm()
        cookie_jar = CookieJar()
        opener = urllib.request.build_opener(
            urllib.request.HTTPBasicAuthHandler(password_manager),
            urllib.request.HTTPCookieProcessor(cookie_jar))
        urllib.request.install_opener(opener)
        request = urllib.request.Request(url)
        response = urllib.request.urlopen(request)
        body = response.read()
        with open(outfile, 'wb') as f:
          f.write(body)
        print (file + " Successfully downloaded from NOAA Atlas 14 webpage")
      except Exception as ex:
        print ("FAILURE - unable to download " + file)
  else:
    print (file + " already exists")
```

2. Get_Atlas14_extra_ams.py

```
import sys, os
import pandas as pd
import numpy as np
import urllib.request, urllib.error
from http.cookiejar import CookieJar


sites_file=r'O:\Projects\Chesapeake Bay Trust\2019 RRsc5 -
IDF\Work\IDFAnalysis\IDF_python\Atlas14_extra_ams.csv'
odir = r"O:\Projects\Chesapeake Bay Trust\2019 RRsc5 -
IDF\Work\IDFAnalysis\IDF_python\Atlas14_ams"

sites_df=pd.read_csv(sites_file)

for idx,site in sites_df.iterrows():
  state=site['State']
  station=site['StationID']

  # Get annual max series
  file = state +"_" + station + "_ams.txt"
  outfile = os.path.join(odir, file)
  if not os.path.exists(outfile):
    try:
      url = "https://hdsc.nws.noaa.gov/pub/hdsc/data/_TimeSeries_stations/" + state + "_" + station +
"_ams.txt"
      password_manager = urllib.request.HTTPPasswordMgrWithDefaultRealm()
```

```
            cookie_jar = CookieJar()
            opener = urllib.request.build_opener(
                  urllib.request.HTTPBasicAuthHandler(password_manager),
                  urllib.request.HTTPCookieProcessor(cookie_jar))
            urllib.request.install_opener(opener)
            request = urllib.request.Request(url)
            response = urllib.request.urlopen(request)
            body = response.read()
            with open(outfile, 'wb') as f:
               f.write(body)
            print (file + " Successfully downloaded from NOAA Atlas 14 webpage")
         except Exception as ex:
            print ("FAILURE - unable to download " + file)
            print (url)
      else:
         print (file + " already exists")
```

3. LOCA_dailymax_hist.py

```
# -*- coding: utf-8 -*-
"""
Created on Mon Dec  2 12:22:10 2019

@author: scott.job
"""

import os
from netCDF4 import Dataset
import numpy as np
import pandas as pd
from datetime import datetime, timedelta



sites_file=r'O:\Projects\Chesapeake Bay Trust\2019 RRsc5 -
IDF\Work\IDFAnalysis\IDF_python\StationGCM_hist.csv'
idir = r"O:\Projects\Chesapeake Bay Trust\2019 RRsc5 - IDF\Work\IDFAnalysis\IDF_python\LOCA_data"
nc_file = 'loca_ACCESS1-0_rcp45_ppt.nc'
odir = r"O:\Projects\Chesapeake Bay Trust\2019 RRsc5 -
IDF\Work\IDFAnalysis\IDF_python\LOCA_output"
ofile = 'DailyMaxPrec_Hist_Results.csv'
startyr = 1950
endyr = 2005

sites_df = pd.read_csv(sites_file)
df_out = pd.DataFrame()
```

```
# Get lat-long grid cell arrays from one of the netCDF files (assumes all are the same)
nc = Dataset(os.path.join(idir,nc_file))
gcmlat = nc.variables['lat'][:]
gcmlong = nc.variables['lon'][:]
gcmlong = list(map(lambda x: x - 360, gcmlong))

for idx,site in sites_df.iterrows():
    station=site['StationID']
    gcm = site['GCM']
    siteLat=float(site['Latitude'])
    siteLong=float(site['Longitude'])
    # find closest gcm cell to station
    lat_idx,lat_val = min(enumerate(gcmlat), key=lambda x: abs(siteLat - x[1]))
    long_idx,long_val = min(enumerate(gcmlong), key=lambda x: abs(siteLong - x[1]))
    # open connection to netCDF file
    file = "loca_" + gcm + "_historical_ppt.nc"
    nc = Dataset(os.path.join(idir,file))
    # set conversion factor to in/day, accounting for varying time units and mm to in
    # netCDF4 module automatically applies scale_factor when data are retrieved, no need to account for
it
    for var in nc.variables.keys():
        if 'pr' in var:
            break
    cfact = 1
    units = str(nc.variables[var].units)
    if 's-1' in units:
        cfact = cfact * 86400
    cfact = cfact * 0.0393701
    # set time array
    CDFtime = nc.variables['time'][:]
    index = np.zeros(len(CDFtime),dtype='datetime64[D]')
    for i in range(0,len(CDFtime)): index[i] = datetime(1900,1,1,0,0,0) + timedelta(days=int(CDFtime[i]))
    # retrieve max daily prec for each year in period
    df = pd.DataFrame(index=index)
    df['MaxDailyPrec'] = nc.variables[var][:,lat_idx,long_idx]
    df = df * cfact
    df = df.loc[str(startyr) + '-1-1':str(endyr) + '-12-31']
    df = df.resample('Y').max()

    df['Station'] = station
    df['GCM'] = gcm
    df_out = pd.concat([df_out,df],sort=False)
    nc.close()
    print('Finished processing: ', station,' ',gcm)

df_out.index.name = 'Year'
ofile = os.path.join(odir,ofile)
```

```
df_out.to_csv(ofile,date_format='%Y')
```

4. LOCA_dailymax_fut.py

```
# -*- coding: utf-8 -*-
"""
Created on Mon Dec  2 12:22:10 2019

@author: scott.job
"""

import os
from netCDF4 import Dataset
import numpy as np
import pandas as pd
from datetime import datetime, timedelta



sites_file=r'O:\Projects\Chesapeake Bay Trust\2019 RRsc5 -
IDF\Work\IDFAnalysis\IDF_python\StationGCM_fut.csv'
idir = r"O:\Projects\Chesapeake Bay Trust\2019 RRsc5 - IDF\Work\IDFAnalysis\IDF_python\LOCA_data"
nc_file = 'loca_ACCESS1-0_rcp45_ppt.nc'
odir = r"O:\Projects\Chesapeake Bay Trust\2019 RRsc5 -
IDF\Work\IDFAnalysis\IDF_python\LOCA_output"
ofile = 'DailyMaxPrec_Fut_Results.csv'

sites_df = pd.read_csv(sites_file)
df_out = pd.DataFrame()

# Get lat-long grid cell arrays from one of the netCDF files (assumes all are the same)
nc = Dataset(os.path.join(idir,nc_file))
gcmlat = nc.variables['lat'][:]
gcmlong = nc.variables['lon'][:]
gcmlong = list(map(lambda x: x - 360, gcmlong))

for idx,site in sites_df.iterrows():
    station=site['StationID']
    period = site['Period']
    startyr = site['StartYr']
    endyr = site['EndYr']
    pcntl = site['Percentile']
    gcm = site['GCM']
    rcp = site['rcp']
    siteLat=float(site['Latitude'])
    siteLong=float(site['Longitude'])
    # find closest gcm cell to station
```

```
    lat_idx,lat_val = min(enumerate(gcmlat), key=lambda x: abs(siteLat - x[1]))
    long_idx,long_val = min(enumerate(gcmlong), key=lambda x: abs(siteLong - x[1]))
    # open connection to netCDF file
    file = "loca_" + gcm + "_" + rcp + "_ppt.nc"
    nc = Dataset(os.path.join(idir,file))
    # set conversion factor to in/day, accounting for varying time units and mm to in
    # netCDF4 module automatically applies scale_factor when data are retrieved, no need to account for
it
    for var in nc.variables.keys():
        if 'pr' in var:
            break
    cfact = 1
    units = str(nc.variables[var].units)
    if 's-1' in units:
        cfact = cfact * 86400
    cfact = cfact * 0.0393701
    # set time array
    CDFtime = nc.variables['time'][:]
    index = np.zeros(len(CDFtime),dtype='datetime64[D]')
    for i in range(0,len(CDFtime)): index[i] = datetime(1900,1,1,0,0,0) + timedelta(days=int(CDFtime[i]))
    # retrieve max daily prec for each year in period
#    df = pd.DataFrame(index=index,columns=['AnnualPrec'])
    df = pd.DataFrame(index=index)
    df['MaxDailyPrec'] = nc.variables[var][:,lat_idx,long_idx]
    df = df * cfact
    df = df.loc[str(startyr) + '-1-1':str(endyr) + '-12-31']
    df = df.resample('Y').max()

    df['Station'] = station
    df['Period'] = period
    df['Percentile'] = pcntl
    df['GCM'] = gcm
    df['rcp'] = rcp
    df_out = pd.concat([df_out,df],sort=False)
    nc.close()
    print('Finished processing: ', station,' ',period, ' ', pcntl)

df_out.index.name = 'Year'
ofile = os.path.join(odir,ofile)
df_out.to_csv(ofile,date_format='%Y')
```

5. Preprocess_AMP.py

```
import os
import pandas as pd
#import numpy as np
```

```
input_dir = r"O:\Projects\Chesapeake Bay Trust\2019 RRsc5 -
IDF\Work\IDFAnalysis\IDF_python\Atlas14_ams\source"
hourly_out_dir = r"O:\Projects\Chesapeake Bay Trust\2019 RRsc5 -
IDF\Work\IDFAnalysis\IDF_python\Atlas14_ams\proc_hourly"
daily_out_dir = r"O:\Projects\Chesapeake Bay Trust\2019 RRsc5 -
IDF\Work\IDFAnalysis\IDF_python\Atlas14_ams\proc_daily"
lookup_file = r"O:\Projects\Chesapeake Bay Trust\2019 RRsc5 -
IDF\Work\IDFAnalysis\IDF_python\MD_sites_Atlas14.csv"

# identifiers cannot begin with a number
hoursList = ['c01h', 'c02h', 'c03h', 'c06h', 'c12h', 'c24h']
durations = ['1-hr','2-hr','3-hr','6-hr','12-hr','24-hr']

df_final = pd.DataFrame()
df_hourly = pd.DataFrame()
drop_year = list()

logfile = r"O:\Projects\Chesapeake Bay Trust\2019 RRsc5 -
IDF\Work\IDFAnalysis\IDF_python\Atlas14_ams\ams_error_log.txt"
loglines = list()

#files = ['WV_46-4763_ams.txt', 'WV_46-1324_ams.txt', 'WV_46-1323_ams.txt']
#for filename in files:
for filename in os.listdir(input_dir):
    lines = []
    file = os.path.join(input_dir,filename)
    with open(file, 'r') as fileY:
        for row in fileY:
            row = row.split()
            lines.append(row)
    fileY.close()

    df = pd.DataFrame(columns=['duration','year','depth'])

    station = filename
    station = station.replace('_ams.txt','')
    writer = 0
    for row in lines:
        if row == []:
            writer = 0
            pass
        elif row[0] == 'Duration:':
            dur = row[1]
            writer = 1
            pass
```

```
        elif writer == 1:
            if float(row[1]) > 1800:
                if float(row[0]) > 0:
                    df = df.append({'duration': 'c' + dur, 'year': row[1], 'depth': float(row[0])}, ignore_index=True)
                else:
                    pass
            else:
                if float(row[1]) > 0:
                    date = row[0].split('/')
                    if int(date[2]) < 1800:
                        loglines.append("Error improper date format. Duration = " + dur + " Station = " + station +
"\n")
                        pass
                    else:
                        df = df.append({'duration': 'c' + dur, 'year': date[2], 'depth': float(row[1])},
ignore_index=True)
                else:
                    pass
        else:
            pass

    df_01d = df.loc[df['duration']=='c01d'].copy()
    if df_01d.empty == False:
        df_01d['station'] = station
        df_final = pd.concat([df_final,df_01d],ignore_index = True)


    if df['duration'].isin(hoursList).any():
        df_hourly = pd.pivot_table(df,values = 'depth',index = 'year',columns='duration')
        df_hourly = df_hourly[hoursList]
        df_hourly.dropna(how='all',inplace=True)
        if df_hourly.isnull().values.any():
            loglines.append(station + " has NaN\n")
            df_hourly.dropna(how='any', inplace=True)
        drop_year.clear()
        for i in range(df_hourly.shape[0]):
            durs = df_hourly.iloc[i]
            if not durs.is_monotonic:
                loglines.append('station ' + station + ', year ' + durs.name + "\n")
                drop_year.append(durs.name)
        for year in drop_year:
            df_hourly.drop(labels=year, inplace=True)
        df_hourly.columns = durations
        ofile = os.path.join(hourly_out_dir,station + '_proc.csv')
        df_hourly.to_csv(ofile)

    print('Processed ',station)
```

```
daily_out_file = os.path.join(daily_out_dir,'daily_ams_all.csv')
df_final.to_csv(daily_out_file)

with open(logfile, 'w') as the_file:
    the_file.writelines(loglines)
    the_file.close

lookup_df = pd.read_csv(lookup_file)

ratios = pd.DataFrame(columns = ['Station', 'Remote_Daily_Station', 'Ratio', 'Matched_Years'])
df_final.drop(['duration'], axis=1, inplace=True)
for idx,stadata in lookup_df.iterrows():
    dailysta = (stadata['State'] + "_" + stadata['StationID'])
    hourlysta = (stadata['HourlyST'] + "_" + stadata['HourlyStaID'])
    remotedailysta = stadata['RemoteDailyStation']
    if dailysta == hourlysta:
        ratios.loc[len(ratios), :] = [dailysta,hourlysta,1,'n/a']
    else:
        df_localsta = df_final.loc[df_final['station']==dailysta].copy()
        df_remotesta = df_final.loc[df_final['station']==remotedailysta].copy()
        df_localsta.set_index('year', inplace = True)
        df_remotesta.set_index('year', inplace = True)
        df_localsta.columns = ['local_depth','local_station']
        df_remotesta.columns = ['remote_depth','remote_station']
        df_join = pd.concat([df_localsta,df_remotesta], axis=1, join='inner')
        ofile = os.path.join(daily_out_dir,dailysta + '_MatchYears.csv')
        df_join.to_csv(ofile)
        if df_join.shape[0] <= 5:
            ratio = 1
        else:
            s_mean = df_join.mean(axis = 0)
            ratio = s_mean.get(key='local_depth') / s_mean.get(key='remote_depth')
        ratios.loc[len(ratios), :] = [dailysta,remotedailysta,ratio,df_join.shape[0]]

ratios.set_index('Station', inplace = True)
ofile = os.path.join(daily_out_dir,'01d_ratios.csv')
ratios.to_csv(ofile)
```

6. Make_IDF_V6.py

```
import os
import inspect
import datetime
from shutil import copyfile
import pandas as pd
import numpy as np
```

```
from lmoments3 import distr
from inspect import getframeinfo, stack
from sklearn.linear_model import LinearRegression

# NB: modified lmoments3 __init__.py to use comb from scipy.special instead of scipy.misc (deprecated)
# NB: lmoments 1.03 tends to sort input array in ascending order for lmom_fit.  Do not pass it arrays that must retain their order for later use

#Python 3.6 -
# v6: Built from v5-Debug.  Added 1-hr and 2-hr constraint factors; changed final renormalization approach.

#debugfile = r"C:\Projects\CBT\Debug\debuglog.txt"
#debugfile = r"O:\Projects\Chesapeake Bay Trust\2019 RRsc5 - IDF\Work\IDFAnalysis\IDF_python\debuglog.txt"
#outf = open(debugfile, "w")

#debug inspection output
def logvar(variable, Vars=vars()):
    #from inspect import getframeinfo, stack
    outf.write("Variable name: ")
    for k in Vars:
        if type(variable) == type(Vars[k]):
            if variable is Vars[k]:
                outf.write(k)
    caller = getframeinfo(stack()[1][0])
    outf.write("\nLine #: " + str(caller.lineno))
    outf.write("\n\n" + str(variable) + "\n\n**********\n")



header_file = r"O:\Projects\Chesapeake Bay Trust\2019 RRsc5 - IDF\Work\IDFAnalysis\IDF_python\IDF_header.csv"
#header_file = r"C:\Projects\CBT\IDF_header.csv"
odir = r"O:\Projects\Chesapeake Bay Trust\2019 RRsc5 - IDF\Work\IDFAnalysis\IDF_python\Results"
#odir = r"C:\Projects\CBT\Debug"

dt = datetime.datetime.now()
dtStr = dt.strftime("%Y%m%d-%H%M")
ofilename = "IDF_Results_" + dtStr + ".csv"
ofile = os.path.join(odir,ofilename)
logfilename = "IDF_log_" + dtStr + ".txt"
logfile = os.path.join(odir,logfilename)
loglines = list()

copyfile(header_file, ofile)
```

```
returnintervals = ['1-yr','2-yr','5-yr','10-yr','25-yr','50-yr','100-yr','200-yr','500-yr','1000-yr']
durations = ['1-hr','2-hr','3-hr','6-hr','12-hr','24-hr']
col1 = '1-hr'
col2 = '2-hr'
col24 = '24-hr'
col1d = '1-day'
col3 = '3-hr'
col4 = '6-hr'
col5 = '12-hr'
##########################################################################################
#################
# Process historic IDF data from Atlas 14 station files
##########################################################################################
#################

atlas14_IDF_dir = r"O:\Projects\Chesapeake Bay Trust\2019 RRsc5 -
IDF\Work\IDFAnalysis\IDF_python\Atlas14_idf"
#atlas14_IDF_dir = r"C:\Projects\CBT\Atlas14_idf"
results = list()

DF_a14_IDF = {}

for filename in os.listdir(atlas14_IDF_dir):

    file = os.path.join(atlas14_IDF_dir,filename)

    station = filename
    station = station.replace('_existing IDF.csv','')

    df = pd.read_csv(file, engine='python', header=None, skiprows=18, index_col=0, names =
returnintervals, skipinitialspace=True, skipfooter=12)
    df.index = df.index.str.replace(r':', '')
    df.rename(index = {'60-min':'1-hr'}, inplace = True)
    df = df.transpose()

    output = [station,'Historic','Atlas14']
    for index, row in df.iterrows():
        for index,value in row.items():
            output.append(value)
    results.append(output)

    DF_a14_IDF[station] = df

##########################################################################################
#################
# Derive future climate results
```

```
##########################################################################################
#################

hourly_ams_dir = r"O:\Projects\Chesapeake Bay Trust\2019 RRsc5 -
IDF\Work\IDFAnalysis\IDF_python\Atlas14_ams\proc_hourly"
ratio_file = r"O:\Projects\Chesapeake Bay Trust\2019 RRsc5 -
IDF\Work\IDFAnalysis\IDF_python\Atlas14_ams\proc_daily\01d_ratios.csv"
run_file = r"O:\Projects\Chesapeake Bay Trust\2019 RRsc5 -
IDF\Work\IDFAnalysis\IDF_python\StationGCM_fut.csv"
#run_file = r"O:\Projects\Chesapeake Bay Trust\2019 RRsc5 -
IDF\Work\IDFAnalysis\IDF_python\StationGCM_fut_2stn.csv"
sta_file = r"O:\Projects\Chesapeake Bay Trust\2019 RRsc5 -
IDF\Work\IDFAnalysis\IDF_python\MD_sites_Atlas14.csv"
hist_GCM_file = r"O:\Projects\Chesapeake Bay Trust\2019 RRsc5 -
IDF\Work\IDFAnalysis\IDF_python\LOCA_output\DailyMaxPrec_Hist_Results.csv"
fut_GCM_file = r"O:\Projects\Chesapeake Bay Trust\2019 RRsc5 -
IDF\Work\IDFAnalysis\IDF_python\LOCA_output\DailyMaxPrec_Fut_Results.csv"
#hourly_ams_dir = r"C:\Projects\CBT\Atlas14_ams\proc_hourly"
#ratio_file = r"C:\Projects\CBT\Atlas14_ams\proc_daily\01d_ratios.csv"
#run_file = r"C:\Projects\CBT\StationGCM_fut.csv"
#run_file = r"C:\Projects\CBT\StationGCM_fut_debug.csv"
#sta_file = r"C:\Projects\CBT\MD_sites_Atlas14.csv"
#hist_GCM_file = r"C:\Projects\CBT\LOCA_output\DailyMaxPrec_Hist_Results.csv"
#fut_GCM_file = r"C:\Projects\CBT\LOCA_output\DailyMaxPrec_Fut_Results.csv"
daily_ams_file = r"O:\Projects\Chesapeake Bay Trust\2019 RRsc5 -
IDF\Work\IDFAnalysis\IDF_python\Atlas14_ams\proc_daily\daily_ams_all.csv"

df_ratio = pd.DataFrame()
df_run = pd.DataFrame()
df_sta = pd.DataFrame()
df_histGCM = pd.DataFrame()
df_futGCM = pd.DataFrame()
histGCM = pd.DataFrame()
futGCM = pd.DataFrame()
df_output = pd.DataFrame()

df_ratio = pd.read_csv(ratio_file, index_col='Station')
df_run = pd.read_csv(run_file)
df_sta = pd.read_csv(sta_file, index_col='StationID')
df_histGCM = pd.read_csv(hist_GCM_file)
df_futGCM = pd.read_csv(fut_GCM_file)

dict_scen ={'Mid10th':'2055-10th',
        'Mid50th_rcp45':'2055-RCP4.5-50th',
        'Mid50th_rcp85':'2055-RCP8.5-50th',
        'Mid90th':'2055-90th',
        'End10th':'2085-10th',
```

```
        'End50th_rcp45':'2085-RCP4.5-50th',
        'End50th_rcp85':'2085-RCP8.5-50th',
        'End90th':'2085-90th'}

DF_ams_dict = {}
df_ams = pd.DataFrame()
DF_ams_1d = pd.DataFrame()
#load the full set of daily AMS data
DF_ams_1d = pd.read_csv(daily_ams_file)  #constrained data correction applied below near line 195
when subset is extracted

#loading the hourly data; typically a reduced set of years compared to the daily data
#historical IDF parms should be computed from the full set of daily data used by Atlas14
#not from the 24-hr sum
for filename in os.listdir(hourly_ams_dir):
    file = os.path.join(hourly_ams_dir,filename)
    station = filename
    station = station.replace('_proc.csv','')
    df_ams = pd.read_csv(file, index_col='year')
    #logvar(df_ams)
    # Atlas14 Volume 2 constrained to unconstrained correction factors - but do not allow 2hr > 3hr or 1 hr
> 2hr
    df_ams[col24] = df_ams[col24] * 1.13
    df_ams[col2] = df_ams[col2] *1.05
    df_ams[col1] = df_ams[col1] * 1.16
    df_ams[col2] = np.where(df_ams[col2] < df_ams[col3], df_ams[col2], df_ams[col3])
    df_ams[col1] = np.where(df_ams[col1] < df_ams[col2], df_ams[col1], df_ams[col2])

    DF_ams_dict[str(station)] = df_ams
    #logvar(df_ams)
data_a14 = pd.DataFrame()

# IDF station loop,
for idx,row in df_run.iterrows():
    station = row['StationID']
    sta_name = df_sta.loc[station,'StationName']
    period = row['Period']
    pcnt = row['Percentile']
    gcm = row['GCM']
    rcp = row['rcp']
    #logvar(station)
    #logvar(period)
    #logvar(pcnt)

    hrly_sta = (df_sta.loc[station,'HourlyST'] + "_" + df_sta.loc[station,'HourlyStaID'])
    df_ams = DF_ams_dict[str(hrly_sta)]
    st_station = ("MD_" + station)
```

```
    ratio = df_ratio.loc[st_station,'Ratio']
    #logvar(ratio)
    df_ams = df_ams * ratio
    #logvar(df_ams)
    #data_hist = df_ams.to_numpy(copy=True)

    #return period
    RT=np.array([1,2,5,10,25,50,100,200,500,1000]);
    #AEP from ARI
    P=1-(1-np.exp(-1/RT));

    df_A14ams_IDF = pd.DataFrame(index=returnintervals, columns=durations)
    # need two cols to force it to remain a dataframe
    df_A14ams_IDF_1d = pd.DataFrame(index=returnintervals, columns=['1-day', 'station'])

    #daily data
    df_ams_1d = DF_ams_1d[DF_ams_1d['station']==st_station]

    # Atlas14 Volume 2 constrained to unconstrained correction factor
    inar = np.asarray(df_ams_1d['depth']).copy() * 1.13
    # for station with hourly data only, no daily, substitute the 24-hr sum
    # note this was already multiplied by the constrained factor above
    if len(inar)==0:
        inar = np.asarray(df_ams[col24]).copy()

    # notice: the parameter order derived by lmoments3 is different from the gev.fit.

    parm_maxfit_ams_1d = distr.gev.lmom_fit(inar,lmom_ratios=4)
    df_A14ams_IDF_1d['1-day'] =
(distr.gev.ppf(P,parm_maxfit_ams_1d['c'],parm_maxfit_ams_1d['loc'],parm_maxfit_ams_1d['scale']))
    df_A14ams_IDF_1d['station'] = st_station
    #logvar(parm_maxfit_ams_1d)

    for col in df_ams:
        inar=np.asarray(df_ams[col]).copy()
        parm_maxfit_ams = distr.gev.lmom_fit(inar,lmom_ratios=4)
        df_A14ams_IDF[col] =
(distr.gev.ppf(P,parm_maxfit_ams['c'],parm_maxfit_ams['loc'],parm_maxfit_ams['scale']))
        #logvar(parm_maxfit_ams)

    histGCM = df_histGCM.loc[(df_histGCM["Station"] == str(station)) & (df_histGCM["GCM"] == str(gcm)),
["Year","MaxDailyPrec"]]
    gcm_con = histGCM.to_numpy(copy=True)
    futGCM = df_futGCM.loc[(df_futGCM["Station"] == str(station)) & (df_futGCM["GCM"] == str(gcm)) &
(df_futGCM["Period"] == str(period)) & (df_futGCM["Percentile"] == str(pcnt)) & (df_futGCM["rcp"] ==
str(rcp)), ["Year","MaxDailyPrec"]]
    gcm_fut = futGCM.to_numpy(copy=True)
```

```
    # Fit extreme value distribution
    # GEV distribution
    # Initialize vectors
    IDF=np.zeros((len(durations),np.size(P)));
    IDF_gen1=np.zeros((len(durations),np.size(P)));

    max_gcm_con=gcm_con[:,1];
    max_gcm_fut=gcm_fut[:,1];
    # Atlas14 Volume 2 constrained to unconstrained correction factor applied to GCM daily output
    max_gcm_con = max_gcm_con * 1.13
    max_gcm_fut = max_gcm_fut * 1.13

    inar=max_gcm_con.copy()
    parm_maxfit_gcm=distr.gev.lmom_fit(inar,lmom_ratios=4);
    inar=max_gcm_fut.copy()
    parm_maxfit_gcm_fut=distr.gev.lmom_fit(inar,lmom_ratios=4);
    #max_gcm_fut = np.flipud(max_gcm_fut);
    # do not need flipud.  These should now be in descending order because not resorted by lmoments3
    #max_gcm_con = np.flipud(max_gcm_con);
    inar=np.asarray(df_ams[col24]).copy()
    parm_maxfit_24h=distr.gev.lmom_fit(inar,lmom_ratios=4);
    #logvar(parm_maxfit_gcm)
    #logvar(parm_maxfit_gcm_fut)
    #logvar(parm_maxfit_24h)

    # adjustment 1
    inar=max_gcm_fut.copy()

pre_model=distr.gev.ppf(distr.gev.cdf(inar,parm_maxfit_gcm_fut['c'],parm_maxfit_gcm_fut['loc'],parm_ma
xfit_gcm_fut['scale']),
                        parm_maxfit_ams_1d['c'],parm_maxfit_ams_1d['loc'],parm_maxfit_ams_1d['scale']);

    # adjustment 2
    inar=max_gcm_fut.copy()

pre_model_fut_reverse=distr.gev.ppf(distr.gev.cdf(inar,parm_maxfit_gcm_fut['c'],parm_maxfit_gcm_fut['lo
c'],parm_maxfit_gcm_fut['scale']),
                        parm_maxfit_gcm['c'],parm_maxfit_gcm['loc'],parm_maxfit_gcm['scale']);

    # adjusted stn future daily data
    pre_model_daily=max_gcm_fut+pre_model-pre_model_fut_reverse;
    #logvar(max_gcm_fut)
    #logvar(pre_model)
    #logvar(pre_model_fut_reverse)
    #logvar(pre_model_daily)
```

```
    # fitting GEV of stn future daily data
    inar=pre_model_daily.copy()
    parm_maxfit_stnfutdaily=distr.gev.lmom_fit(inar,lmom_ratios=4);

    # IDFs for model output, historic and future periods
    IDF[5,:]= (distr.gev.ppf(P,parm_maxfit_gcm['c'],parm_maxfit_gcm['loc'],parm_maxfit_gcm['scale']));

IDF_gen1[5,:]=(distr.gev.ppf(P,parm_maxfit_stnfutdaily['c'],parm_maxfit_stnfutdaily['loc'],parm_maxfit_stnf
utdaily['scale']));

    # subdaily QM
    inar=pre_model_daily.copy()
    test1 = distr.gev.cdf(inar,parm_maxfit_24h['c'],parm_maxfit_24h['loc'],parm_maxfit_24h['scale'])
    #logvar(pre_model_daily)
    test1[np.where(test1<1.0E-5)] = 1.0E-5
    test1[np.where(test1>0.99999)] = 0.99999
    #logvar(test1)
    #logvar(parm_maxfit_24h)
    for i in range(0,len(durations) - 1):
        print (station, gcm, rcp, i)
        #logvar(i)
        max_hist_con=np.asarray(df_ams[durations[i]])
        #logvar(max_hist_con)
        #fitting GEV distribution
        parm_maxfit_hist= distr.gev.lmom_fit(max_hist_con, lmom_ratios=4);
        #logvar(parm_maxfit_hist)
        #smoothed model future subdaily - scaled to 1-day IDF

pre_model_sub=distr.gev.ppf(test1,parm_maxfit_hist['c'],parm_maxfit_hist['loc'],parm_maxfit_hist['scale']);
        #logvar(pre_model_sub)

#pre_model_sub=distr.gev.ppf(distr.gev.cdf(inar,parm_maxfit_24h['c'],parm_maxfit_24h['loc'],parm_maxfit
_24h['scale']),
        #                        parm_maxfit_hist['c'],parm_maxfit_hist['loc'],parm_maxle']);
        # regression with intercept using polyfit
        #post_para=np.polyfit(pre_model_daily,pre_model_sub,1);
        #pre_model1=np.polyval(post_para,pre_model_daily);
        # no intercept regression using sklearn LinearRegression
        arr1 = pre_model_daily.reshape(-1, 1).copy()
        arr2 = pre_model_sub.reshape(-1, 1).copy()
        reg = LinearRegression(fit_intercept = False).fit(arr1, arr2)
        arr3 = reg.predict(arr1)
        pre_model1 = arr3.reshape((arr3.shape[0],))
        #logvar(reg.coef_)
        #logvar(reg.intercept_)
        #logvar(pre_model_daily)
        #logvar(df_ams)
```

```
        #logvar(pre_model_sub)
        #logvar(pre_model1)

        #smoothed model historic subdaily
        inar=max_gcm_con.copy()
        test2 = distr.gev.cdf(inar,parm_maxfit_24h['c'],parm_maxfit_24h['loc'],parm_maxfit_24h['scale'])
        test2[np.where(test2<1.0E-5)] = 1.0E-5
        test2[np.where(test2>0.99999)] = 0.99999

        pre_model_sub0=distr.gev.ppf(test2,
parm_maxfit_hist['c'],parm_maxfit_hist['loc'],parm_maxfit_hist['scale']);

        # no intercept regression using sklearn LinearRegression
        arr1 = max_gcm_con.reshape(-1, 1).copy()
        arr2 = pre_model_sub0.reshape(-1, 1).copy()
        reg = LinearRegression(fit_intercept = False).fit(arr1, arr2)
        arr3 = reg.predict(arr1)
        pre_model0 = arr3.reshape((arr3.shape[0],))

        #historical model IDF
        inar=pre_model0.copy()
        parm_maxfit_gcm0=distr.gev.lmom_fit(inar, lmom_ratios=4);
        IDF[i,:]=(distr.gev.ppf(P,parm_maxfit_gcm0['c'],parm_maxfit_gcm0['loc'],parm_maxfit_gcm0['scale']));

        #future adjusted IDF
        inar=pre_model1.copy()
        parm_maxfit_gcm1=distr.gev.lmom_fit(inar, lmom_ratios=4);
        #logvar(parm_maxfit_gcm1)

IDF_gen1[i,:]=(distr.gev.ppf(P,parm_maxfit_gcm1['c'],parm_maxfit_gcm1['loc'],parm_maxfit_gcm1['scale'])
);

    df_IDF = pd.DataFrame(IDF, index=durations, columns=returnintervals)
    df_IDF = df_IDF.transpose()
    df_IDF_gen1 = pd.DataFrame(IDF_gen1, index=durations, columns=returnintervals)
    df_IDF_gen1 = df_IDF_gen1.transpose()

    #logvar(df_A14ams_IDF)
    #logvar(df_A14ams_IDF_1d)
    #logvar(df_IDF)
    #logvar(df_IDF_gen1)

    data_a14 = DF_a14_IDF[station]
    #logvar(data_a14)
    idf_project = pd.DataFrame(index=returnintervals, columns=durations)
    alt_ratio = data_a14[col24]/df_A14ams_IDF_1d[col1d]
    #logvar(alt_ratio)
```

```
    idf_project[col24]=alt_ratio*list(df_IDF_gen1[col24])

    #alt_ratio2 = idf_project[col24]/df_IDF_gen1[col24]
    #logvar(alt_ratio2)
    for i in range(0,len(durations) - 1):
        mycol = durations[i]
        #alt_ratio2 = data_a14[mycol]/df_IDF[mycol]
        #alt_ratio2 = data_a14[mycol]/df_A14ams_IDF[mycol]
        #idf_project[durations[i]]=alt_ratio2*list(df_IDF_gen1[durations[i]])
        #subdaily results tend to be unstable at high recurrences so estimate based on ratio of GCM fit for
dur relative to
        #GCM fit for 24 hr data times the 1-day result calculated with the parms from the longer ams series
        idf_project[durations[i]] = df_A14ams_IDF[mycol]/df_A14ams_IDF[col24] * idf_project[col24]

    # final adjustments where values across durations for a given recurrence is not monotonically
increasing
    # per p. 39 in Atlas 14 v. 2.  Do this from the top down as the 1-hr tends to be most unstable
    #logvar(data_a14)
    #logvar(idf_project)
    for j in range(0, len(returnintervals)):
        #for i in range(1, len(durations)):
        for i in range(len(durations)-1, 0, -1):
            if idf_project.iat[j, i] < idf_project.iat[j, i-1]:
                idf_project.iat[j, i-1] = idf_project.iat[j, i]
    #logvar(idf_project)

    # test if monotonically increasing across durations and recurrence intervals
    for i in range(idf_project.shape[0]):
        rets = idf_project.iloc[i]
        if not rets.is_monotonic_increasing:
            loglines.append("Station ID: "+ station + " Station Name: " + sta_name + " Future period: " +
period + " Percentile: " + pcnt + " GCM: " + gcm + " rcp: " + rcp + " " + rets.name + " is not monotonically
increasing.\n" + str(rets) + "\n")

    for i in range(idf_project.shape[1]):
        durs = idf_project.iloc[:,i]
        if not durs.is_monotonic_increasing:
            loglines.append("Station ID: "+ station + " Station Name: " + sta_name + " Future period: " +
period + " Percentile: " + pcnt + " GCM: " + gcm + " rcp: " + rcp + " " + durs.name + " is not monotonically
increasing.\n" + str(durs) + "\n")

#output the results
    output = [station,dict_scen[(period + pcnt)],(gcm + "_" + rcp)]

    for index, row in idf_project.iterrows():
        for index,value in row.items():
```

```
                output.append(value)
    results.append(output)
    print (idx, station, gcm, rcp)

with open(ofile, 'a') as file:
    for line in results:
        file.write(','.join([str(x) for x in line]) + '\n')
    file.close()

with open(logfile, 'w') as the_file:
    if len(loglines) == 0:
        the_file.writelines("All durations and return intervals are monotonically increasing\n")
    else:
        the_file.writelines(loglines)
    the_file.close
#debug output
#outf.close()
```

A-2. PEAKS-OVER-THRESHOLD ANALYSIS

```
# -*- coding: utf-8 -*-
"""
Created on Fri Nov  1 10:18:30 2019

@author: tan.zi
"""

# -*- coding: utf-8 -*-
"""
Created on Mon Sep 30 11:56:34 2019

@author: tan.zi
"""

import numpy as np
from scipy.stats import genpareto as gpd
from scipy.io import netcdf
import statsmodels.api as sm
import pandas as pd
from scipy.signal import argrelextrema
import os
import urllib.request, urllib.error
from http.cookiejar import CookieJar
from netCDF4 import Dataset
from datetime import datetime
```

```
from datetime import date

def LOCA_download(userLat, userLong, saveLocation, GCMs, rcp):

    odir =saveLocation
    if not os.path.exists(odir): os.makedirs(odir)

    minLat = str(round(userLat - 0.05, 6))
    minLong = str(round(userLong - 0.05, 6))
    maxLat = str(round(userLat + 0.05, 6))
    maxLong = str(round(userLong + 0.05, 6))


    line = "Downloading historical LOCA data\n"

    # HISTORICAL
    scn = GCMs

    if scn == 'CCSM4':
        url = 'https://cida.usgs.gov/thredds/ncss/loca_historical?var=pr_' + scn + '_r6i1p1_historical&'

    elif scn == 'GISS-E2-H' and rcp == 'rcp85':
        url = 'https://cida.usgs.gov/thredds/ncss/loca_historical?var=pr_' + scn + '_r6i1p1_historical&'
    elif scn == 'GISS-E2-H' and rcp == 'rcp45':
        url = 'https://cida.usgs.gov/thredds/ncss/loca_historical?var=pr_' + scn + '_r6i1p1_historical&'

    elif scn == 'GISS-E2-R' and rcp == 'rcp85':
        url = 'https://cida.usgs.gov/thredds/ncss/loca_historical?var=pr_' + scn + '_r6i1p1_historical&'
    elif scn == 'GISS-E2-R' and rcp == 'rcp45':
        url = 'https://cida.usgs.gov/thredds/ncss/loca_historical?var=pr_' + scn + '_r6i1p1_historical&'

    elif scn == 'EC-EARTH' and rcp == 'rcp85':
        url = 'https://cida.usgs.gov/thredds/ncss/loca_historical?var=pr_' + scn + '_r1i1p1_historical&'

    else:
        url = 'https://cida.usgs.gov/thredds/ncss/loca_historical?var=pr_' + scn + '_r1i1p1_historical&'
    url = url + 'north=' + maxLat + '&west=' + minLong + '&east=' + maxLong + '&south=' + minLat
    url = url + '&disableProjSubset=on&horizStride=1&time_start=1950-01-
01T12%3A00%3A00Z&time_end=2005-12-31T12%3A00%3A00Z&timeStride=1'
    print(url)
    out_name = 'historical_loca_' + str(userLat) + "_" + str(userLong) + "_" + scn + '_ppt' + '.nc'
    local = os.path.join(odir,out_name)
    if not os.path.exists(local):
        try:
            password_manager = urllib.request.HTTPPasswordMgrWithDefaultRealm()
            cookie_jar = CookieJar()
            opener = urllib.request.build_opener(
```

```
            urllib.request.HTTPBasicAuthHandler(password_manager),
            urllib.request.HTTPCookieProcessor(cookie_jar))
        urllib.request.install_opener(opener)
        request1 = urllib.request.Request(url)
        response1 = urllib.request.urlopen(request1)
        body1 = response1.read()
        with open(local, 'wb') as f:
          f.write(body1)



  # FUTURE

  if scn == 'CCSM4':
    url = 'https://cida.usgs.gov/thredds/ncss/loca_future?var=pr_' + scn + '_r6i1p1_' + rcp + '&'

  elif scn == 'GISS-E2-H' and rcp == 'rcp85':
    url = 'https://cida.usgs.gov/thredds/ncss/loca_future?var=pr_' + scn + '_r2i1p1_' + rcp + '&'
  elif scn == 'GISS-E2-H' and rcp == 'rcp45':
    url = 'https://cida.usgs.gov/thredds/ncss/loca_future?var=pr_' + scn + '_r6i1p3_' + rcp + '&'

  elif scn == 'GISS-E2-R' and rcp == 'rcp85':
    url = 'https://cida.usgs.gov/thredds/ncss/loca_future?var=pr_' + scn + '_r2i1p1_' + rcp + '&'
  elif scn == 'GISS-E2-R' and rcp == 'rcp45':
    url = 'https://cida.usgs.gov/thredds/ncss/loca_future?var=pr_' + scn + '_r6i1p1_' + rcp + '&'

  elif scn == 'EC-EARTH' and rcp == 'rcp45':
    url = 'https://cida.usgs.gov/thredds/ncss/loca_future?var=pr_' + scn + '_r8i1p1_' + rcp + '&'
  elif scn == 'EC-EARTH' and rcp == 'rcp85':
    url = 'https://cida.usgs.gov/thredds/ncss/loca_future?var=pr_' + scn + '_r2i1p1_' + rcp + '&'

  else:
    url = 'https://cida.usgs.gov/thredds/ncss/loca_future?var=pr_' + scn + '_r1i1p1_' + rcp + '&'
  url = url + 'north=' + maxLat + '&west=' + minLong + '&east=' + maxLong + '&south=' + minLat
  url = url + '&disableProjSubset=on&horizStride=1&time_start=2006-01-
01T12%3A00%3A00Z&time_end=2100-12-31T12%3A00%3A00Z&timeStride=1'
  print(url)
  out_name = rcp + '_loca_' + str(userLat) + "_" + str(userLong) + "_" + scn + '_ppt' + '.nc'
  local = os.path.join(odir,out_name)
  if not os.path.exists(local):
    try:
      password_manager = urllib.request.HTTPPasswordMgrWithDefaultRealm()
      cookie_jar = CookieJar()
      opener = urllib.request.build_opener(
            urllib.request.HTTPBasicAuthHandler(password_manager),
            urllib.request.HTTPCookieProcessor(cookie_jar))
      urllib.request.install_opener(opener)
```

```
        request1 = urllib.request.Request(url)
        response1 = urllib.request.urlopen(request1)
        body1 = response1.read()
        with open(local, 'wb') as f:
            f.write(body1)


def Pull_RCM_DailyRainfall(netcdf_folder,GCM_csv_folder,userLat,userLong,GCMs,rcp):

    loca_repo = netcdf_folder

    scenario=GCMs
    historical_file = loca_repo + "\\historical_loca_" + str(userLat) + "_" + str(userLong) + "_" + scenario +
"_ppt.nc"
    rcp_file = loca_repo + "\\" + rcp + "_loca_" + str(userLat) + "_" + str(userLong) + "_" + scenario +
"_ppt.nc"
    mhistf = netcdf.netcdf_file(historical_file, 'r')
    mfutf = netcdf.netcdf_file(rcp_file, 'r')


    s=datetime(1950,1,1)
    e=datetime(2005,12,31)
    ts=pd.date_range(s,e,freq='d')


    if scenario == 'CCSM4':
        scenariocall = 'pr_' + scenario + '_r6i1p1_historical'
        t1=mhistf.variables[scenariocall][:,0,1]
    elif scenario == 'GISS-E2-H' and rcp == 'rcp85':
        scenariocall = 'pr_' + scenario + '_r6i1p1_historical'
        t1=mhistf.variables[scenariocall][:,0,1]
    elif scenario == 'GISS-E2-H' and rcp == 'rcp45':
        scenariocall = 'pr_' + scenario + '_r6i1p1_historical'
        t1=mhistf.variables[scenariocall][:,0,1]
    elif scenario == 'GISS-E2-R' and rcp == 'rcp45':
        scenariocall = 'pr_' + scenario + '_r6i1p1_historical'
        t1=mhistf.variables[scenariocall][:,0,1]
    elif scenario == 'GISS-E2-R' and rcp == 'rcp85':
        scenariocall = 'pr_' + scenario + '_r6i1p1_historical'
        t1=mhistf.variables[scenariocall][:,0,1]
    else:
        scenariocall = 'pr_' + scenario + '_r1i1p1_historical'
        t1=mhistf.variables[scenariocall][:,0,1]

    #check units and scale factor and convert to mm
    if mhistf.variables[scenariocall].units in ['kg m-2 s-1',b'kg m-2 s-1']:
        t1=t1*86400
```

```
    if hasattr(mhistf.variables[scenariocall], 'scale_factor'):
        t1=t1*mhistf.variables[scenariocall].scale_factor
    t1=t1*0.0393701
    rcm_hist_df=pd.DataFrame(columns=['Date','P_inch'])
    rcm_hist_df['Date']=pd.Series(ts)
    rcm_hist_df['P_inch']=pd.Series(t1)
    rcm_hist_df.to_csv(GCM_csv_folder+'\\'+scenario+'_hist_'+ str(userLat) + "_" + str(userLong)+'.csv',
index=False)

    fut_yr_start=2006
    fut_yr_end=2100
    sp=datetime(fut_yr_start,1,1)
    ep=datetime(fut_yr_end,12,31)
    tsp=pd.date_range(sp,ep,freq='d')

    if scenario == 'CCSM4':
        scenariocall = 'pr_' + scenario + '_r6i1p1_' + rcp
        tp1=mfutf.variables[scenariocall][:,0,1]
    elif scenario == 'GISS-E2-H' and rcp == 'rcp45':
        scenariocall = 'pr_' + scenario + '_r6i1p3_' + rcp
        tp1=mfutf.variables[scenariocall][:,0,1]
    elif scenario == 'GISS-E2-H' and rcp == 'rcp85':
        scenariocall = 'pr_' + scenario + '_r2i1p1_' + rcp
        tp1=mfutf.variables[scenariocall][:,0,1]
    elif scenario == 'GISS-E2-R' and rcp == 'rcp45':
        scenariocall = 'pr_' + scenario + '_r6i1p1_' + rcp
        tp1=mfutf.variables[scenariocall][:,0,1]
    elif scenario == 'GISS-E2-R' and rcp == 'rcp85':
        scenariocall = 'pr_' + scenario + '_r2i1p1_' + rcp
        tp1=mfutf.variables[scenariocall][:,0,1]
    elif scenario == 'EC-EARTH' and rcp =='rcp45':
        scenariocall = 'pr_' + scenario + '_r8i1p1_' + rcp
        tp1=mfutf.variables[scenariocall][:,0,1]
    elif scenario == 'EC-EARTH' and rcp =='rcp85':
        scenariocall = 'pr_' + scenario + '_r2i1p1_' + rcp
        tp1=mfutf.variables[scenariocall][:,0,1]
    else:
        scenariocall = 'pr_' + scenario + '_r1i1p1_' + rcp
        tp1=mfutf.variables[scenariocall][:,0,1]



    if mfutf.variables[scenariocall].units in ['kg m-2 s-1',b'kg m-2 s-1']:
        tp1=tp1*86400
    if hasattr(mfutf.variables[scenariocall], 'scale_factor'):
        tp1=tp1*mfutf.variables[scenariocall].scale_factor
```

```
        tp1=tp1*0.0393701
        rcm_fut_df=pd.DataFrame(columns=['Date','P_inch'])
        rcm_fut_df['Date']=pd.Series(tsp)
        rcm_fut_df['P_inch']=pd.Series(tp1)
        rcm_fut_df.to_csv(GCM_csv_folder+'\\'+scenario+'_'+rcp+'_'+ str(userLat) + "_" +
str(userLong)+'.csv', index=False)


def Screen_GCMs(site_id,Prism_file,GCM_list, Screen_folder,userLat,userLong, fut_yr_st,fut_yr_ed):


    lat_ind=int((userLat-23.40625)/0.0625)   # LOCA dataset lat starts at 23.40625 with 0.0625 interval
    lon_ind=int(((360+userLong)-234.03125)/0.0625)  # LOCA dataset long starts at 234.03125 with
0.0625 interval

    ratio_dict={}
    ratior45_dict={}
    ratior85_dict={}


    hist_data =np.genfromtxt(Prism_file,delimiter=",",missing_values=" ",skip_header=1)
    hist_p=hist_data[hist_data>0]
    hist_90th=np.quantile(hist_p,q=0.9)
    hist_lg_90th=sum(hist_p[hist_p>=hist_90th])/len(hist_data)

    fut_url='http://cida.usgs.gov/thredds/dodsC/loca_future'
    fut_dataset = Dataset(fut_url)


    for GCM in GCM_list:

        # FUTURE
        first_date = date(2006, 1, 1)
        s_date = date(fut_yr_st, 1, 1)
        e_date = date(fut_yr_ed, 12, 31)
        delta_s = s_date - first_date
        delta_e=e_date-first_date

        rcp='rcp45'

        if scn == 'CCSM4':
            var = 'pr_' + scn + '_r6i1p1_' + rcp
        elif scn == 'GISS-E2-H':
            var = 'pr_' + scn +  '_r6i1p3_' +rcp
        elif scn == 'GISS-E2-R':
            var = 'pr_' + scn +  '_r6i1p1_'+rcp
        elif scn == 'EC-EARTH':
```

```
    var = 'pr_' + scn +  '_r8i1p1_'+rcp
else:
    var = 'pr_' + scn + '_r1i1p1_'+rcp

print('rcp45_'+GCM)

futr45_slice=fut_dataset.variables[var]

futr45_data=futr45_slice[delta_s.days:delta_e.days,lat_ind,lon_ind].data

futr45_p=futr45_data[futr45_data>0]

if len(futr45_p) and len (hist_p)>0:

    if futr45_slice.units=='kg m-2 s-1':
        futr45_p=futr45_p*86400

    futr45_lg_90th=sum(futr45_p[futr45_p>=hist_90th])/len(futr45_data)
    change_ratio=(futr45_lg_90th-hist_lg_90th)/hist_lg_90th
    ratio_dict.update({scn+'_'+rcp:change_ratio})
    ratior45_dict.update({scn+'_'+rcp:change_ratio})

rcp='rcp85'

if scn == 'CCSM4':
    var = 'pr_' + scn + '_r6i1p1_' + rcp
elif scn == 'GISS-E2-H':
    var = 'pr_' + scn +  '_r2i1p1_' +rcp
elif scn == 'GISS-E2-R':
    var = 'pr_' + scn +  '_r2i1p1_'+rcp
elif scn == 'EC-EARTH':
    var = 'pr_' + scn +  '_r2i1p1_'+rcp
else:
    var = 'pr_' + scn + '_r1i1p1_'+rcp

print('rcp85_'+GCM)
futr85_slice=fut_dataset.variables[var]

futr85_data=futr85_slice[delta_s.days:delta_e.days,lat_ind,lon_ind].data

futr85_p=futr85_data[futr85_data>0]

if len(futr85_p) and len (hist_p)>0:

    if futr85_slice.units=='kg m-2 s-1':
        futr85_p=futr85_p*86400
```

```
            futr85_lg_90th=sum(futr85_p[futr85_p>=hist_90th])/len(futr85_data)
            change_ratio=(futr85_lg_90th-hist_lg_90th)/hist_lg_90th
            ratio_dict.update({scn+'_'+rcp:change_ratio})
            ratior85_dict.update({scn+'_'+rcp:change_ratio})

        # return the 10th, 50th, 90th percentile models
    if bool(ratio_dict):
        gcm90=list(ratio_dict.keys())[np.abs(list(ratio_dict.values()) -
np.percentile(list(ratio_dict.values()),90)).argmin()]
        r45gcm50=list(ratior45_dict.keys())[np.abs(list(ratior45_dict.values()) -
np.percentile(list(ratior45_dict.values()),50)).argmin()]
        r85gcm50=list(ratior85_dict.keys())[np.abs(list(ratior85_dict.values()) -
np.percentile(list(ratior85_dict.values()),50)).argmin()]
        gcm10=list(ratio_dict.keys())[np.abs(list(ratio_dict.values()) -
np.percentile(list(ratio_dict.values()),10)).argmin()]
    else:
        gcm90=''
        r45gcm50=''
        r85gcm50=''
        gcm10=''
    print(gcm10,r45gcm50,r85gcm50,gcm90)

    # OUTPUT screen results
    with open(Screen_folder+'\\'+str(site_id)+'_Screen'+'_'+str(fut_yr_st)+'_'+str(fut_yr_ed)+'.csv','w') as f:
    writer = csv.writer(f)
    for key, value in ratio_dict.items():
        writer.writerow([key, value])

    return ([gcm10,r45gcm50,r85gcm50,gcm90])


def Define_Threshold(raints):

    rain=np.sort(raints[raints>0])

    Ee=[]
    var_E=[]
    weights=[]
    for i in range(len(rain)-10):
        e=rain-rain[i]
        Ee.append(np.mean(e[e>0]))
        var_E.append(np.var(e[i:]))
        weights.append((len(rain)-i)/var_E[i])

    wls_results=[]

    for j in range(len(rain)-20):
```

```
        # WLS regression
        WLS =sm.WLS( Ee[j:],sm.add_constant(rain[j:-10]), sample_weight=weights[j:])
        res_wls=WLS.fit()
        y_prime=res_wls.fittedvalues
        wmse=sum(weights[j:]*(y_prime-Ee[j:])**2)/len(weights[j:])
        wls_results.append(np.hstack((j,wmse,res_wls.params[0],res_wls.params[1])))

    wls_df=pd.DataFrame(wls_results, columns=('Index','WMSE','intercept','slope'))
    minm = argrelextrema(np.array(wls_df['WMSE']), np.less)   # find local minimum
    threshold=rain[int(minm[0][0])]
    slope=wls_df['slope'][int(minm[0][0])]
    intercept=wls_df['intercept'][int(minm[0][0])]
    shape=slope/(1+slope)
    scale=intercept*(1-shape)+shape*threshold

    return threshold,shape,scale


def GPD_fit(Prism_file,GCM_csv_folder,Scenlist,userLat,userLong,GDP_fit_file, fut_yr_st,fut_yr_ed):


    data=np.genfromtxt(Prism_file,delimiter=",",missing_values=" ",skip_header=1)
    threshold,shape0,scale0=Define_Threshold(data[:,1])

    rain=np.sort(data[data[:,1]>0,1])
    hist_90th=np.quantile(rain,q=0.9)


    GPD_fit_list=[]
    GPD_fit_list.append(['PRISM',hist_90th])

    for scn in Scenlist:
        for rcp in ['rcp45','rcp85']:
            print(scn)
            GCM=scn.split('_')[0]
            gcmcon_file=GCM_csv_folder+'\\'+siteID+'_'+GCM+'_historical'+'.csv'
            gcmfut_file=GCM_csv_folder+'\\'+siteID+'_'+GCM+'_'+rcp+'.csv'
            gcm_con_daily_df=pd.read_csv(gcmcon_file)
            gcm_con_daily_df['year'] = pd.DatetimeIndex(gcm_con_daily_df['Date']).year
            # 30 years of historical modeling results
            gcm_con_daily=np.array(gcm_con_daily_df['P_inch'] )
            gcm_con=np.sort(gcm_con_daily[gcm_con_daily>0])


            gcm_fut_daily_df=pd.read_csv(gcmfut_file)
            gcm_fut_daily_df['year'] = pd.DatetimeIndex(gcm_fut_daily_df['Date']).year
```

```
        # 30 years of future modeling results
        gcm_fut_daily=np.array(gcm_fut_daily_df[(gcm_fut_daily_df['year']>=fut_yr_st) &
(gcm_fut_daily_df['year']<=fut_yr_ed)]['P_inch'] )
        gcm_fut=np.sort(gcm_fut_daily[gcm_fut_daily>0])




        gcm_con_t=gcm_con[gcm_con>threshold]
        gcm_fut_t=gcm_fut[gcm_fut>threshold]
        prob_threshold=len(gcm_fut_t)/len(gcm_fut)

        # fit GDP with the initial guess values from historical data
        gcm_con_param=gpd.fit(gcm_con_t,shape0, loc=threshold, scale=scale0)
        gcm_fut_param=gpd.fit(gcm_fut_t,shape0, loc=threshold, scale=scale0)

        ########################################################################
        # conditional distribution matching
        ########################################################################

        # adjustment 1

P_fut_adj1=gpd.ppf(gpd.cdf(gcm_fut_t,gcm_fut_param[0],threshold,gcm_fut_param[2]),shape0,threshold,
scale0);

        # adjustment 2

P_fut_adj2=gpd.ppf(gpd.cdf(gcm_fut_t,gcm_fut_param[0],threshold,gcm_fut_param[2]),gcm_con_param[
0],threshold,gcm_con_param[2]);

        # adjusted stn future daily data
        P_fut=gcm_fut_t+P_fut_adj1- P_fut_adj2;  # conditional distribution only for x > threshold


    # Covert probability from truncated dataset to full dataset with conditional probability
        stnfut_param=gpd.fit(P_fut,gcm_fut_param[0],loc=threshold,scale=gcm_fut_param[2])

        x=np.linspace(min(P_fut),max(P_fut),100)

        cdf_fit=gpd.cdf(x,*stnfut_param)

        model_fut_prob=1-prob_threshold*(1-cdf_fit)

        st_fut_ary=np.transpose(np.vstack((x,model_fut_prob)))

        st_fut_df=pd.DataFrame(st_fut_ary,columns=('Rain','Prob'))
```

```
            hi_prob=model_fut_prob[model_fut_prob > 0.9].min()

            low_prob=model_fut_prob[model_fut_prob < 0.9].max()

            p90_plus=float(st_fut_df[st_fut_df['Prob']==hi_prob]['Rain'])

            p90_minus=float(st_fut_df[st_fut_df['Prob']==low_prob]['Rain'])

            st_90th_fut_p=(0.9-low_prob)/(hi_prob-low_prob)*(p90_plus-p90_minus)+p90_minus

            GPD_fit_list.append([GCM+'_'+rcp,st_90th_fut_p])

    pd.DataFrame(GPD_fit_list,columns=['Scenarios','P_90th']).to_csv(GDP_fit_file,index=None)
```

```
def main(netcdf_folder,GCM_csv_folder,Prism_folder,sites_file,Screen_folder,results_folder):
#    The streamlined function to batch process the POT analysis of all MD sites.
#    First, screen GCMs based on each site  (Screen_GCMs)
#    Then, based on the screening results, pull and process GCM data  (LOCA_download,
Pull_RCM_Dailyrainfall)
#    Last, project future changes to 90th rainfall event  (GDP_fit), threshold and GDP parameters were
estimated with Define_Threshold function.



#    main(netcdf_folder,GCM_csv_folder,Prism_folder,sites_file,Screen_folder,results_folder)
#    netcdf_folder=r'C:\Tan\Projects\CBT\POT\data_test\Loca_data'
#    GCM_csv_folder=r'C:\Tan\Projects\CBT\POT\data_test\GCM_CSV'
#    Prism_folder=r'C:\Tan\Projects\CBT\POT\data_test\PRISM_data'
#    sites_file=r'C:\Tan\Projects\CBT\POT\data_test\MD_sites2.csv'
#    Screen_folder=r'C:\Tan\Projects\CBT\POT\data_test\Screen_results'
#    results_folder=r'C:\Tan\Projects\CBT\POT\data_test\Results'
#

    GCM_list=['ACCESS1-0','ACCESS1-3','CCSM4','CESM1-BGC','CESM1-CAM5','CMCC-CMS','CMCC-
CM',
            'CNRM-CM5','CSIRO-Mk3-6-0','CanESM2','EC-EARTH','FGOALS-g2','GFDL-CM3',
             'GFDL-ESM2G','GFDL-ESM2M','GISS-E2-H','GISS-E2-R','HadGEM2-AO','HadGEM2-CC',
             'HadGEM2-ES','IPSL-CM5A-LR','IPSL-CM5A-MR','MIROC-ESM-CHEM','MIROC-ESM',
             'MIROC5','MPI-ESM-LR','MPI-ESM-MR','MRI-CGCM3','NorESM1-M','bcc-csm1-1-m']
```

```
    sites_df=pd.read_csv(sites_file)
    for idx,site in sites_df.iterrows():
        userLat=float(site['Latitude'])
        userLong=float(site['Longitude'])
        site_id=site['StationID']
        print(site['StationID'])


        Prism_file=Prism_folder+'\\PRISM_'+str(float(site.Latitude))+'_'+str(float(site.Longitude)) + '_ppt.csv'

        fut_yr_st=2040
        fut_yr_ed=2069

        Scenlist=[]
        Scenlist=Screen_GCMs(site_id,Prism_file,GCM_list, Screen_folder,userLat,userLong,
fut_yr_st,fut_yr_ed)

        if len(Scenlist[0])>0:
        #downlaod and processing LOCA data
            for scn in Scenlist:
                GCM=scn.split('_')[0]
                rcp=scn.split('_')[1]
                LOCA_download(userLat, userLong, netcdf_folder, GCM, rcp)
                Pull_RCM_DailyRainfall(netcdf_folder,GCM_csv_folder,userLat,userLong,GCM,rcp)


            GDP_fit_file=results_folder+'\\'+str(site['Station ID'])+'_2055.csv'
            GPD_fit(Prism_file,GCM_csv_folder,Scenlist,userLat,userLong,GDP_fit_file, fut_yr_st,fut_yr_ed)

        fut_yr_st=2070
        fut_yr_ed=2099

        Scenlist=[]
        Scenlist=Screen_GCMs(site_id,Prism_file,GCM_list, Screen_folder,userLat,userLong,
fut_yr_st,fut_yr_ed)

        if len(Scenlist[0])>0:
        #downlaod and processing LOCA data
            for scn in Scenlist:
                GCM=scn.split('_')[0]
                rcp=scn.split('_')[1]
                LOCA_download(userLat, userLong, netcdf_folder, GCM, rcp)
                Pull_RCM_DailyRainfall(netcdf_folder,GCM_csv_folder,userLat,userLong,GCM,rcp)


            GDP_fit_file=results_folder+'\\'+str(site['Station ID'])+'_2085.csv'
```

```
        GPD_fit(Prism_file,GCM_csv_folder,Scenlist,userLat,userLong,GDP_fit_file, fut_yr_st,fut_yr_ed)


if __name__ == '__main__':
    main(sys.argv[1],sys.argv[2],sys.argv[3],sys.argv[4],sys.argv[5],sys.argv[6])
```

A-3. SWMM SIMULATIONS

Separate code is provided for the simulations with and without the BMP in place.

1. SWMM_IDF_NoBMP_Looped.py

```
# -*- coding: utf-8 -*-
"""
Created on Fri Mar 27 15:05:13 2020

@author: PETER.KWON
"""

import sys
import io
import ftplib
import os
import os, math
from scipy.optimize import minimize
import time
import datetime as dt
import pandas as pd
import numpy as np
from pandas import ExcelWriter
from pyswmm import Simulation, Nodes, LidGroups, Subcatchments

def main():

    ###USER_INPUT###
    file_to_use =
r"C:\Users\peter.kwon\Projects\Chesapeake_Bay_Trust\Python\Looping_Code\Input\SWMM_Input_Gene
ration_Launch_Loop_Input.xlsx"
            BMP = 'Bioret_NoBMP'

    #import POT Rainfall estimates
    IDF_INPUT = pd.read_excel(file_to_use, sheet_name = 'IDF')
    #Cumulative rainfall tab that will become Rainfall.dat export for SWMM input
    CUM_RATIO = pd.read_excel(file_to_use, sheet_name = 'CUM_RATIO')
    #type of BMP to run. BMP_TYPE sheet should have only one item selected.
    BMP_TYPE = pd.read_excel(file_to_use, sheet_name = 'BMP_TYPE')
    #Station Inputs - WQ_Depth, CPv_Time, 1yr_24hr, and 100yr_24hr values by station.
```

```
    #Bioretention uses WQ_Depth, Wet Ponds uses all columns
    STATIONINPUTS = pd.read_excel(file_to_use, sheet_name = 'STATION_INPUTS')
    #Create List of Percent Impervious scenarios to analyze
    P_IMP = [25,50,80]
    #Create List of IDF scenarios
    IDF_SCENARIO = ['1-yr 24-hr','2-yr 24-hr','10-yr 24-hr','100-yr 24-hr']

    ###End User Inputs###

    ###In-code processing###

    #Create list of loopable index
    ROWCOUNT = IDF_INPUT['RowCount'].tolist()

    #Prepare a dataframe for the final output depending on BMP type
    if BMP == 'Bioret_NoBMP':
        column_names =
['StationName','StationID','Year','GCM_RCP','BMP_Type','ANALYSIS_Type','RAINFALL_DEPTH',
                    'EVENT_Type','P_IMPERV','Site_peak_flow_cfs','Site_volume_cf']
    if BMP == 'WetP_NoBMP':
        column_names =
['StationName','StationID','Year','GCM_RCP','BMP_Type','ANALYSIS_Type','RAINFALL_DEPTH',
                    'EVENT_Type','P_IMPERV','Site_peak_flow_cfs','Site_volume_cf']
    DF_OUTPUT = pd.DataFrame(columns=column_names)

    #Start loop over each row
    for a, aa in enumerate(ROWCOUNT):
        STATION_NAME = IDF_INPUT.loc[IDF_INPUT['RowCount']==aa,'Atlas14_Station'].item()
        STATION_ID = IDF_INPUT.loc[IDF_INPUT['RowCount']==aa,'Atlas14_StationID'].item()
        YEAR = IDF_INPUT.loc[IDF_INPUT['RowCount']==aa,'Year'].item()
        GCM_RCP = IDF_INPUT.loc[IDF_INPUT['RowCount']==aa,'GCM_RCP'].item()
        WQ_DEPTH =
STATIONINPUTS.loc[STATIONINPUTS['StationID']==STATION_ID,'WQ_Depth'].item()
        #Start loop for 4 rainfall eventss
        for b,bb in enumerate(IDF_SCENARIO):
            if bb == '1-yr 24-hr':
                PRECIP = IDF_INPUT.loc[IDF_INPUT['RowCount']==aa,'1-yr 24-hr'].item()
            if bb == '2-yr 24-hr':
                PRECIP = IDF_INPUT.loc[IDF_INPUT['RowCount']==aa,'2-yr 24-hr'].item()
            if bb == '10-yr 24-hr':
                PRECIP = IDF_INPUT.loc[IDF_INPUT['RowCount']==aa,'10-yr 24-hr'].item()
            if bb == '100-yr 24-hr':
                PRECIP = IDF_INPUT.loc[IDF_INPUT['RowCount']==aa,'100-yr 24-hr'].item()
            #Create Rainfall.dat file
            CUM_RATIO['PRECIP'] = PRECIP
            CUM_RATIO['CUM_RAINFALL'] = np.nan
            #print(aa)
```

```
        #print(CUM_RATIO.columns)
        RATIO_LIST = CUM_RATIO.RATIO.tolist()
        PRECIP_LIST = CUM_RATIO.PRECIP.tolist()
        CUM_RATIO['CUM_RAINFALL'] = np.multiply(RATIO_LIST,PRECIP_LIST)
        CUM_RATIO = CUM_RATIO.round({"CUM_RAINFALL":6})
        RAINFALL =
CUM_RATIO[['STATION_ID','YEAR','MONTH','DAY','HOUR','MINUTE','CUM_RAINFALL']]
        if BMP == 'Bioret_NoBMP':

RAINFALL.to_csv(r'C:\Users\peter.kwon\Projects\Chesapeake_Bay_Trust\Python\Looping_Code\Proces
sing\Bioret_NoBMP\Rainfall.dat',sep=' ',header=False, index=False)
        if BMP == 'WetP_NoBMP':

RAINFALL.to_csv(r'C:\Users\peter.kwon\Projects\Chesapeake_Bay_Trust\Python\Looping_Code\Proces
sing\WetP_NoBMP\Rainfall.dat',sep=' ',header=False, index=False)

        #loop grabbing SWMM input file created by Scott Job for each percent impervious value
        for c, cc in enumerate(P_IMP):
            if BMP == 'Bioret_NoBMP':
                folder_name =
r'C:\Users\peter.kwon\Projects\Chesapeake_Bay_Trust\Python\Looping_Code\Processing\Bioret_NoBMP
'
                os.chdir(folder_name)
                #.inp files for SWMM provided by Scott Job
                if cc == 25:
                    infile = 'SWMM_Bioret_Imp25.inp'
                if cc == 50:
                    infile = 'SWMM_Bioret_Imp50.inp'
                if cc == 80:
                    infile = 'SWMM_Bioret_Imp80.inp'
                #Design parameters provided by Scott Job
                Rv = 0.05 + 0.009 * cc                  # volumetric runoff coefficient
                SiteArea = 1                            # acres
                WQv = WQ_DEPTH * Rv * SiteArea * 43560 / 12     # WQ_DEPTH inches, WQv cu ft
                Bio_pd = 1                              # Ponding depth above media, ft
                Bio_footprint = WQv / Bio_pd
            if BMP == 'WetP_NoBMP':
                folder_name =
r'C:\Users\peter.kwon\Projects\Chesapeake_Bay_Trust\Python\Looping_Code\Processing\WetP_NoBMP'
                os.chdir(folder_name)

                #.inp files for SWMM provided by Scott Job
                if cc == 25:
                    infile = 'SWMM_WetPond_Imp25.inp'
                if cc == 50:
                    infile = 'SWMM_WetPond_Imp50.inp'
                if cc == 80:
```

```
                infile = 'SWMM_WetPond_Imp80.inp'

            #Run pyswmm simulation
            if BMP == 'Bioret_NoBMP':
                with Simulation(infile) as sim:
                    sc1 = Subcatchments(sim)["SC1"]
                    for step in sim:
                        pass
                    site_peakflow = sc1.statistics.get('peak_runoff_rate')
                    site_volume = sc1.statistics.get('runoff')

                    sim.close()

                # Report    Statistic               Value
                #           Site peak flow (cfs)     site_peakflow
                #           Site volume (cf)        site_volume
                #
                # For BMP_Type, report "Bioretention site, no BMP"
            if BMP == 'WetP_NoBMP':
                with Simulation(infile) as sim:
                    sc1 = Subcatchments(sim)["SC1"]
                    for step in sim:
                        pass
                    site_peakflow = sc1.statistics.get('peak_runoff_rate')
                    site_volume = sc1.statistics.get('runoff')

                    sim.close()
                # Report    Statistic               Value
                #           Site peak flow (cfs)     site_peakflow
                #           Site volume (cf)        site_volume
                #
                # For BMP_Type, report "Wet Pond site, no BMP"
            #Create row to iterate into datafrme
            if BMP == "Bioret_NoBMP":
                ROW_TO_ADD = [STATION_NAME,STATION_ID,YEAR,GCM_RCP,"Bioretention site, no
BMP",ANALYSIS,PRECIP,bb,cc,site_peakflow,site_volume]
            if BMP == "WetP_NoBMP":
                ROW_TO_ADD = [STATION_NAME,STATION_ID,YEAR,GCM_RCP,"Wet Pond site, no
BMP",ANALYSIS,PRECIP,bb,cc,site_peakflow,site_volume]
            ROW_TO_ADD = pd.Series(ROW_TO_ADD,index=DF_OUTPUT.columns)
            #Loop for 3 percent impervious conditions (25%,50%,80%)
            if c == 0:
                DF_OUTPUT_FINAL = DF_OUTPUT.append(ROW_TO_ADD,ignore_index=True)
            if c > 0:
                DF_OUTPUT_FINAL = DF_OUTPUT_FINAL.append(ROW_TO_ADD,ignore_index=True)
        #Loop for 4 rainfall events (1,2,10,100 years 24-hr events)
        if b == 0:
```

```
            DF_OUTPUT_FINAL2 = DF_OUTPUT_FINAL
        if b > 0:
            DF_OUTPUT_FINAL2 =
DF_OUTPUT_FINAL2.append(DF_OUTPUT_FINAL,ignore_index=True)
    #Loop for each row of input design storm information
    if a == 0:
        DF_OUTPUT_FINAL3 = DF_OUTPUT_FINAL2
    if a > 0:
        DF_OUTPUT_FINAL3 =
DF_OUTPUT_FINAL3.append(DF_OUTPUT_FINAL2,ignore_index=True)
  #Export dataframe to master output
  if BMP == 'Bioret_NoBMP':

DF_OUTPUT_FINAL3.to_csv(r'C:\Users\peter.kwon\Projects\Chesapeake_Bay_Trust\Python\Looping_C
ode\Output\SWMM_IDF_OUTPUT_SUMMARY_BIORET_NOBMP.csv',index=False)
  if BMP == 'WetP_NoBMP':

DF_OUTPUT_FINAL3.to_csv(r'C:\Users\peter.kwon\Projects\Chesapeake_Bay_Trust\Python\Looping_C
ode\Output\SWMM_IDF_OUTPUT_SUMMARY_WETP_NOBMP.csv',index=False)
  ###End In-code processing###

if __name__=="__main__":
  main()
```

2. SWMM_IDF_BMP_Looped.py

```
# -*- coding: utf-8 -*-
"""
Created on Fri Mar 27 15:05:13 2020

@author: PETER.KWON
"""

#import sys
#import io
#import ftplib
#import os
import os, math
from scipy.optimize import minimize
import time
import datetime as dt
import pandas as pd
import numpy as np
#from pandas import ExcelWriter
from pyswmm import Simulation, Nodes, LidGroups

def main():
```

```
    ###USER_INPUT###
    file_to_use = r"C:\Temp\CBT
Climate\SWMM\python\Looping_Code\Input\SWMM_Input_Generation_Launch_Loop_Input.xlsx"
            BMP = 'Bioretention'

    #import POT Rainfall estimates
    IDF_INPUT = pd.read_excel(file_to_use, sheet_name = 'IDF')
    #Cumulative rainfall tab that will become Rainfall.dat export for SWMM input
    CUM_RATIO = pd.read_excel(file_to_use, sheet_name = 'CUM_RATIO')
    #Station Inputs - WQ_Depth, CPv_Time, 1yr_24hr, and 100yr_24hr values by station.
    #Bioretention uses WQ_Depth, Wet Ponds uses all columns
    STATIONINPUTS = pd.read_excel(file_to_use, sheet_name = 'STATION_INPUTS')
    #Create List of Percent Impervious scenarios to analyze
    P_IMP = [25,50,80]
    #output file
    outfile = r"C:\Temp\CBT
Climate\SWMM\python\Looping_Code\Output\SWMM_IDF_OUTPUT_SUMMARY_BIORETENTION.csv"
    #Create List of IDF scenarios
    IDF_SCENARIO = ['1-yr 24-hr','2-yr 24-hr','10-yr 24-hr','100-yr 24-hr']

    ###End User Inputs###

    ###In-code processing###

    #Create list of loopable index
    ROWCOUNT = IDF_INPUT['RowCount'].tolist()

    #Prepare a dataframe for the final output depending on BMP type
    if BMP == 'Bioretention':
        column_names =
['StationName','StationID','Year','GCM_RCP','BMP_Type','P_IMPERV','ANALYSIS_Type','EVENT_Type',
                    'STORM_Depth','Site_PeakFlow_cfs','Overflow_cf','Underdrain_outflow_cf']
    if BMP == 'Wet Pond':
        column_names =
['StationName','StationID','Year','GCM_RCP','BMP_Type','P_IMPERV','ANALYSIS_Type','EVENT_Type',
                    'STORM_Depth','CPv_stage_ft','Site_PeakFlow_cfs','Site_volume_cf']
    DF_OUTPUT = pd.DataFrame(columns=column_names)

    #Start loop over each row
    for a, aa in enumerate(ROWCOUNT):
        STATION_NAME = IDF_INPUT.loc[IDF_INPUT['RowCount']==aa,'Atlas14_Station'].item()
        STATION_ID = IDF_INPUT.loc[IDF_INPUT['RowCount']==aa,'Atlas14_StationID'].item()
        YEAR = IDF_INPUT.loc[IDF_INPUT['RowCount']==aa,'Year'].item()
        GCM_RCP = IDF_INPUT.loc[IDF_INPUT['RowCount']==aa,'GCM_RCP'].item()
        WQ_DEPTH =
STATIONINPUTS.loc[STATIONINPUTS['StationID']==STATION_ID,'WQ_Depth'].item()
```

```
        #Start loop for 4 rainfall eventss
        for b,bb in enumerate(IDF_SCENARIO):
            if bb == '1-yr 24-hr':
                PRECIP = IDF_INPUT.loc[IDF_INPUT['RowCount']==aa,'1-yr 24-hr'].item()
            if bb == '2-yr 24-hr':
                PRECIP = IDF_INPUT.loc[IDF_INPUT['RowCount']==aa,'2-yr 24-hr'].item()
            if bb == '10-yr 24-hr':
                PRECIP = IDF_INPUT.loc[IDF_INPUT['RowCount']==aa,'10-yr 24-hr'].item()
            if bb == '100-yr 24-hr':
                PRECIP = IDF_INPUT.loc[IDF_INPUT['RowCount']==aa,'100-yr 24-hr'].item()
            #Create Rainfall.dat file
            CUM_RATIO['PRECIP'] = PRECIP
            CUM_RATIO['CUM_RAINFALL'] = np.nan
            RATIO_LIST = CUM_RATIO.RATIO.tolist()
            PRECIP_LIST = CUM_RATIO.PRECIP.tolist()
            CUM_RATIO['CUM_RAINFALL'] = np.multiply(RATIO_LIST,PRECIP_LIST)
            CUM_RATIO = CUM_RATIO.round({"CUM_RAINFALL":6})
            #Python lesson: DF[COLUMN]*DF[COLUMN] runs into a KeyError due to pandas trying to
            #identify the column name, not the column contents. Use format, DF.COLUMNS
            #CUM_RATIO['CUM_RAINFALL'] = CUM_RATIO['CUM_RATIO']*CUM_RATIO['PRECIP']
            #CUM_RATIO['CUM_RAINFALL'] = '{0:.6f}'.format(CUM_RATIO['CUM_RAINFALL'])
            RAINFALL =
CUM_RATIO[['STATION_ID','YEAR','MONTH','DAY','HOUR','MINUTE','CUM_RAINFALL']]
            if BMP == 'Bioretention':
                RAINFALL.to_csv(r'C:\Temp\CBT
Climate\SWMM\python\Looping_Code\Processing\Bioretention\Rainfall.dat',sep=' ',header=False,
index=False)
            if BMP == 'Wet Pond':
                RAINFALL.to_csv(r'C:\Temp\CBT
Climate\SWMM\python\Looping_Code\Processing\Wet_Pond\Rainfall.dat',sep=' ',header=False,
index=False)

            #loop grabbing SWMM input file created by Scott Job for each percent impervious value
            for c, cc in enumerate(P_IMP):
                if BMP == 'Bioretention':
                    folder_name = r'C:\Temp\CBT
Climate\SWMM\python\Looping_Code\Processing\Bioretention'
                    os.chdir(folder_name)
                    #.inp files for SWMM provided by Scott Job
                    if (cc == 25) & (WQ_DEPTH == 0.9):
                        infile = 'SWMM_0p9_25.inp'
                    if (cc == 50) & (WQ_DEPTH == 0.9):
                        infile = 'SWMM_0p9_50.inp'
                    if (cc == 80) & (WQ_DEPTH == 0.9):
                        infile = 'SWMM_0p9_80.inp'
                    if (cc == 25) & (WQ_DEPTH == 1.0):
                        infile = 'SWMM_1p0_25.inp'
```

```
            if (cc == 50) & (WQ_DEPTH == 1.0):
                infile = 'SWMM_1p0_50.inp'
            if (cc == 80) & (WQ_DEPTH == 1.0):
                infile = 'SWMM_1p0_80.inp'
            #Design parameters provided by Scott Job
            Rv = 0.05 + 0.009 * cc                  # volumetric runoff coefficient
            SiteArea = 1                            # acres
            WQv = WQ_DEPTH * Rv * SiteArea * 43560 / 12     # WQ_DEPTH inches, WQv cu ft
            Bio_pd = 1                              # Ponding depth above media, ft
            Bio_footprint = WQv / Bio_pd
        if BMP == 'Wet Pond':
            folder_name = r'C:\Temp\CBT Climate\SWMM\python\Looping_Code\Processing\Wet_Pond'
            os.chdir(folder_name)

            #Designate variables per Scott Job's code
            StationID = STATION_ID
            pcnt_imp = cc

            #Read in station, geometry, and design parameter files

            station_file = r"C:\Temp\CBT
Climate\SWMM\python\Looping_Code\Input\StationLoookups.csv"
            df_station = pd.read_csv(station_file, index_col='StationID')
            WQ_dep = df_station.loc[StationID,'WQ_Depth']
            CPv_time = df_station.loc[StationID,'CPv_Time']

            geom_file = r"C:\Temp\CBT
Climate\SWMM\python\Looping_Code\Input\WetPond_Geom.csv"
            df_geom = pd.read_csv(geom_file, index_col=['PcntImp','WQ_dep'])
            L1 = df_geom.loc[(pcnt_imp,WQ_dep),'L1']
            H1 = df_geom.loc[(pcnt_imp,WQ_dep),'H1']
            curve = df_geom.loc[(pcnt_imp,WQ_dep),'Stage00':]

            design_params_file = r"C:\Temp\CBT
Climate\SWMM\python\Looping_Code\Input\Design_out.csv"
            df_design = pd.read_csv(design_params_file, index_col=['StationID','PcntImp'])
            vol_1yr = df_design.loc[(StationID,pcnt_imp),'1yr_vol']
            peak_1yr = df_design.loc[(StationID,pcnt_imp),'1yr_peak']
            peak100yr = df_design.loc[(StationID,pcnt_imp),'100yr_peak']

            #Define site area, acres
            site_area = 25

            # power curves for MD Stormwater Manual nomengraph page D.11.3
            nomen = [[12,19.618,-0.911],[24,13.917,-0.965]]
            df_nomen = pd.DataFrame(nomen, columns = ['T','coeff','exp'])
            df_nomen.set_index('T', inplace = True, append = False)
```

```
coeff = df_nomen.loc[CPv_time,'coeff']
exp = df_nomen.loc[CPv_time,'exp']

# CPv storage volume calcs
Qa = vol_1yr * 12 / site_area / 43560
area_sqmi = site_area / 640
qu = peak_1yr / Qa / area_sqmi
qo_qi = coeff * qu ** exp
k = [0.683,-1.43,1.64,-0.804]
Vs_Vr = k[0] + k[1]*qo_qi + k[2]*qo_qi**2 + k[3]*qo_qi**3
Vs_in = Vs_Vr * Qa
Vs_cf = Vs_in / 12 * site_area * 43560 #storage volume needed in wet pond to address channel protection volume, less than channel protection volume, allows inflow for 24hr flow

# Optimize on Vs_cf, L1, H1 --> return H2

def opt(x,a,b,c): #x is variable to find, a,b,c are arguments
   result = abs(((a+a*x/b)*(2*(b+x))**2)/3 - (a*(2*b)**2)/3 - c)
   return result

x0 = [20]   # starting value #value of 20 will vary #x0 is L2, item of optimization
out = minimize(opt, x0, bounds = [(0,100)], args=(H1,L1,Vs_cf))
L2 = out.x[0]
H2 = L2 * H1 / L1


# Orifice diameter (ft)
qo = qo_qi * peak_1yr
O_diam = round(2 * math.sqrt(qo / (0.6 * math.pi * math.sqrt(2 * 32.2 * H2))), 4)

# Weir width (ft)
freeboard = 1  # ft
W_width = round(peak100yr / 3 / freeboard ** 1.5, 2)


# Build SWMM INP file

N_1 = 0.011
N_2 = 0.24
S_1 = 0.05
S_2 = 0.15
PCT_S = 2
SH = 8.6
Kst = 0.06
IMDx = 0.208
interval = "0:06"
```

```
model_file = "SWMM.inp"
SWMMinput = os.path.join(folder_name, model_file)
with open(SWMMinput, 'w') as z:
    z.write('[TITLE]\n')
    z.write(';;Project Title/Notes\n\n')
    z.write('[OPTIONS]\n')
    z.write(';;Option\t\tValue\n')
    z.write('FLOW_UNITS           CFS\n')
    z.write('INFILTRATION         GREEN_AMPT\n')
    z.write('FLOW_ROUTING         DYNWAVE\n')
    z.write('LINK_OFFSETS         DEPTH\n')
    z.write('MIN_SLOPE            0\n')
    z.write('ALLOW_PONDING        NO\n')
    z.write('SKIP_STEADY_STATE    NO\n\n')
    z.write('START_DATE           12/24/2018\n')
    z.write('START_TIME           00:00:00\n')
    z.write('REPORT_START_DATE    12/24/2018\n')
    z.write('REPORT_START_TIME    00:00:00\n')
    z.write('END_DATE             12/26/2018\n')
    z.write('END_TIME             00:00:00\n')
    z.write('SWEEP_START          01/01\n')
    z.write('SWEEP_END            12/31\n')
    z.write('DRY_DAYS             0\n')
    z.write('REPORT_STEP          00:01:00\n')
    z.write('WET_STEP             00:00:10\n')
    z.write('DRY_STEP             00:00:10\n')
    z.write('ROUTING_STEP         00:00:01\n\n')
    z.write('INERTIAL_DAMPING     PARTIAL\n')
    z.write('NORMAL_FLOW_LIMITED  BOTH\n')
    z.write('FORCE_MAIN_EQUATION  H-W\n')
    z.write('VARIABLE_STEP        0.75\n')
    z.write('LENGTHENING_STEP     0\n')
    z.write('MIN_SURFAREA         12.566\n')
    z.write('MAX_TRIALS           8\n')
    z.write('HEAD_TOLERANCE       0.005\n')
    z.write('SYS_FLOW_TOL         5\n')
    z.write('LAT_FLOW_TOL         5\n')
    z.write('MINIMUM_STEP         0.5\n')
    z.write('THREADS              1\n\n')
    z.write('[EVAPORATION]\n')
    z.write(';;Data Source    Parameters\n')
    z.write(';;-------------- ----------\n')
    z.write('CONSTANT         0.142\n')
    z.write('DRY_ONLY         YES\n\n')
    z.write('[RAINGAGES]\n')
    z.write(';;Name           Format    Interval SCF      Source\n')
    z.write(';;-------------- --------- ------ ------ ----------\n')
```

```
                string1 = 'RG1             CUMULATIVE    %s     1.0      FILE       "Rainfall.dat" Station1
IN\n\n' % (interval)
                z.write(string1)
                z.write('[SUBCATCHMENTS]\n')
                z.write(';;Name          Rain Gage       Outlet          Area     %Imperv  Width    %Slope
CurbLen  SnowPack\n')
                z.write(';;--------------- ---------------- ---------------- -------- -------- -------- -------- -------- ----------------
-\n')
                string2 = 'SC1             RG1             S1              %s       %s      1044      %s       0\n\n' %
(site_area, pcnt_imp, PCT_S)
                z.write(string2)
                z.write('[SUBAREAS]\n')
                z.write(';;Subcatchment   N-Imperv   N-Perv     S-Imperv   S-Perv     PctZero    RouteTo
PctRouted\n')
                z.write(';;--------------- ---------- ---------- ---------- ---------- ---------- ----------\n')
                string3 = 'SC1             %s      %s       %s       %s       0          OUTLET\n\n' % (N_1, N_2,
S_1, S_2)
                z.write(string3)
                z.write('[INFILTRATION]\n')
                z.write(';;Subcatchment   Suction    Ksat       IMD\n')
                z.write(';;--------------- ---------- ---------- ----------\n')
                string4 = 'SC1             %s       %s       %s\n\n' % (SH, Kst, IMDx)
                z.write(string4)
                z.write('[JUNCTIONS]\n')
                z.write(';;Name          Elevation  MaxDepth   InitDepth  SurDepth   Aponded\n')
                z.write(';;--------------- ---------- ---------- ---------- ---------- ----------\n')
                z.write('J1              8.9        10         0          0          0\n')
                z.write('J2              9          10         0          0          0\n')
                z.write('J3              9          10         0          0          0\n\n')
                z.write('[OUTFALLS]\n')
                z.write(';;Name          Elevation  Type       Stage Data       Gated    Route To\n')
                z.write(';;--------------- ---------- ---------- ---------------- -------- ----------------\n')
                z.write('OF1             8.8        FREE                        NO\n\n')
                z.write('[STORAGE]\n')
                z.write(';;Name          Elev.    MaxDepth   InitDepth  Shape      Curve Name/Params
N/A      Fevap    Psi      Ksat     IMD\n')
                z.write(';;--------------- -------- ---------- ---------- ---------- ---------------------------- -------- --------
-------- -------- --------\n')
                z.write('S1              10       15         0          TABULAR    Curve_S1                     0
1\n\n')
                z.write('[CONDUITS]\n')
                z.write(';;Name          From Node       To Node         Length     Roughness  InOffset
OutOffset  InitFlow   MaxFlow\n')
                z.write(';;--------------- ---------------- ---------------- ---------- ---------- ---------- ---------- ---------- -----
-----\n')
                z.write('C1              J1              OF1             10         0.01       0          0          0          0\n')
                z.write('C2              J2              J1              10         0.01       0          0          0          0\n')
```

```
                z.write('C3             J3              J1              10        0.01      0         0         0         0\n\n')
                z.write('[ORIFICES]\n')
                z.write(';;Name          From Node       To Node         Type        Offset     Qcoeff     Gated
CloseTime\n')
                z.write(';;--------------- ---------------- ---------------- ------------ ---------- ---------- -------- ----------\n')
                z.write('O1             S1              J3              SIDE        0         0.60      NO       0\n\n')
                z.write('[WEIRS]\n')
                z.write(';;Name          From Node       To Node         Type        CrestHt    Qcoeff     Gated
EndCon   EndCoeff   Surcharge  RoadWidth  RoadSurf   Coeff. Curve\n')
                z.write(';;--------------- ---------------- ---------------- ------------ ---------- ---------- -------- --------
--- ---------- ---------- ---------- ----------------\n')
                z.write('W1             S1              J2              TRANSVERSE   ' + str(round(H2,2)) + '
3.00       NO       0        0         YES\n\n')
                z.write('[XSECTIONS]\n')
                z.write(';;Link          Shape       Geom1          Geom2      Geom3      Geom4      Barrels
Culvert\n')
                z.write(';;--------------- ------------ ---------------- ---------- ---------- ---------- ---------- ----------\n')
                z.write('C1             CIRCULAR    8              0         0         0         1\n')
                z.write('C2             CIRCULAR    8              0         0         0         1\n')
                z.write('C3             CIRCULAR    4              0         0         0         1\n')
                string5 = 'O1             CIRCULAR     %s             0         0         0\n' % (O_diam)
                z.write(string5)
                string6 ='W1             RECT_OPEN    10             %s      0         0\n\n' % (W_width)
                z.write(string6)
                z.write('[CURVES]\n')
                z.write(';;Name          Type       X-Value    Y-Value\n')
                z.write(';;--------------- ---------- ---------- ----------\n')
                z.write("Curve_S1        Storage    0          " + str(curve['Stage00']) + "\n")
                z.write("Curve_S1                   1          " + str(curve['Stage01']) + "\n")
                z.write("Curve_S1                   2          " + str(curve['Stage02']) + "\n")
                z.write("Curve_S1                   3          " + str(curve['Stage03']) + "\n")
                z.write("Curve_S1                   4          " + str(curve['Stage04']) + "\n")
                z.write("Curve_S1                   5          " + str(curve['Stage05']) + "\n")
                z.write("Curve_S1                   6          " + str(curve['Stage06']) + "\n")
                z.write("Curve_S1                   7          " + str(curve['Stage07']) + "\n")
                z.write("Curve_S1                   8          " + str(curve['Stage08']) + "\n")
                z.write("Curve_S1                   9          " + str(curve['Stage09']) + "\n")
                z.write("Curve_S1                   10         " + str(curve['Stage10']) + "\n")
                z.write("Curve_S1                   11         " + str(curve['Stage11']) + "\n")
                z.write("Curve_S1                   12         " + str(curve['Stage12']) + "\n")
                z.write("Curve_S1                   13         " + str(curve['Stage13']) + "\n")
                z.write("Curve_S1                   14         " + str(curve['Stage14']) + "\n")
                z.write("Curve_S1                   15         " + str(curve['Stage15']) + "\n")
                z.write('\n')
                z.write('[REPORT]\n')
                z.write(';;Reporting Options\n')
                z.write('AVERAGES   YES\n')
```

```
                z.write('SUBCATCHMENTS ALL\n')
                z.write('NODES ALL\n')
                z.write('LINKS ALL\n\n')
                z.write('[TAGS]\n\n')
                z.write('[MAP]\n')
                z.write('DIMENSIONS 0.000 0.000 10000.000 10000.000\n')
                z.write('Units      None\n\n')
                z.write('[COORDINATES]\n')
                z.write(';;Node           X-Coord            Y-Coord\n')
                z.write(';;-------------- ------------------ ------------------\n')
                z.write('J1              10771.429          5857.143\n')
                z.write('J2              10437.037          6770.370\n')
                z.write('J3              10555.556          4903.704\n')
                z.write('OF1              12051.852          5822.222\n')
                z.write('S1              8028.571           5857.143\n\n')
                z.write('[VERTICES]\n')
                z.write(';;Link           X-Coord            Y-Coord\n')
                z.write(';;-------------- ------------------ ------------------\n')
                z.write('O1              9514.286           4828.571\n')
                z.write('W1              9600.000           6857.143\n\n')
                z.write('[Polygons]\n')
                z.write(';;Subcatchment   X-Coord            Y-Coord\n')
                z.write(';;-------------- ------------------ ------------------\n')
                z.write('SC1             5114.286           7428.571\n')
                z.write('SC1             5085.714           4114.286\n')
                z.write('SC1             2171.429           4200.000\n')
                z.write('SC1             2228.571           7457.143\n\n')
                z.write('[SYMBOLS]\n')
                z.write(';;Gage           X-Coord            Y-Coord\n')
                z.write(';;-------------- ------------------ ------------------\n')

            z.close()

        #Run pyswmm simulation
        if BMP == 'Bioretention':
            with Simulation(infile) as sim:
                j1 = Nodes(sim)["J1"]
                lid_on_sub = LidGroups(sim)["SC1"]
                for step in sim:
                    pass

                PEAKFLOW = str(j1.statistics.get('peak_total_inflow'))
                OVERFLOW = str(lid_on_sub[0].water_balance.surface_flow / 12 * Bio_footprint)
                UNDERDRAIN_OUTFLOW = str(lid_on_sub[0].water_balance.drain_flow / 12 *
Bio_footprint)

                sim.close()
```

```
            if BMP == 'Wet Pond':
                infile = ("SWMM.inp")
                with Simulation(infile) as sim:
                    of1 = Nodes(sim)["OF1"]
                    for step in sim:
                        pass

                    site_peakflow = of1.statistics.get('peak_total_inflow')
                    site_volume = of1.cumulative_inflow

            #Create row to iterate into datafrme
            if BMP == "Bioretention":
                ROW_TO_ADD =
[STATION_NAME,STATION_ID,YEAR,GCM_RCP,BMP,cc,ANALYSIS,bb,PRECIP,PEAKFLOW,OVERF
LOW,UNDERDRAIN_OUTFLOW]
            if BMP == "Wet Pond":
                ROW_TO_ADD =
[STATION_NAME,STATION_ID,YEAR,GCM_RCP,BMP,cc,ANALYSIS,bb,PRECIP,H2,site_peakflow,site
_volume]

            DF_OUTPUT.loc[len(DF_OUTPUT)] = ROW_TO_ADD

        print ("Row complete: " + str(aa))

    #Export dataframe to master output
    DF_OUTPUT.to_csv(outfile,index=False)

    ###End In-code processing###

    #set end time
    ENDTIME = time.time()

    #indicate process finish and time taken
    print('Date today: %s' % dt.date.today())
    print("program finished")
    print("It took {0:.2f} minutes to execute this".format((ENDTIME - STARTTIME) / 60.))

if __name__=="__main__":
    main()
```